TRW SYSTEMS

SECOND QUARTERLY PROGRESS REPORT

(19 August - 18 November)

"Study and Analysis

of

Satellite Power Systems Configurations

for

Maximum Utilization of Power"

Contract Number NAS 5-9178
(NASA Goddard Space Flight Center)

W. G. Binckley
W. G. Binckley, Project Manager

Approved: H. Riess
H. Riess, Head
Systems Engineering Section

Approved: A. Krausz
A. Krausz, Manager
Electric Power Department

Approved: P. F. Glaser
P. F. Glaser, Director
Space Power & Support Systems

1. INTRODUCTION

This report is the second quarterly report covering work performed under the GSFC contract for study and analysis of satellite power system configurations for maximum utilization of power. The study as a whole is organized around six major tasks:

1. A survey of the power requirements of spaceborne equipment in typical unmanned satellites.

2. A survey of typical spacecraft electrical power system designs.

3. Collection and presentation of electrical, thermal and physical data on the individual elements of power systems (i.e., power control, energy storage, and power conditioning equipment).

4. Analysis of typical space missions to be identified by GSFC with respect to their electrical power requirements and to the characteristics of photovoltaic power systems which could meet those requirements. Various power systems will be evaluated with respect to efficiency, reliability, weight, and interface considerations.

5. Investigation of possible means of standardizing electrical power requirements of satellite equipment as well as design of power systems and their components.

6. Investigation of the characteristics of alternate electrical power systems using radioisotope thermoelectric generators rather than photovoltaic sources.

The culmination of the first four tasks is obviously Task 5, which will include recommendations as to how standardization can be furthered without unduly compromising efficiency. It is evident that any degree of standardization which can be achieved will offer significant advantages with respect to cost, development time, and reliability; an attempt will be made to determine the point at which these advantages are outweighed by reduced efficiency, taking into consideration the various types of missions identified by GSFC.

2. PRESENT STATUS OF THE STUDY

It is estimated that by the end of the second quarter the planned program was approximately 45 percent complete. To date, all effort has been devoted to the first three tasks, with the following results:

<u>Task 1</u> Complete, except for additional data regarding experiment power requirements to be furnished by GSFC in January 1966. Results are presented in the first quarterly report and in the present document.

<u>Task 2</u> Complete. Results are presented in this report.

<u>Task 3</u> Approximately 90 percent complete, with results presented in this report. The remaining data will be available in January 1966 from results of company-funded research projects now under way in the fields of power controls, power conditioning, and batteries.

It is planned that the third quarter will be devoted primarily to Task 4, system analysis for the various missions. These are to be identified by GSFC in January 1966. A schedule revised to reflect the GSFC inputs to the study is attached.

It should be noted that the results of the first three tasks are not of interest in themselves, since their only function is to serve as inputs to Task 4. These results are presented here primarily to provide an indication of the nature of the data on which the analysis of Task 4 will be based.

PROGRAM SCHEDULE

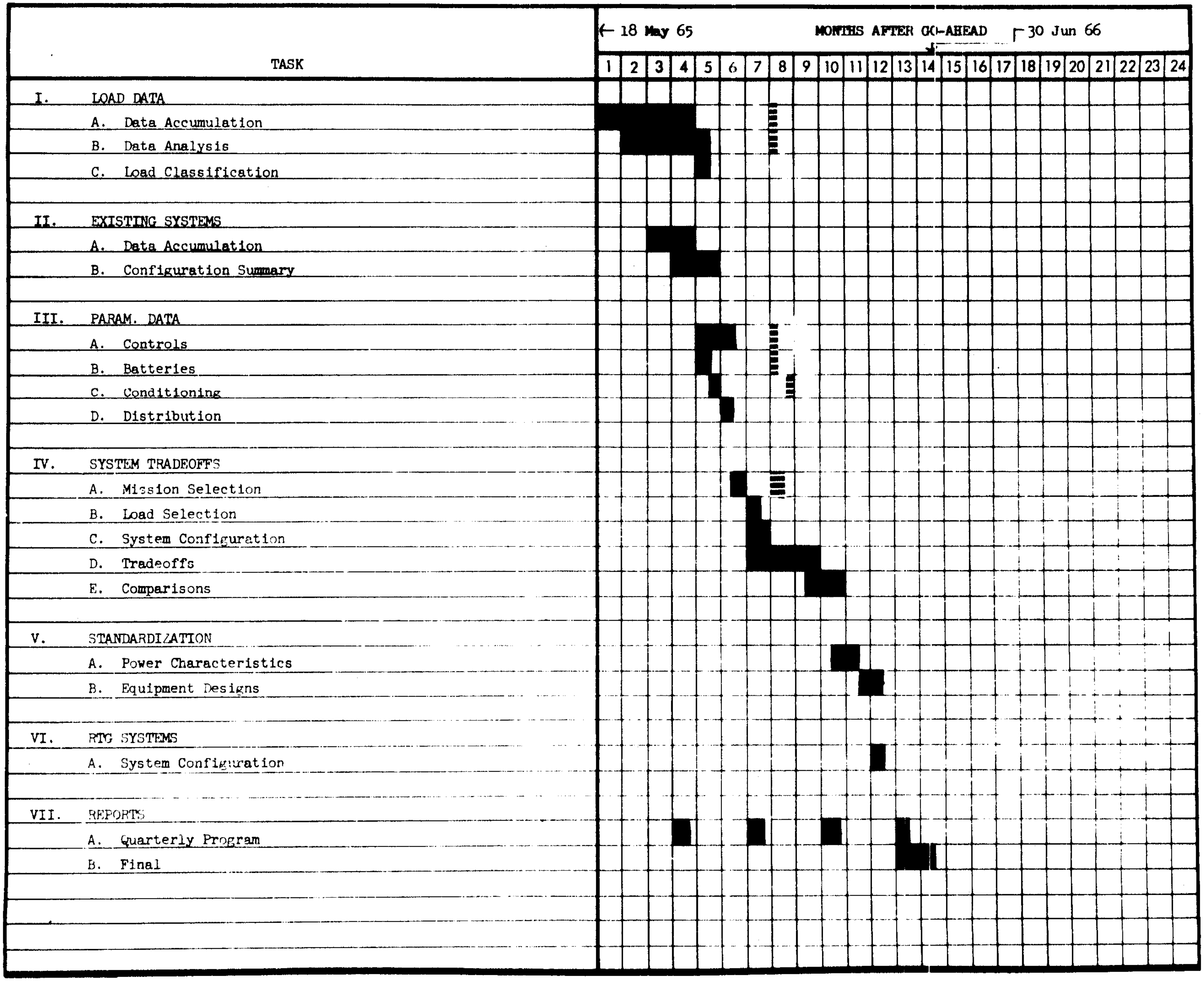

3. STUDY RESULTS

3.1 ANALYSIS OF LOADS

As indicated in the first quarterly progress report, the loads supplied by satellite power systems will be considered under three major headings:

- Communications and data handling equipment
- Stabilization and control equipment
- Experiments

The data accumulated for the first category was presented in the previous report. The second and third will be covered here, except for the additional experiment data to be obtained in January 1966.

3.1.1 Stabilization and Control Equipment

Tables I, II, and III summarize the results of the survey of electrical power requirements of typical stabilization and control equipment. Stabilization and control systems typically consist of sensors and reaction devices, connected through a set of electronics which provides the required data processing and logic functions. Table I shows voltage, voltage regulation, frequency and frequency regulation, ripple, duty cycle, and average power for samples of the three types of sensor commonly used (inertial, optical, electromechanical transducers). Table II provides the same data for the standard types of reaction devices, and Table III shows the requirements for typical digital and analog signal processing and logic units.

A review of these tables indicates the great variety of power requirements imposed by stabilization and control equipment, not only with regard to voltage and voltage regulation, but for ripple and noise as well. Consultations were held with responsible design engineers to determine the reasons for this wide variety. It was found that in most cases, a component or part was chosen because it was available and met the functional requirements of the system, and was therefore accepted along with its particular power requirements, without any consideration of whether these requirements could be simplified by selection of another part or component which might also meet the

TABLE I

STABILIZATION AND CONTROL
SENSORS

Sensor Type	Attitude Control System - Type	Required Voltage and Regulation	Required Freq. and Regulation	Ripple p - p	Duty Cycle	Average Power	Usage
I. Inertial							
Rate Gyro	Active 3 Axis Control	26/18 VAC +20VDC ± 2% -20VDC ± 2% $+28 \, ^{+5.5}_{-4.5}$ VDC	400 ± 0.1% 2ø - - -	- 300 MV 300 MV 300 MV	100% until stabilized in orbit	6.0 W 0.46 W 0.17 W 0.30 W	OGO
Rate Gyro	Spin Stabilized with active orientation	$+22 \, ^{+2}_{-3}$ VDC	-	200 MV	100% until normal orbit attained	4 W plus 8 W heaters	VELA
Position Gyro	Active 3 Axis Control	$+28 \, ^{+5.5}_{-4.5}$ VDC	-	300 MV	100% 60%	4.84 W 12.0 W heaters	OGO
Accelerometer	Spin Stab. Probe	+45VDC +20 -20 ± 10%	-		Command	9 MW 160 MW 160 MW	ABLE V
II. Optical							
Earth Detector	Active 3 Axis Control	+20VDC ± 1.5% -20VDC ± 1.5%	- -		100% 100%	4.35 W 4.35 W	OGO
Earth Detector	Active Spin Stab.	$+22 \, ^{+2}_{-3}$ VDC	-	200 MV	100%	3.0 W	VELA
Earth Detector	Active Spin Stab.	+26.5±4.5 VDC	-	200 MV	100%	0.75 W	COMSAT
Sun Detector	Active Spin Stab.	+15 VDC ± 1.5%	-	±2%	100%	Negligible	PIONEER
Sun Detector	Active 3 Axis Stab.	NONE	-	-	-	-	OGO
Sun Detector	Active Spin Stab.	NONE	-	-	-	-	COMSAT
III. Transducers							
Resolver	Shaft Position	115 VAC ±1.5%	400 ± 0.1%	-	100%	150 MW	OGO
Pressure Transducer	Pneumatic Press	+5 VDC ±1%	-	50 MV	100%	10 MW	OGO

TABLE II

STABILIZATION AND CONTROL
REACTION DEVICES

Device Type	Operating Mode	Required Voltage and Regulation	Required Freq. and Regulation	Ripple p - p	Duty Cycle	Average Power	Usage
I. Reaction Wheel							
Yaw Motor	Stall or Acceleration	125 ± 10VAC 135 ± 10VAC	400 cps ± 5% 400 cps ± 5%	- -	51% 51%	22.7 W	OGO
	Full Speed	125 ± 10VAC 135 ± 10VAC	400 cps ± 5% 400 cps ± 5%	- -	46% 46%	8.1 W	
Pitch or Roll	Stall or Acceleration	125 ± 10VAC 135 ± 10VAC	400 cps ± 5% 400 cps ± 5%	- -	40% 40%	6.5 W	OGO
	Full Speed	125 ± 10 VAC 135 ± 10 VAC	400 cps ± 5% 400 cps ± 5%	- -	57% 57%	3.6 W	
Yaw or Roll	All Modes	$+22^{+2}_{-3}$ VDC	-	200 MV	100%	3.0 W	VELA
II. Solenoids							
Yaw, Pitch, or Roll	Acquisition Mode	26^{+5}_{-4} VDC	-	200 MV	100%	3.4 W	OGO
	Orbit Mode	26^{+5}_{-4} VDC	-	200 MV	0.02%	0.7 MW	
Radial or Axial	Acquisition Mode	26 ± 4.5 VDC	-	400 MV	Command	4.2 W (on)	COMSAT
	Orbit Mode	26 ± 4.5 VDC	-	400 MV	Command	4.2 W (on)	
Yaw, Pitch, or Roll	All Modes	22^{+2}_{-3} VDC	-	200 MV	Command	12.5 W (on)	VELA
Roll	Spin-up	16 ± 0.5 VDC	-	-	0.06%	1.0 MW	PIONEER
III. Thrusters							
Heaters	Despin	22^{+2}_{-3} VDC	-	200 MV	Command	33.0 W	VELA
	ΔV	22^{+2}_{-3} VDC	-	200 MV	Command	132.0 W	
IV. Motors							
Solar Array or OPEP Drive Motors	De-energized	125/135 ± 10VAC	400 cps ± 5%	-	90%	20 MW	OGO
	Accelerating	125/135 ± 10VAC	400 cps ± 5%	-	3%	170 MW	
	Full Speed	125/135 ± 10VAC	400 cps ± 5%	-	7%	213 MW	

TABLE III

STABILIZATION AND CONTROL
ELECTRONICS

Circuit Type	Function	Required Voltage and Regulation	Required Freq. and Regulation	Ripple p - p	Duty Cycle	Average Power	Usage
I. Digital **Electrical Integration Assembly**	Input to ADCS*	+26.5 ± 4.5 VDC	-	200 MV	100%	100 MW	COMSAT
		+10 VDC ± 3%	-	200 MV	100%	200 MW	
		+6 VDC ± 3%	-	200 MV	100%	3 MW	
* **Attitude Determination and Control System**	Control ACS	+15 VDC ± 3%	-	200 MV	100%	150 MW	COMSAT
		-15 VDC ± 3%	-	200 MV	100%	150 MW	
		+6 VDC ± 3%	-	200 MV	100%	350 MW	
		-6 VDC ± 3%	-	200 MV	100%	350 MW	
Control Electronics Assembly	Control ACS	+22 $^{+2}_{-3}$ VDC	-	200 MV	100%	14 W	VELA
Valve Drivers	De-Energized	+28 $^{+5.5}_{-4.5}$	-	400 MV	99.98%	11 MW	OGO
	Energized	+28 $^{+5.5}_{-4.5}$ VDC	-	400 MV	0.02%	0.7 MW	
Reference Signal	Horizon Scanner Demodulator	+20 VDC ± 1.5%	-	300 MV	100%	40 MW	OGO
		+10 VDC ± 1.5%	-	600 MV	100%	40 MW	
		+28 $^{+5.5}_{-4.5}$ VDC	-	600 MV	100%	40 MW	
Drive Electronics	Solar Array or OPEP Drive	115 VAC ± 2%	2461 cps ± 0.1%	-	100%	950 MW	OGO
		+20 VDC ± 1.5%	-	300 MV	100%	100 MW	
		+10 VDC ± 3%	-	300 MV	100%	60 MW	
		28 $^{+5.5}_{-4.5}$ VDC	-	300 MV	10%	1.4 W	
		28 VAC ± 3%	400 cps ± 5%	-	10%	750 MW	
II. Analog Horizon Scanner Central Electronics	Process Horizon Sensor Signals	+20 VDC ± 1.5%	-	300 MV	100%	4.35 W	OGO
		-20 VDC ± 1.5%	-	300 MV	100%	4.35 W	
OPEP Gyro Electronics	Process Gyro Signals	+28 $^{+5.5}_{-4.5}$ VDC	-	400 MV	100%	3.54 W	OGO
Inertial Reference Unit	Provide Reference Signals	+28 $^{+5.5}_{-4.5}$ VDC	-	400 MV	Hot 4.84W Cold 16.84W	12 W	OGO
Signal Conditioner	Signal Conditioning	+10 ± 0.2% VDC	-	50 MV	5%	300 MW	VELA
Signal Conditioner	Telemetry Signal	-20 VDC ± 1.5%	-	50 MV	100%	20 MW	OGO
		+20 VDC ± 1.5%	-	50 MV	100%	50 MW	
		+10 VDC ± 1.5%	-	50 MV	100%	30 MW	
Valve Driver	Bias	-20 VDC ± 2%	-	400 MV	100%	340 MW	OGO
Yaw Motor Driver	Stall or Acceleration	125/135 ± 10VAC	400 cps ± 5%	-	51%	16.6 W	OGO
	Full Speed	125/135 ± 10VAC	400 cps ± 5%	-	46%	6.6 W	
Pitch or Roll Motor Drive	Stall or Acceleration	125/135 ± 10VAC	400 cps ± 5%	-	40%	4.9 W	OGO
	Full Speed	125/135 ± 10VAC	400 cps ± 5%	-	57%	3.3 W	
Bi-Stable Mag-Amp	De-Energized	115 VAC ± 2%	2461 cps ± 0.1%	-	50%	23 MW	OGO
	Energized	115 VAC ± 2%	2461 cps ± 0.1%	-	50%	350 MW	

functional requirements. In short, the lack of standardization results in part from a lack of attention to the matter; it was the consensus of opinion that if the equipment were to be redesigned or modified, it would be possible to standardize on a smaller range of electrical power requirements.

3.1.2 Scientific Experiments

Table IV lists the 58 experiments which were reviewed for the present study to date. They are classified in the table in nine basic functional categories which appear to cover the range of nearly all present or anticipated satellite experiments. It can be seen that in many cases two experiments may differ only in the range of the parameters they measure.

It appears that the general practice with respect to power for scientific experiments has been to provide the experiment with the nominal spacecraft bus voltage, leaving any required conversion, inversion, or additional regulation to be performed within the experiment. This practice simplifies the definition of interfaces and undoubtedly expedites the overall program, but at the cost of considerable waste of power. It is not unreasonable to estimate that half the power supplied to the experiments has been wasted in power conditioning equipment within the experiment package.

Table V summarizes the electrical power requirements for each of the experiment packages listed. It is hoped that additional data for this table will be available during the next quarter, but from the data shown here it is clear that the variety of requirements is greater than for the stabilization and control equipment. Not only is there a wide range, but in some cases, the requirements differ so slightly (for example, different experiments require 5, 6, 7, 8, 9, and 10 volts respectively) that it seems very probable that some standardization would be possible.

From this cursory review it is evident that the standardization of power requirements for scientific experiments should be investigated in considerable detail. It is planned that part of the work during the third quarter of the study will be to define feasible and reasonable standard voltages and power characteristics for scientific experiments.

TABLE IV

CLASSIFICATION OF EXPERIMENTS

I.	Radio Frequency		
	1)	#5001 Radio Astronomy - 2.5 mc cosmic noise	OGO-C
	2)	#5002 VLF Propagation - 0.2 -100 kc	OGO-C
	3)	Range and Range Rate 2270 mc	OGO-C
	4)	#PC-1.05 Radio Propagation - Stanford	Pioneer
	5)	#4917 - VLF Noise and Propagation 0.2 to 100 kc	OGO-A
	6)	#4918 - Radio Astronomy 2-4 mc	OGO-A
II.	Audio Frequency		
	1)	#5003 Whistlers and Audio Frequency Electromagnetic Waves 500 cps - 18 kc	OGO-C
III.	Magnetic Fields		
	1)	#5005 Low Frequency Magnetic Field Fluctuations	OGO-C
	2)	#5006 Rubidium Vapor Magnetometer - Magnetic Field Survey	OGO-C
	3)	#PC-1.02 Magnetometer - GSFC	Pioneer
	4)	Flux Gate Magnetometer	Able V
	5)	Spin Coil Magnetometer	Able V
	6)	#4910 Low Frequency Magnetic Field Variations 0.01 cps to 3 kc	OGO-A
	7)	#4911 Magnetic Field Strength and Direction 3γ to 0.14 gauss	OGO-A
IV.	Plasma Measurements		
	1)	#PC-1.03 Plasma Probe - MIT	Pioneer
	2)	#PC-1.08 Plasma Probe - ARC	Pioneer
	3)	Plasma Probe	Able V
	4)	#4902 Plasma (Electronstatic Analyzer) 100 ev to 200 Kev	OGO-A
	5)	#4903 Plasma (Faraday Cup) 100 ev to 10 Kev	OGO-A

TABLE IV (CONTINUED)

CLASSIFICATION OF EXPERIMENTS (Cont.)

V.	Light Frequencies		
	1)	#5012 Airglow and Aurora Photometer	OGO-C
	2)	#5013 Lyman Alpha and U.V. Airglow 1216-1550Å	OGO-C
	3)	#5014 Ultraviolet Spectra of the Earth's Atmosphere 1100 to 3300Å	OGO-C
	4)	#5019 Ionosphere Composition and Solar U.V. Flux	OGO-C
	5)	#5020 Solar U.V. Emissions 170-1700 Å	OGO-C
	6)	#4919 Geocoronal Lyman-Alpha Scattering (1216Å)	OGO-A
	7)	#4920 Gegenschein Photometry	OGO-A
VI.	Particle Radiation		
	1)	#5008 Low Energy Proton - Alpha Telescope Protons 0.5 - 40 mev - Alpha 2-160 mev	OGO-C
	2)	#5009 Galactic and Solar Cosmic Rays 40 mev - 1 bev	OGO-C
	3)	#5010 Corpuscular Radiation - Electrons 40 kev and > 120 kev	OGO-C
	4)	#5011 Low Energy Trapped Radiation and Auroral Particles 10 - 100 kev electrons, 100 kev to 10 mev protons, 10 kev to 10 mev total flux	OGO-C
	5)	#5007 Cosmic Ray and Polar Region Ionization	OGO-C
	6)	#5017 Neutral Particle Measurements (density, temp)	OGO-C
	7)	#5021 Solar X-Ray Emissions 0.5-Å, 2-8Å, 8-16Å, 44-60Å	OGO-C
	8)	#PC-1.04 Cosmic Ray - Univ. Chicago	Pioneer
	9)	#PC-1.06 Cosmic Ray - GRCSW	Pioneer
	10)	Solid State Detector - Proton Flux 0.5 - 10 mev	Able V
	11)	Low Energy Scintillometer - Electron and Proton	Able V
	12)	Ion Chamber and Geiger Counter	Able V
	13)	Cosmic Ray Telescope	Able V
	14)	Scintillation Spectrometer - Protons	Able V

TABLE IV (CONTINUED)

CLASSIFICATION OF EXPERIMENTS (Cont.)

	15)	#4901 Solar Protons 2-100 mev	OGO-A
	16)	#4904 - Positron Search and Gamma Rays	OGO-A
	17)	#4905 - Trapped Radiation (Scintillation Counter) Electrons and Protons	OGO-A
	18)	#4906 - Isotopic Abundance and Galactic Cosmic Rays	OGO-A
	19)	#4907 - Cosmic Ray Spectra and Fluxes 0.3 mev - 4 bev	OGO-A
	20)	#4908 - Trapped Radiation (Geiger Counter)(electrons 40 kev - 2 bev)(protons 0.5 mev - 23 mev)	OGO-A
	21)	#4909 - Trapped Radiation (Electron Spectrometer) 50 kev to 4 mev	OGO-A
	22)	#4912 Thermal Charged Particles - electrons and ions 0.2 ev to μ kev	OGO-A
	23)	#4913 - Thermal Charged Particles - ± ions low energy	OGO-A
	24)	#4914 - Electron Density by RF Propagation - electron density	OGO-A
VII.	Mass		
	1)	#5015 Neutral and Ion Mass Spectrometer 1 - 50 AMU	OGO-C
	2)	#5016 Positive Ion Composition 1 - 45 AMU	OGO-C
	3)	#4915 - Atmospheric Composition 1 - 45 AMU Positive Ions	OGO-A
VIII.	Meteorites		
	1)	#5018 Micrometeorites - spatial density and mass distribution 10^{-13} to 10^{-19} grams	OGO
	2)	#PC-1.07 Micrometeoroid Detector - ARC	Pioneer
	3)	Micrometeorites	Able V
	4)	#4916 - Micron Dust Particles (mass, velocity, direction, intensity, time and spatial variations)	OGO-A
IX.	Biological or Mineral Detectors		
	1)	Microbiological Detector	Surveyor

TABLE V

EXPERIMENTS

Experiment Identification	Required Voltage and Regulation	Required Freq. and Regulation	Ripple p - p	Duty Cycle	Average Power	Usage
I. Stanford Radio Propagation	-3 VDC	-	-	?	1.4 W	PIONEER
	+2.5 VDC	-	-	?		
	+5 VDC	-	-	?		
	+12 VDC	-	-	?		
II. 5003 Whistlers and Audio Frequency Electromagnetic Waves - 500 cps - 18 cps						
III. Magnetometer (UCLA)	+6 VDC ± 0.1%	-	0.1%	Command	168 MW	OGO
	+8 VDC ± 1%	-	20 MV	Command	960 MW	
	-8 VDC ± 1%	-	20 MV	Command	120 MW	
	+20 VDC ± 0.1%	-	0.1%	Command	800 MW	
	-20 VDC ± 1%	-	20 MV	Command	200 MW	
	+3 VDC ± 1%	-	20 MV	Command	300 MW	
Spin Coil Magnetometer	+10 VDC ± 1%	-	1%	100%	100 MW	ABLE V
	-16 VDC ± 1%	-	1%	100%	120 MW	
	± 6 VDC ± 5%	-	1 MV max	100%	?	
Flux Gate Magnetometer	+6 VDC ± 1%	-	1%	100%	180 MW	ABLE V
	-6 VDC ± 1%	-	1%	100%	12 MW	
	+18 VDC ± 2%	-	(Special)	0-5 sec	3.24 W	
	+18 VDC ± 2%	-	(Battery)	0-5 sec	72 W	
IV. MIT Plasma Probe	±6 VDC	-	?		Lo Avg 0.9 W Hi Avg 2.1 W Peak 7.9 W	PIONEER
	±12 VDC	-	?			
	±10 VDC	-	?			
	-25 VDC	-	?			
	-30 VDC	-	?			
	+75 VDC	-	?			
ARC Plasma Probe	-3 VDC	-	?	?	1.5 W	PIONEER
	± 6 VDC	-	?	?		
	±12 VDC	-	?	?		
	-18 VDC	-	?	?		
	± 150 VDC	-	?	?		
	±165 VDC	-	?	?		
V. White Light Coronagraph (*3 KV varied on command with superimposed variable 1 KV)	± 10 VDC ± 0.1%	-	0.1%	100%	10 W	AOSO
	±3VDC ± 0.1%	-	0.1%	100%		
	±3000 VDC*	-	1%	30 W max		
VI. Proton Spectrometer (UCLA)	+1250 VDC ± 0.1%	-	0.1%	Command	250 MW	OGO
	-20 VDC ± 1%	-	20 MV	Command	90 MW	
	+3 VDC ± 1%	-	20 MV	Command	177 MW	
	+7 VDC ± 1%	-	20 MV	Command	1.3 W	
	-7 VDC ± 1%	-	20 MV	Command	262 MW	
	-6 VDC ± 0.1%	-	0.1%	Command	150 MW	
	+5.1 VDC ± 0.1%	-	0.1%	Command	122 MW	
	-3 VDC ± 1%	-	20 MV	Command	118 MW	

TABLE V (CONTINUED)

EXPERIMENTS

Experiment Identification	Required Voltage and Regulation	Required Freq. and Regulation	Ripple p - p	Duty Cycle	Average Power	Usage
VI. (Cont.)						
GRCSW Cosmic Ray	+1200 VDC ± 0.1%	-	0.1%		1.5 W	PIONEER
	+3.1 VDC ± 1%	-	1%			
	+12 VDC ± 1%	-	1%			
Cosmic Ray Telescope	+6 VDC ± 1%	-	1%	100%	240 MW	ABLE V
Ion Chamber and Geiger Counter	+6 VDC ± 1%	-	1%	100%	90 MW	ABLE V
Solid State Detector	+6 VDC ± 1%	-	1%	100%	55 MW	ABLE V
	+6 VDC ± 1%	-	1%	100%	1.6 MW	
Scintillation Spectrometer	+1200 VDC ± 0.1%	-	0.1%	100%	100 MW	ABLE V
	+16 VDC ± 1%	-	1%	100%	240 MW	
	-16 VDC ± 1%	-	1%	100%	20 MW	
	+10 VDC ± 1%	-	1%	100%	12 MW	
	+6 VDC ± 1%	-	1%	100%	15 MW	
	-6 VDC ± 1%	-	1%	100%	23 MW	
	18 ± 3 VDC	-	-	one 1/2 sec pulse	2.5 W	
	18 ± 3 VDC	-	-		54 W	
	+10 ± 0.5 VDC	-	200 MV max	?	?	
	+3 ± 0.5 VDC	-	200 MV max	?	?	
	+8 ± 0.5 VDC	-	200 MV max	?	?	
Low Energy Scintillometer	+1200 VDC ± 0.1%	-	0.1%	100%	100 MW	ABLE V
	+16 VDC ± 1%	-	1%	100%	208 MW	
	+6 VDC ± 1%	-	1%	100%	132 MW	
Cosmic Ray and Gamma Ray	+10 VDC ± 0.1%	-	0.1%	100%	650 MW	OSO-C
	+1200 VDC ± 0.1%	-	0.1%	100%	50 MW	
X-Ray Instrument	+10 VDC ± 0.1%	-	0.1%	100%	450 MW	OSO-C
	+1200 VDC ± 0.1%	-	0.1%	100%	50 MW	
Primary Electron Detector	+10 VDC ± 0.5%	-	0.5%	100%		OGO-E
	+2.5 VDC ± 2%	-	0.2%	100%	1 W	
	+1350 VDC ± 0.1%	-	0.1%	100%		
VII.						
VIII. Micrometeorite	+6 VDC ± 1%	-	1%	100%	72 MW	ABLE V
IX. Microbiological Detector	± 10 VDC ± 0.25%	-	2%	100%	200 MW	VOYAGER
	+10 VDC ± 1%	-	2%	1W on 2 sec	[illegible]	

3.2 POWER SYSTEM CHARACTERISTICS

A spacecraft electrical power system can be simply defined in terms of the characteristics of the power available on its main power bus. These are basically the following:

- Voltage
- Voltage regulation
- Average or peak power
- Ripple and noise

Table VI lists these characteristics for eight different satellites. The range of values shown here will probably cover the requirements for most future unmanned spacecraft. For this reason, a detailed examination of these eight systems offers a promising avenue to explore the possibilities of standardization.

3.3 ANALYSIS OF EXISTING POWER SYSTEMS

Figures 1 through 8 are overall block diagrams showing the electrical power system configuration used in each of the eight satellites listed in Table VI. In each case the system makes use of solar cell arrays combined with batteries, so that in general the same functions must be performed and therefore the same basic elements are found. The differences result to a large extent from the varying emphasis on one or another requirements, such as the very long lifetime required for Comsat, the intermittent heavy load in Relay, the stress on off-the-shelf designs for Vela, the heavy loads and complex equipment on EOGO and POGO, and so on.

Another major influence on electrical power system design is the planned orbit for the spacecraft. Table VII indicates the characteristics of the orbits for the eight satellites discussed here. Orbit characteristics affect power system design by dictating such important parameters as length and frequency of eclipses, integrated radiation flux, and range of angles of incidence of solar radiation. These parameters are reflected in battery cycling requirements and in power control requirements.

TABLE VI

LOAD BUS POWER

Unregulated Bus Volts	Unregulated Bus %	Load Bus Power Watts	Batteries: Number Cells	Batteries: Amp Hours	Batteries: Type	Load Bus: Impedance	Load Bus: Ripple	Load Bus: Transients	Usage	Maximum Solar Array Power
-28	-25 +10	50	21 x 2	4.0	Ni-Cd	-	-	-	TIROS	90 Watts
28	+25 -10	50	22 x 2	4.0	Ni-Cd	-	20 MV p-p	34 VDC Peak for 0.5 sec.	RELAY	90 Watts
28	+20 -16	300	22 x 2	12.0	Ni-Cd	< 0.5 Ω	0.3 V p-p	≤ 50 VDC Peak for < 10 msec.	OGO	600 Watts
28	+20 -16	500	22 x 2	12.0	Ag-Cd	0.5 to 3Ω	0.3 V p-p	≤50 VDC Peak for < 10 msec.	POGO	600 Watts
28	+18 -16	55	18	1.0	Ag-Zn	< 13Ω	150MV p-p	±2.25 V Peak	PIONEER	81 Watts
22	+10 -15	75	16 x 2	6.0	Ni-Cd	< 1.0Ω	200 MV p-p	± 2.20 V Peak	VELA	100 Watts
18	+28 -22	35	14 x 2	4.0	Ni-Cd (F type)	< 0.4Ω	0.5 V p-p		ABLE V	40 Watts
28	+15 -15	105	20	6.0	Ni-Cd	< 1.0Ω	< 5MV 0-10KC	≤50 VDC Peak for < 10 msec.	COMSAT	161 Watts

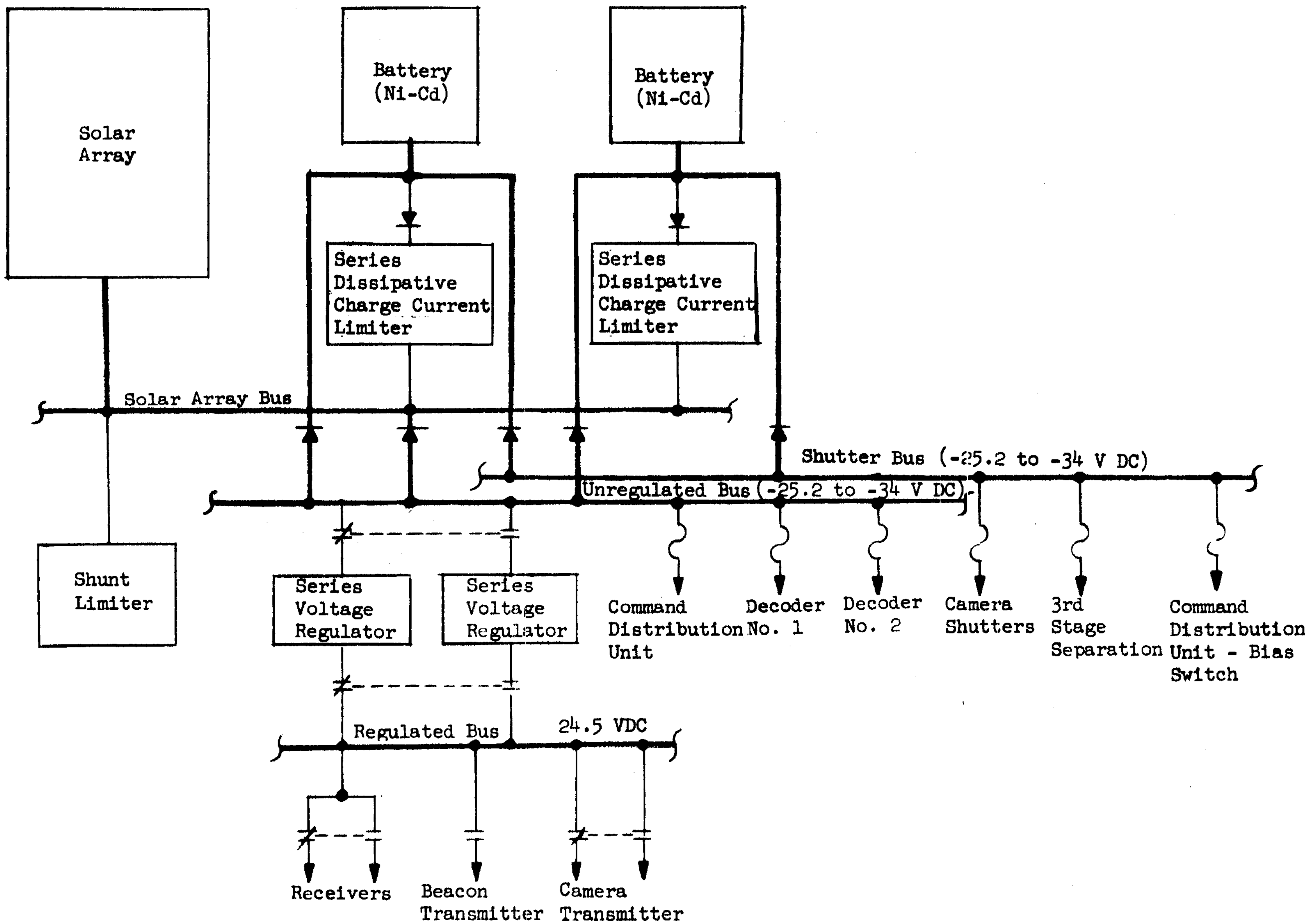

Figure 1
Tiros, Electric Power Subsystem

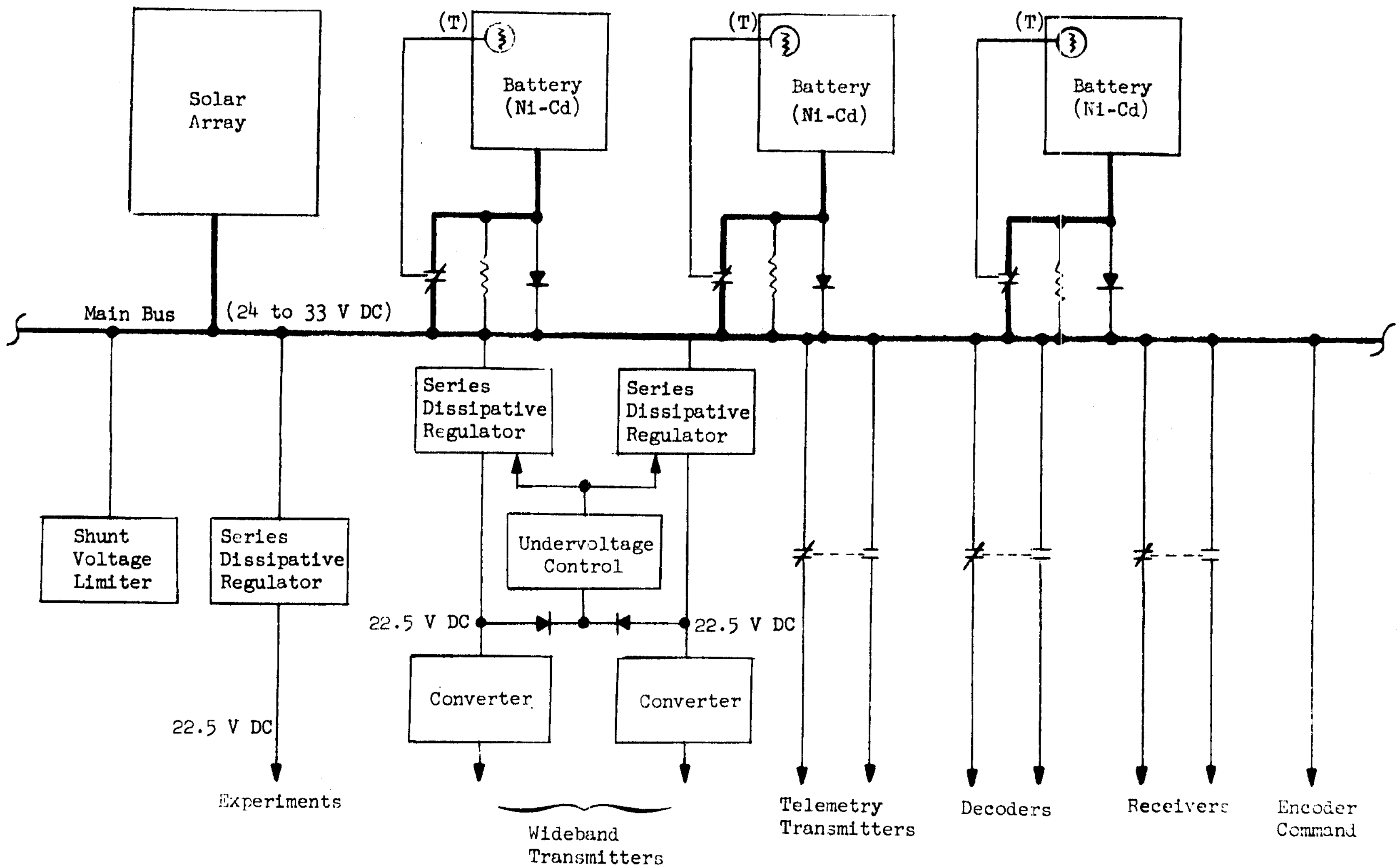

Figure 2

Relay, Electric Power Subsystem

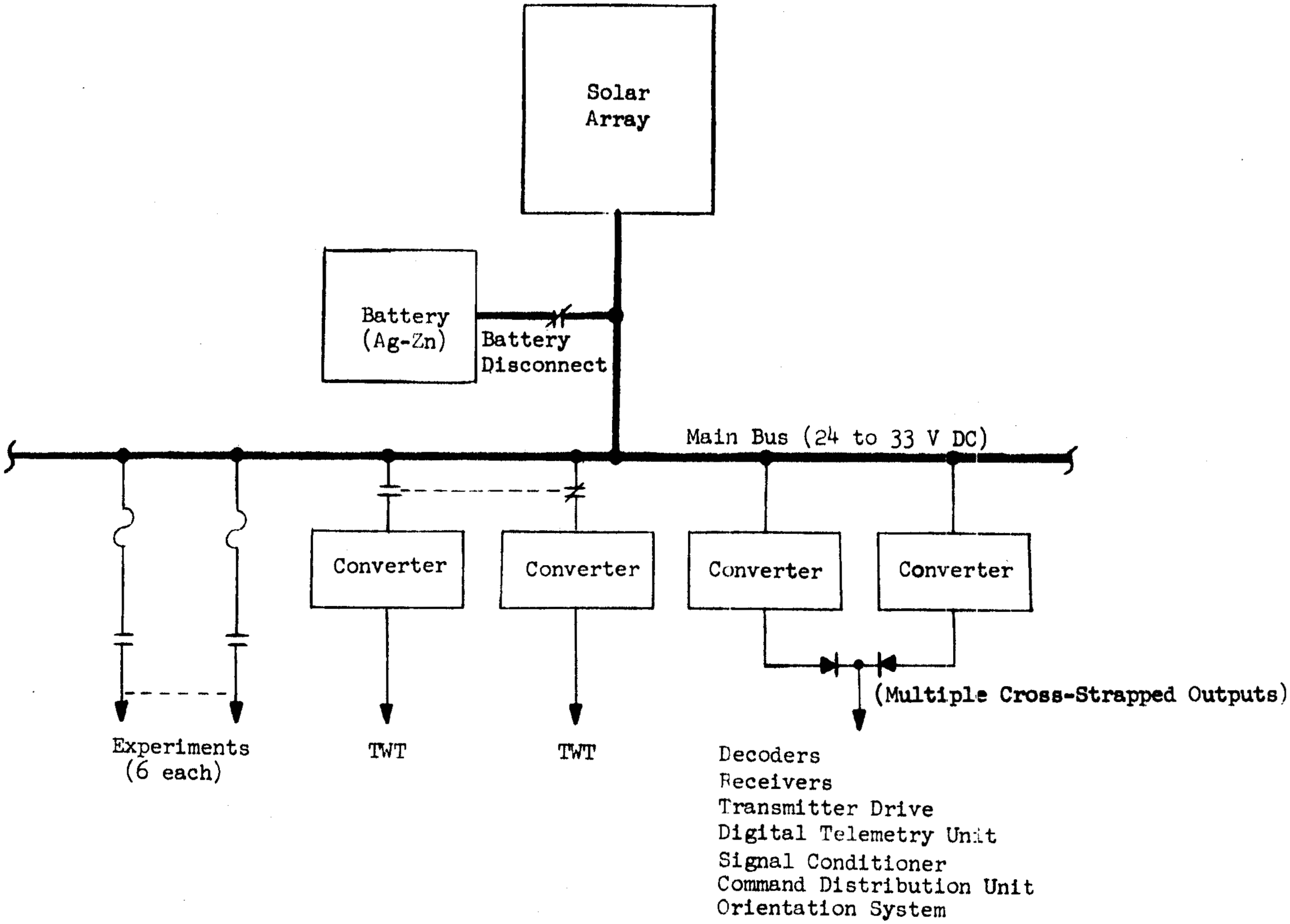

Figure 3
Pioneer, Electric Power Subsystem

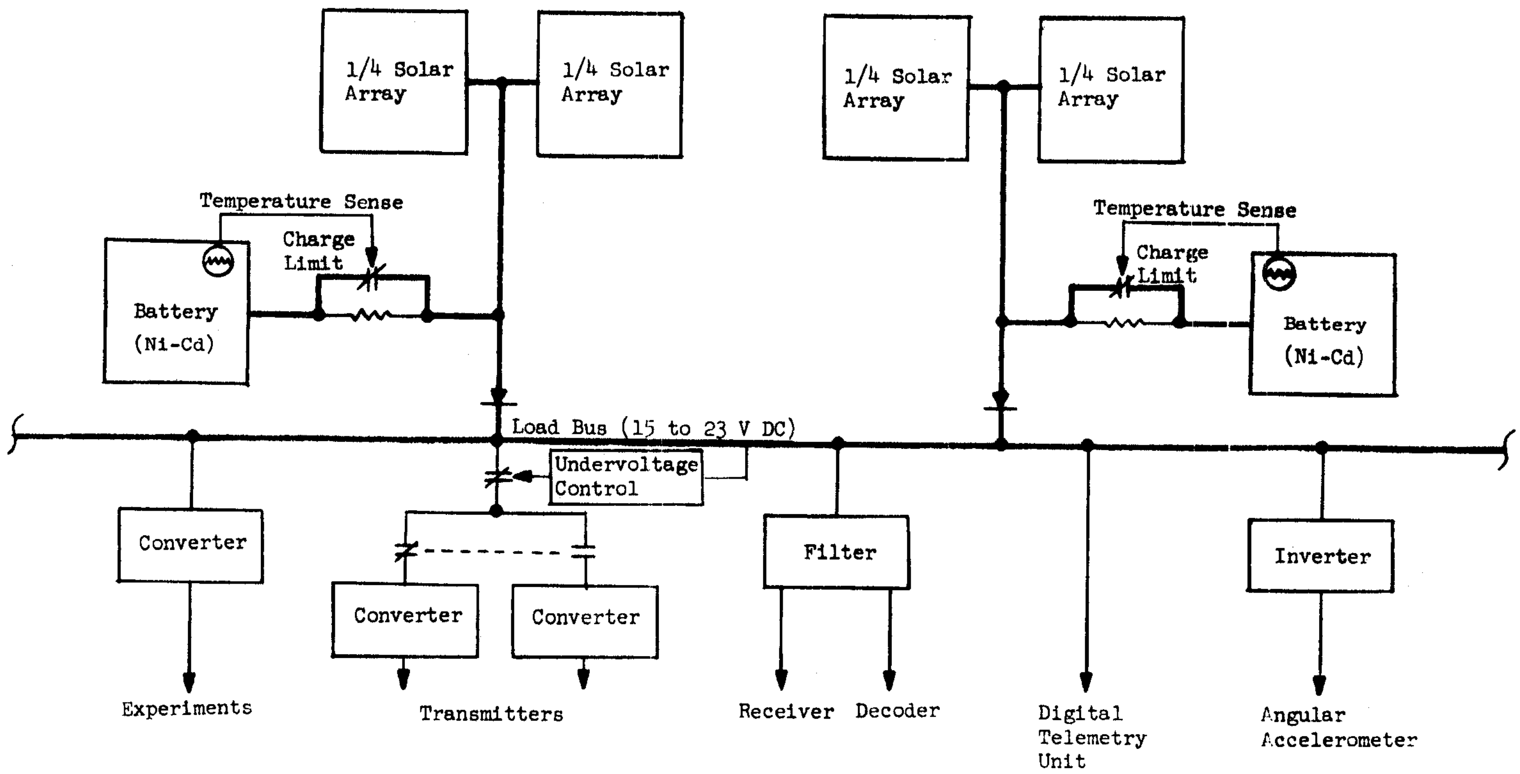

Figure 4
ABLE V, Electric Power Subsystem

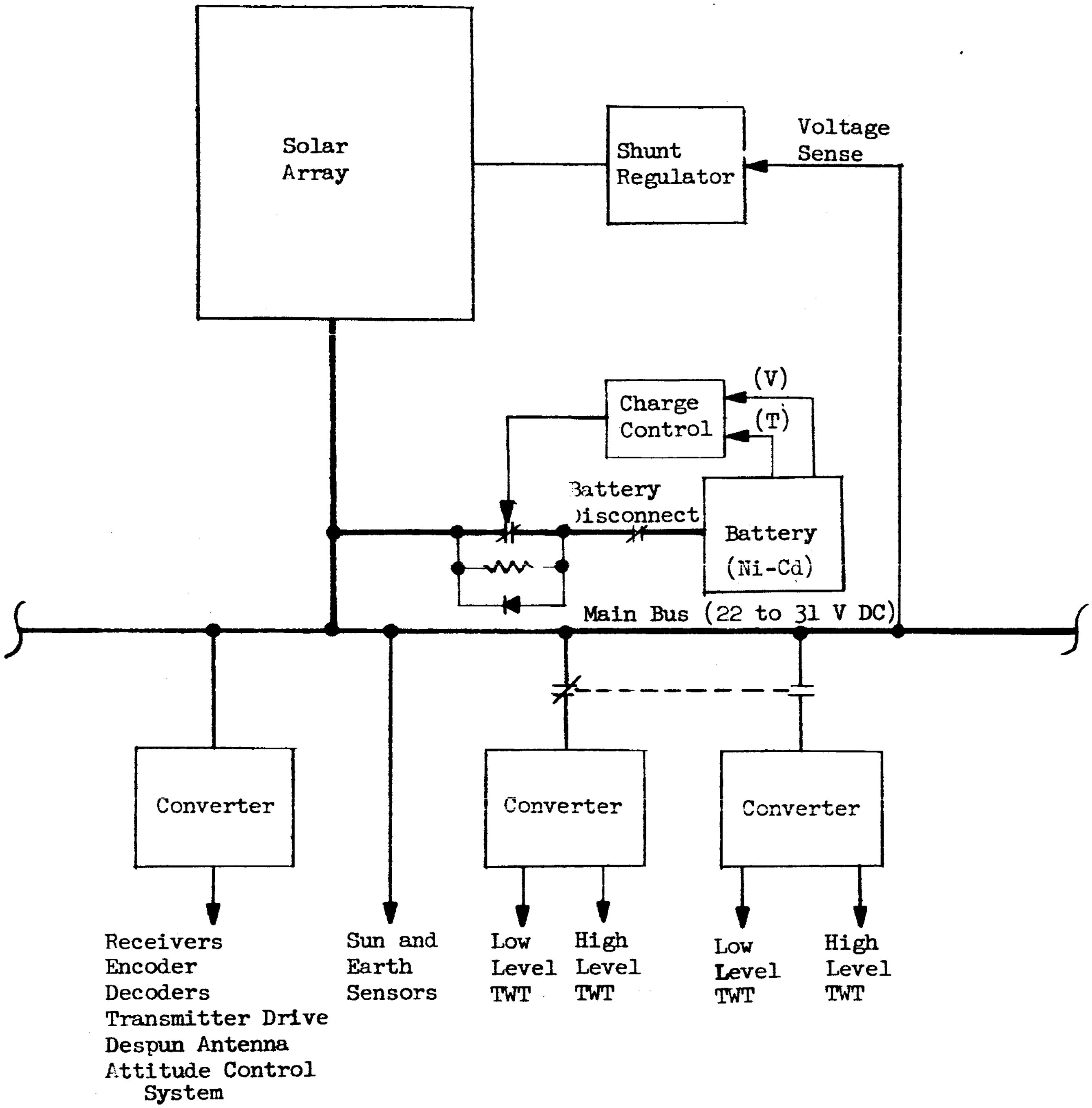

Figure 5

COMSAT, Electric Power Subsystem

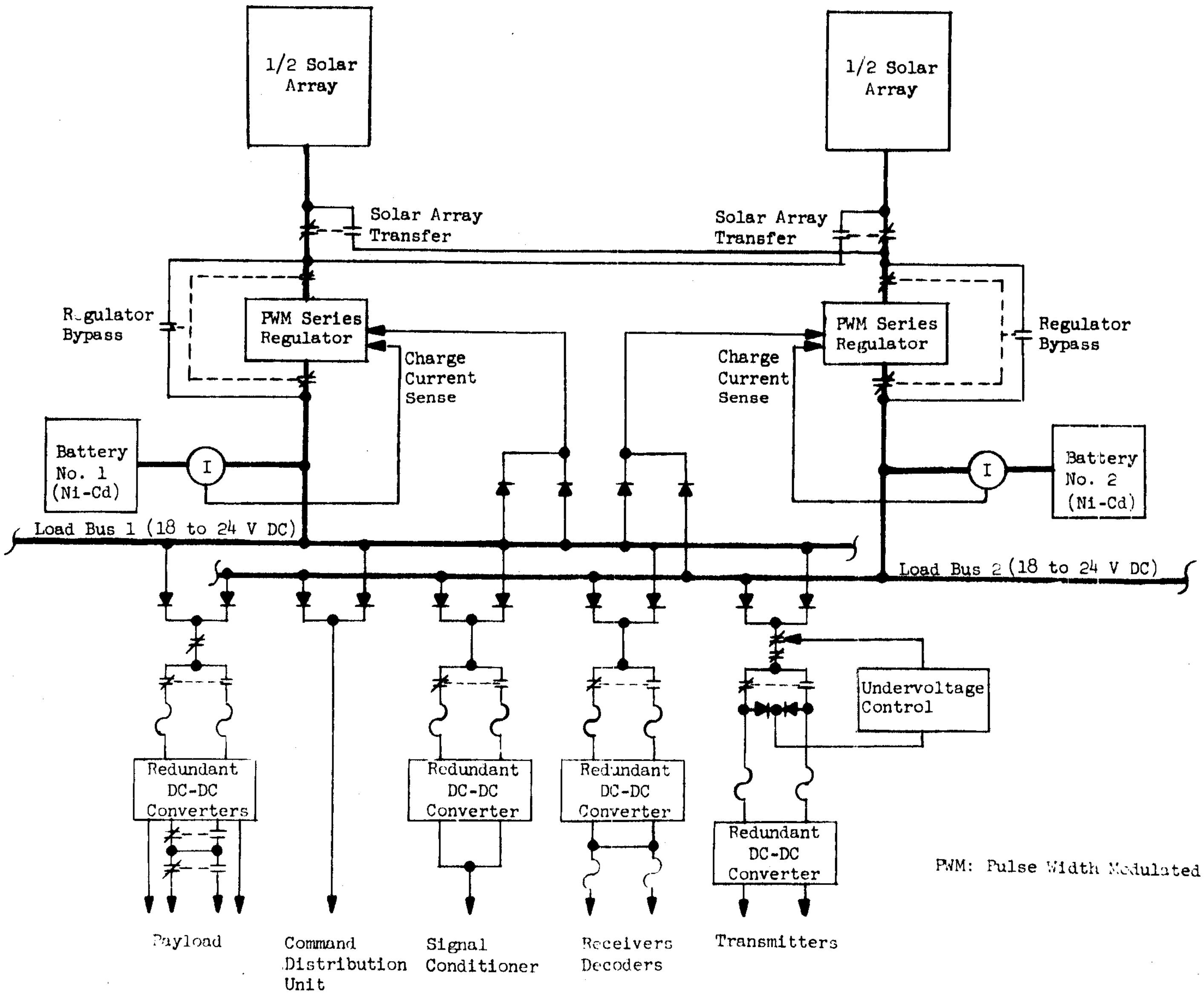

Figure 6

VELA, Electric Power Subsystem

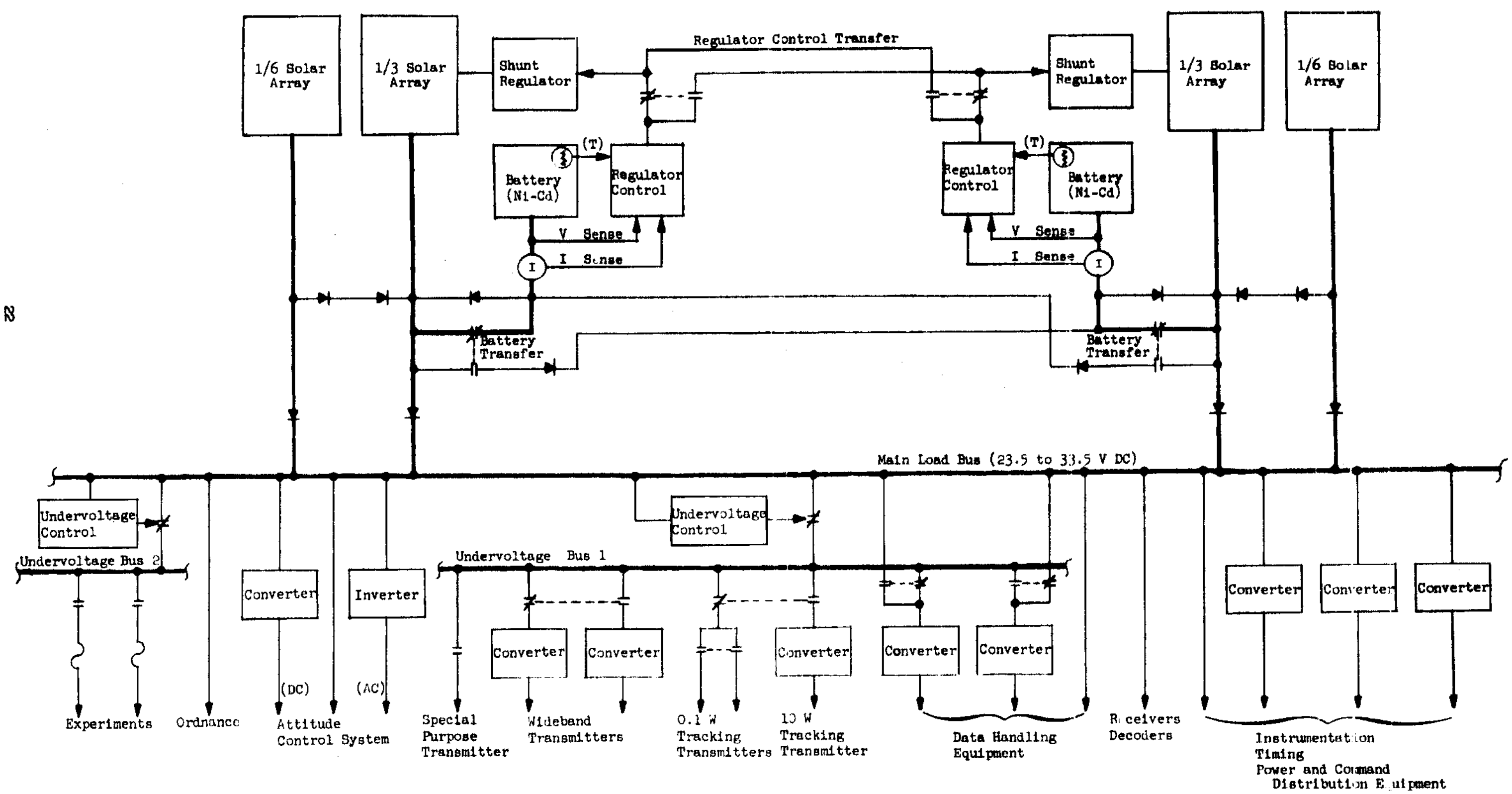

Figure 7

OGO Electric Power Subsystem

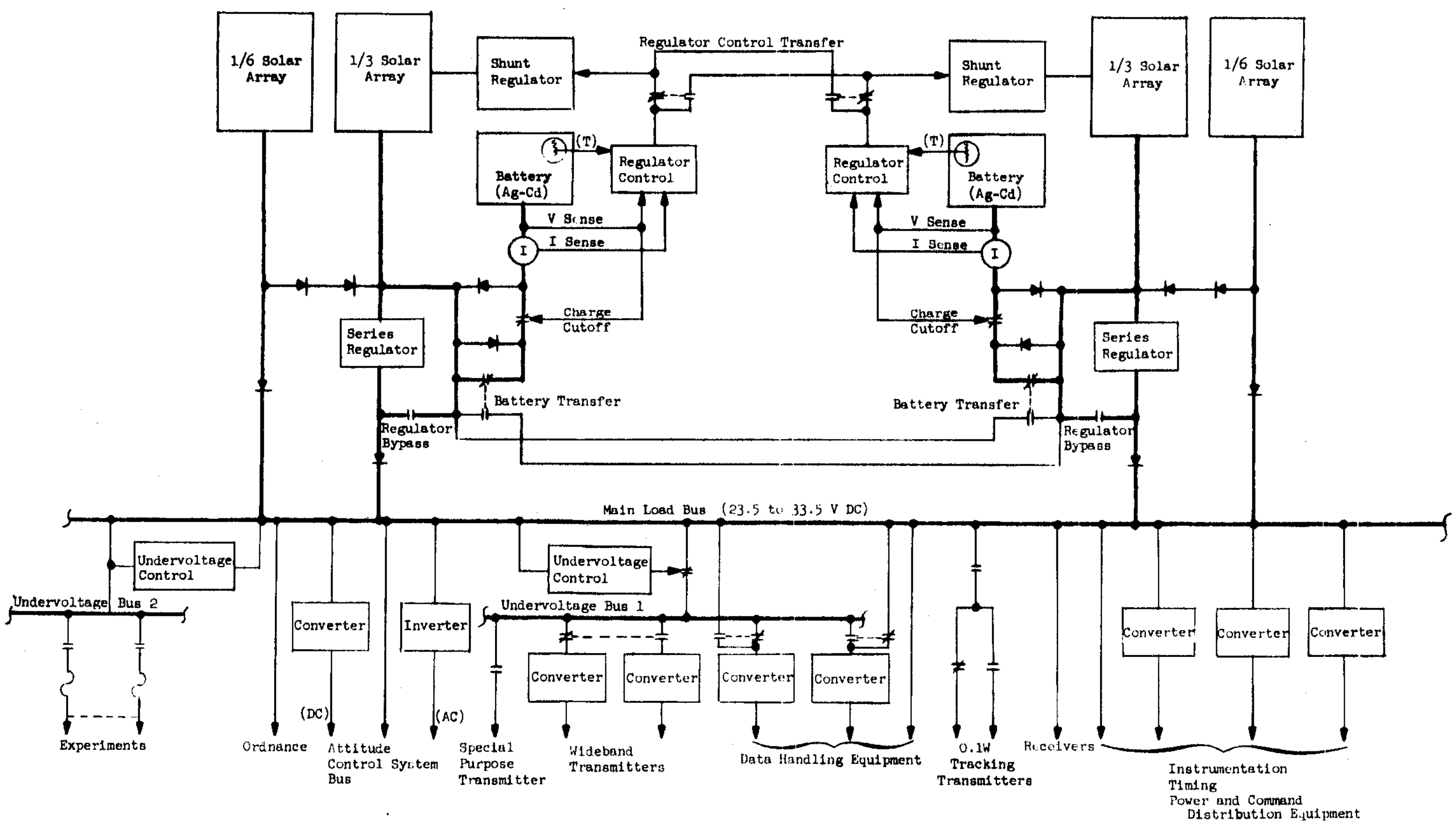

Figure 8
POGO, Electric Power Subsystem

TABLE VII

ORBITAL CHARACTERISTICS

Program	Orbit Time	Predicted Life Time	Type - Inclination
COMSAT	24 hr.	5 yr.	Equatorial - Synchronous
OGO	3839 min.	1 yr.	31° inclined
POGO	104 min.	1 yr.	Polar - 87°
PIONEER	Probe	6 mo.	Solar
RELAY	185.1 min.	1 yr.	48° inclined
VELA	110 hr.	3 yr.	31° inclined
TIROS	113.5 min.	6 mo.	Polar - 101°

3.3.1 Power Source Control

Power source control is the term applied to the function of regulating the voltage and/or current delivered by the solar array. In all cases, the voltage delivered by the array must be kept below a value which might damage spacecraft equipment; under certain conditions (emergence from eclipse, for example), the array may generate an excessive voltage for a short period of time. In addition, battery charging must be controlled to prevent overcharging of the batteries. In some cases, it is also desired to maintain bus voltage at a minimum value even when the array voltage has fallen below this value.

The types of regulation used to perform these functions are in general the following:

- o Series dissipative
- o Shunt Dissipative
- o Pulse width modulated (bucking, boost, or buck-boost).

Table VIII summarizes the methods of power source control used in the eight satellite power systems considered here.

Series Dissipative Regulation. This type of regulation requires that the input voltage be higher than the regulated output voltage. Maximum dissipation occurs at maximum load and maximum voltage difference, as shown in Figure 9. It can be seen from the figure that with an array temperature variation of 145°C, the dissipation is over 100 percent of the load, reducing efficiency below 50 percent. Nevertheless, this relatively simple type of regulation may be attractive in cases where input voltage variation, and the consequent loss in efficiency, are small. Weight of the regulator varies as a function of the power loss associated with variations in input voltage.

Shunt Dissipative Regulation. This is another dissipative type of regulator, and requires that the input voltage (i.e., the full solar array voltage) be at least equal to the desired bus voltage under the worst conditions. The advantage of partial shunt regulation as compared to a full shunt or series dissipative

TABLE VIII

POWER SOURCES CONTROLS

Usage	Battery Charge Control	Protection Feature	Battery Temperature Control	Regulator Limits	Type of Regulator
ABLE	Trickle Charge Switch	Undervoltage Bus	Thermal Control to Trickle Charge (43°C)	± 20%	None
VELA	Current Limited	Undervoltage Bus	- -	± 5%	Pulse width modulated series regulator
PIONEER	Floats on Bus	ON-OFF Battery Switch (Command)	- -	Unregulated	None
RELAY	Current Limited	Undervoltage Bus	Thermal Control to Trickle Charge 26°C to 28°C		Full shunt voltage limiter and series regulator for selected loads.
TIROS	Constant Current to Voltage Limit		- -		Full shunt voltage limiter and series regulator selected loads.
COMSAT	Voltage Limited (Individual Cell Monitoring)	Undervoltage Bus	Thermal Control to Trickle Charge	± 0.4 V	Partial shunt voltage limiter.
EOGO	Constant Current to Voltage Limit	Undervoltage Bus	Thermal Control to Trickle Charge (35°C)	± 5%	Partial shunt voltage limiter.
POGO	Constant Current to Voltage Limit	Undervoltage Bus	Stop Charging at 43°C	± 5%	Partial shunt voltage limiter.

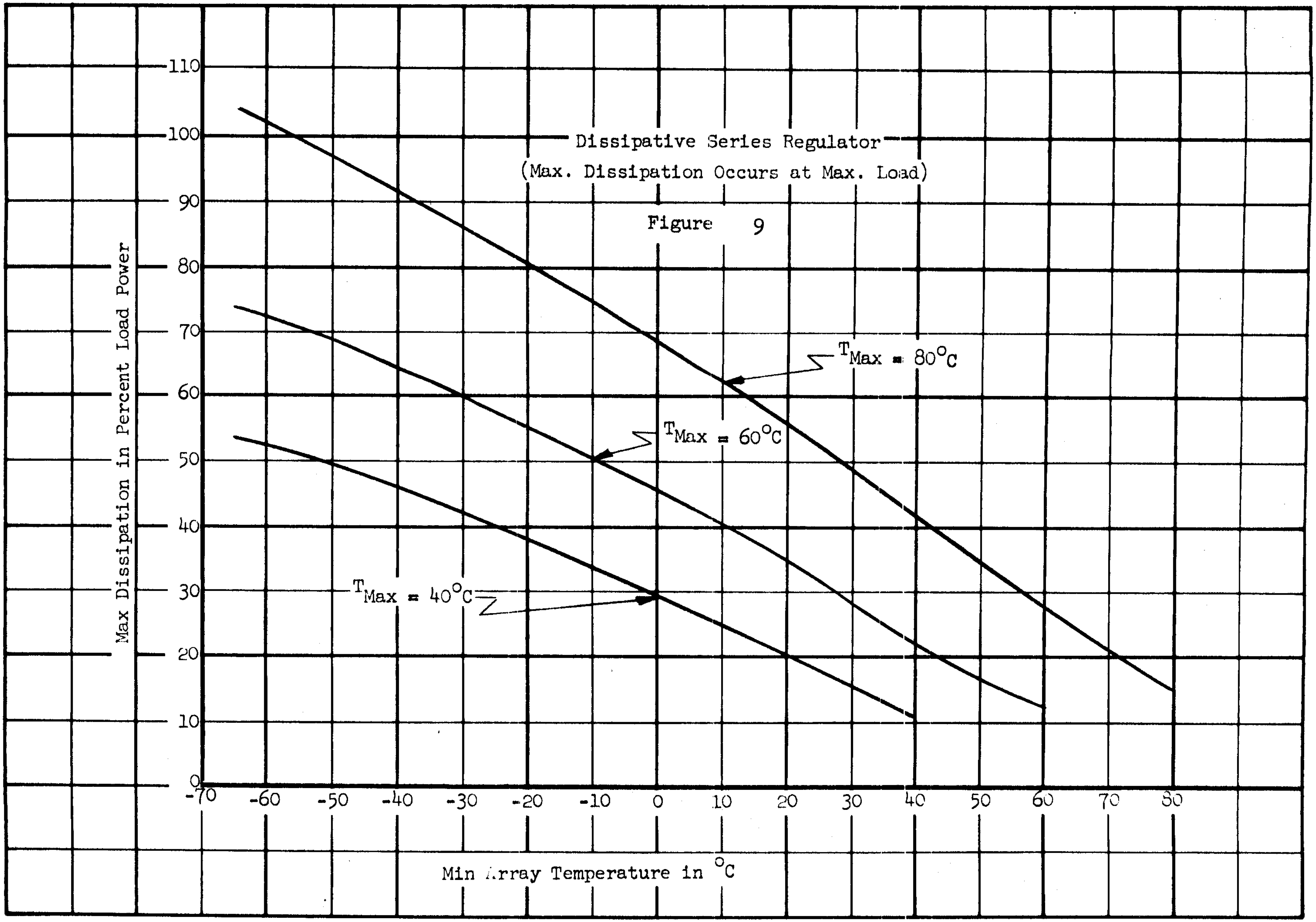
Dissipative Series Regulator
(Max. Dissipation Occurs at Max. Load)
Figure 9
TMax = 80°C
TMax = 60°C
TMax = 40°C
Max Dissipation in Percent Load Power
Min Array Temperature in °C
110
100
90
80
70
60
50
40
30
20
10
0
-70
-60
-50
-40
-30
-20
-10
0
10
20
30
40
50
60
70
80

configuration is that dissipation is reduced by having part of the solar array continuously feeding the bus, with the output of the remaining portion regulated by the shunt, which dissipates only as much power as necessary to keep the total voltage of the two portions combined below the specified value. The shunt is connected to a tap in the solar array selected in such a way that at maximum array voltage (minimum temperature), the shunt elements are driven into saturation and the array voltage is equal to the unshunted series section voltage plus the saturated drop of the shunt elements. With this type of regulation maximum dissipation occurs generally at minimum load. The graphs of Figures 10, 11, and 12, show dissipation of a partial shunt regulator as a function of minimum array temperature and minimum load for maximum array temperatures of 80, 60, and 40°C respectively.

The variation of dissipation with load becomes much less pronounced at smaller temperature variations, as does the amount of dissipation required. The effect of variation in maximum array temperature (and therefore in temperature range) can be seen by comparing the three figures. For example, the no-load curve of Figure 10 indicates 48 percent dissipation when the temperature varies from a minimum of -60°C to a rather hot 80°C maximum. If the maximum is held to 60 or 40°C, the corresponding dissipation become 38 or 32 percent respectively (for the same minimum temperature).

Figure 13 shows the relation of shunt dissipation to electrical load on the system, indicating that maximum dissipation occurs, as already noted, at minimum load for typical solar array temperature ranges. This characteristic illustrates a significant advantage of the partial shunt type of regulation, since it shows that losses are minimum when the load requirements approach the solar array power capability.

Pulse Width Modulating Regulation. Regulators of this type utilize power transistors in a switching mode with controlled duty cycle to effect the voltage regulation, and generally offer higher efficiencies than do dissipative regulators at the cost of a loss in frequency response and output impedance. They approach maximum efficiency as the difference between input and output voltages becomes smaller, which makes them suitable for power control functions. In this type of application the input and output voltages are usually similar and normally do not reach a ratio as high as 2:1. The following paragraphs discuss the characteristics of three types of pulse width modulating regulators: bucking, boost, and buck-boost.

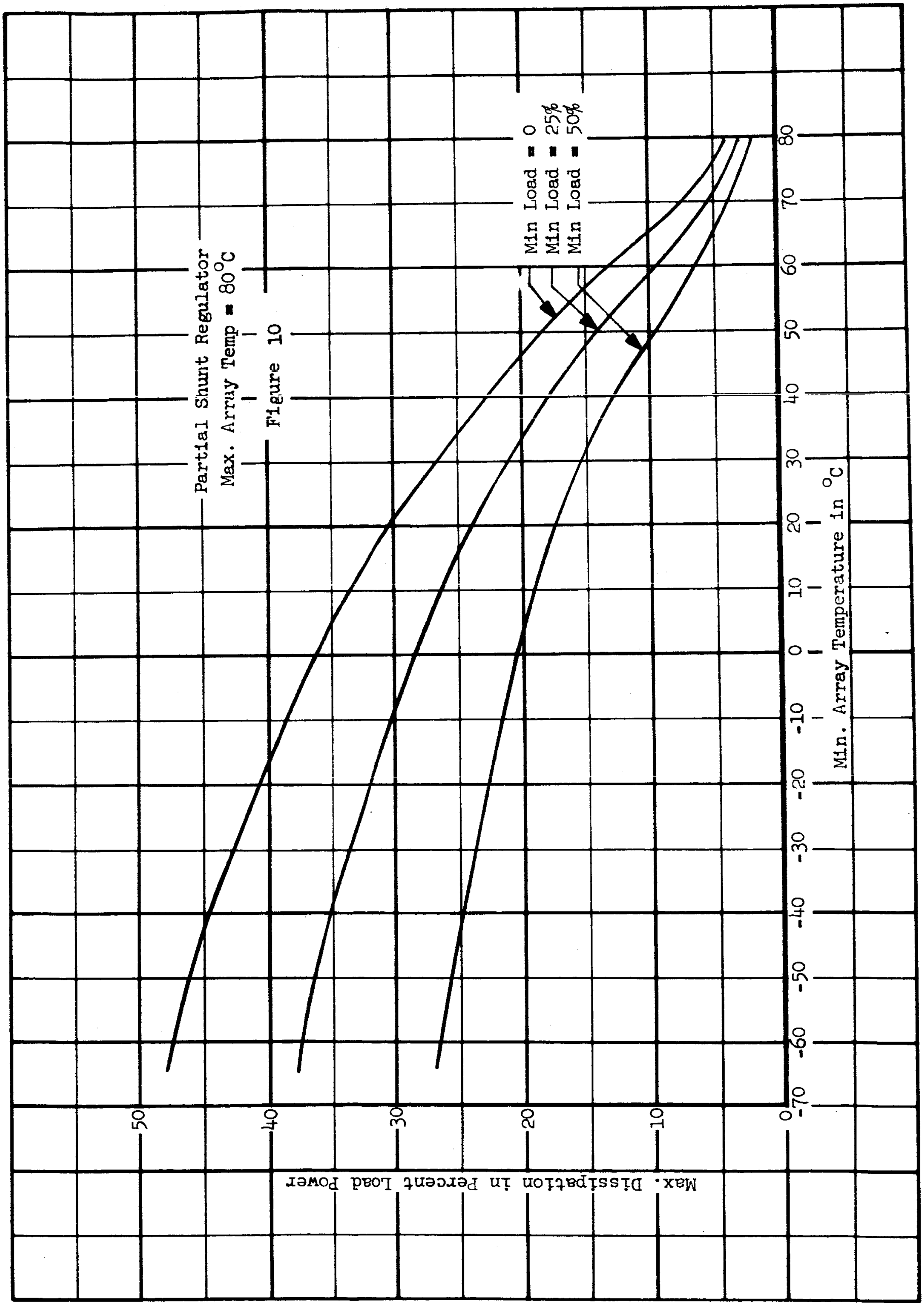

Partial Shunt Regulator
Max. Array Temp = 80°C

Figure 10

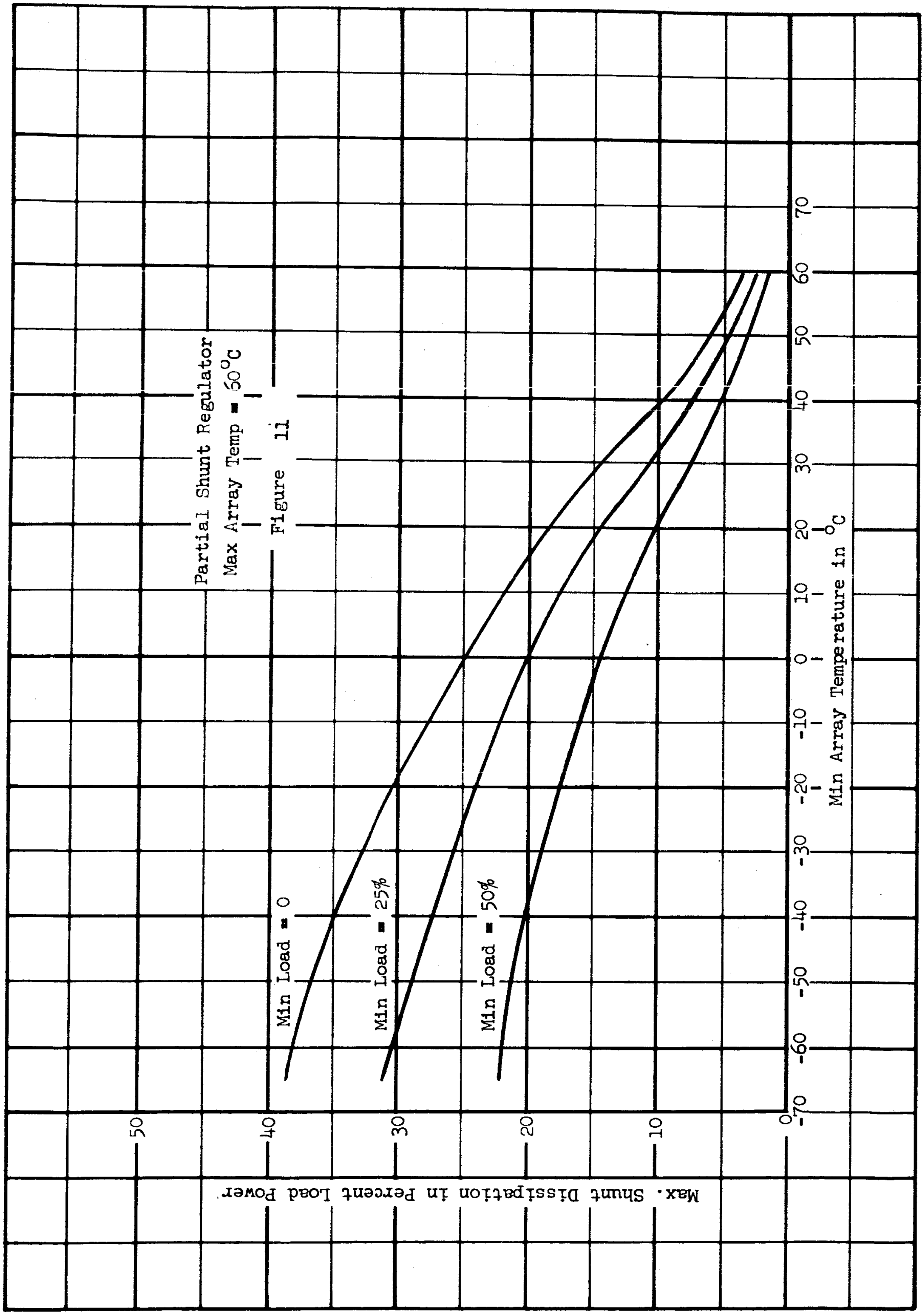
Partial Shunt Regulator
Max Array Temp = 60°C
Figure 11
Min Load = 0
Min Load = 25%
Min Load = 50%
Min Array Temperature in °C
-70
-60
-50
-40
-30
-20
-10
0
10
20
30
40
50
60
70
Max. Shunt Dissipation in Percent Load Power
0
10
20
30
40
50

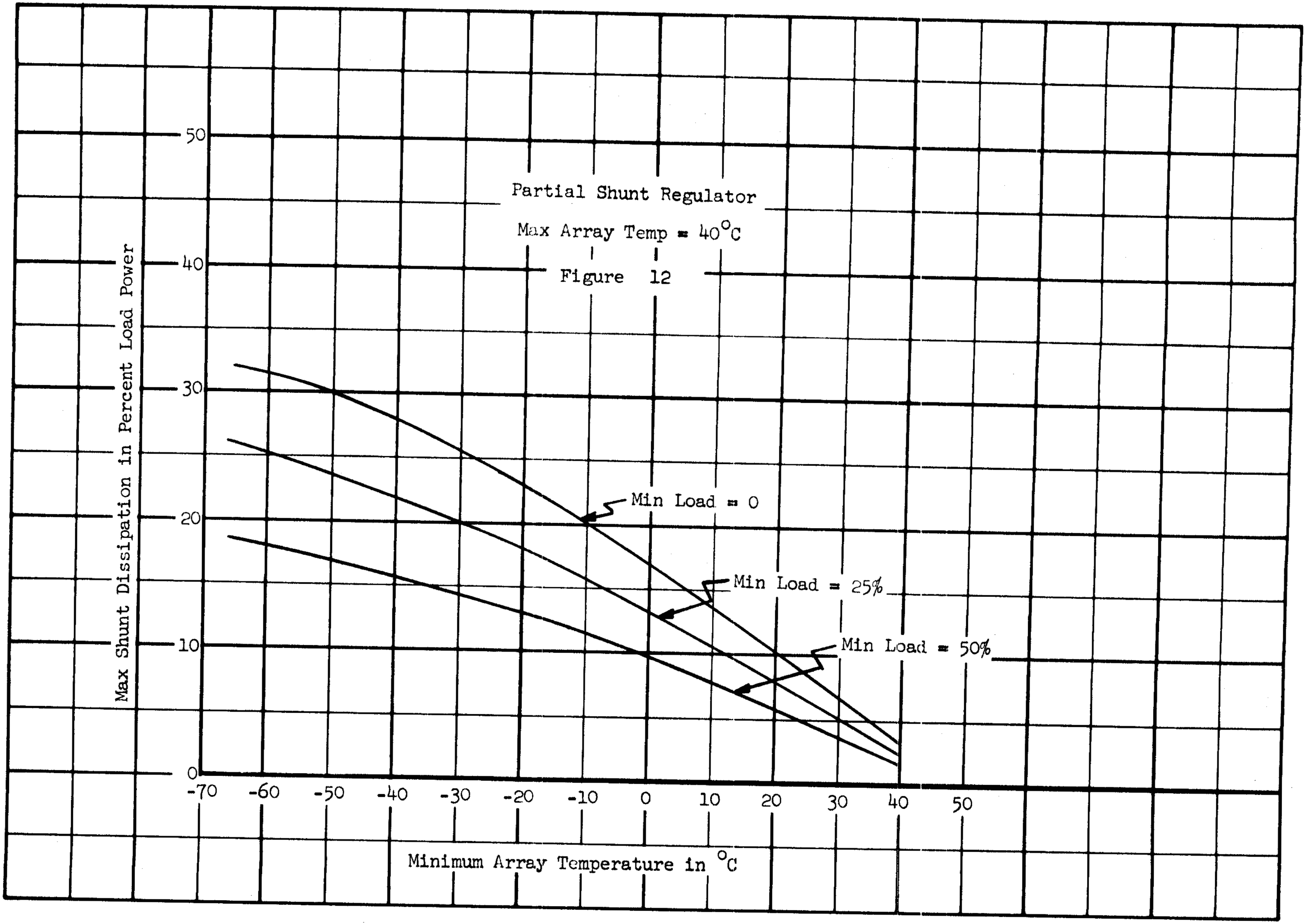
Partial Shunt Regulator
Max Array Temp = 40°C
Figure 12
Min Load = 0
Min Load = 25%
Min Load = 50%
Max Shunt Dissipation in Percent Load Power
0
10
20
30
40
50
-70
-60
-50
-40
-30
-20
-10
0
10
20
30
40
50
Minimum Array Temperature in °C

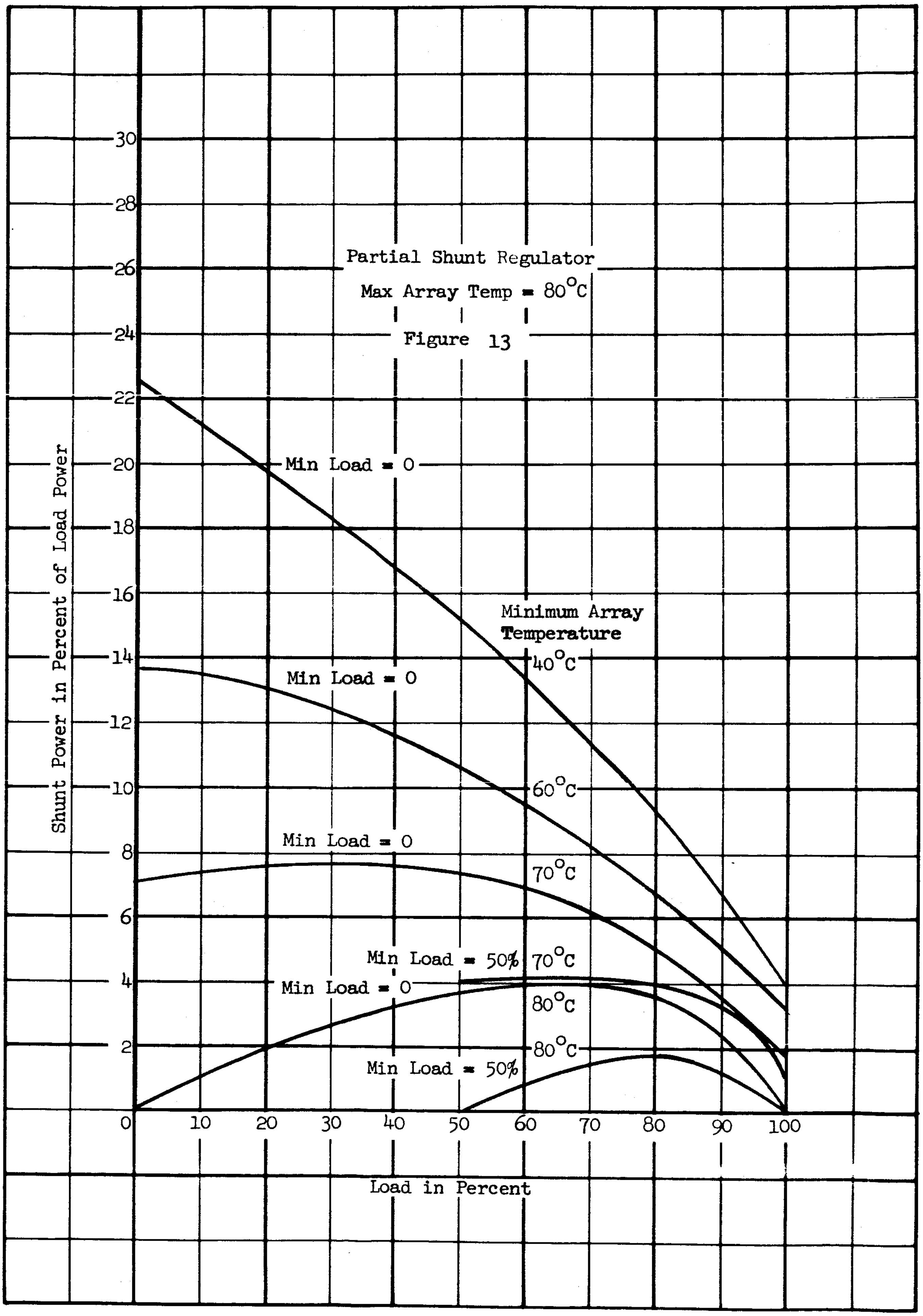
Partial Shunt Regulator
Max Array Temp = 80°C
Figure 13
Minimum Array Temperature
Min Load = 0
40°C
Min Load = 0
60°C
Min Load = 0
70°C
Min Load = 50%
70°C
Min Load = 0
80°C
80°C
Min Load = 50%
Shunt Power in Percent of Load Power
0
2
4
6
8
10
12
14
16
18
20
22
24
26
28
30
10
20
30
40
50
60
70
80
90
100
Load in Percent

As its name suggests, a bucking regulator is one for use where the input voltage is always higher than the output voltage. The basic block diagram for this type of regulator is shown in Figure 14. The output voltage is related to the input voltage by the ratio t_{on}/T, where t_{on} is the ON time of the switch and T is the total drive period. Figure 15 shows typical series losses for a range of output currents under saturated conditions, when losses are a function of output current only. Figure 16 indicates how efficiency varies with output power and with output voltage; these curves represent the losses which occur just prior to full saturation of the switching elements, when off time is minimum. They show that higher efficiencies are associated with higher output voltages.

Variation in efficiency with change in input voltage (assuming a constant output voltage) is shown in Figure 17 for two output voltages. The increase in losses as the voltage ratio increases results primarily from greater switching losses. Regulators of this type have been implemented with weight-to-load power ratios of 0.75 pounds per watt.

A boost regulator is one used where the input voltage is always less than the output voltage. Figure 18 is a block diagram of a constant-frequency boost regulator of the pulse width modulated type. This case is the inverse of the bucking regulator, the ratio of input to output voltage being the ratio of T to t_{off}, with T the total drive period and t_{off} the off time of the shunt switching element.

Maximum efficiency of this type of regulator occurs not when the two voltages are the same, but when the input voltage is slightly higher than the output voltage (not a normal condition for this type of regulator). The shunt element is open in this case, with all losses confined to the series elements. This condition occurs when the power available from the solar array is maximum (i.e., low temperature in sunlight). Figure 19 shows the losses of this type of regulator as a function of load current, and Figure 20 shows the efficiency as a function of output power for varying output voltages. As in the previous case, the curves are taken for t_{off} almost equal to T, and losses are greater

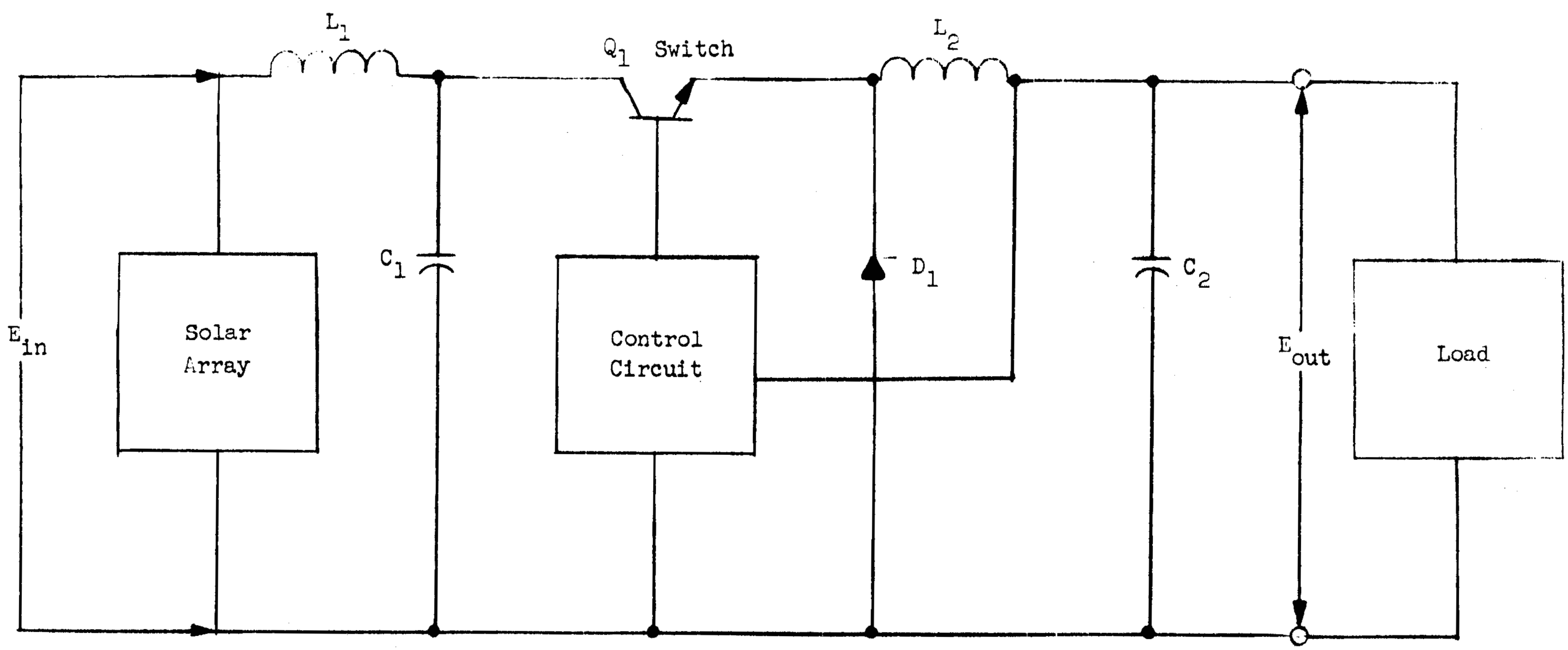

Pulse Width Modulated Bucking Regulator Block Diagram

Figure 14

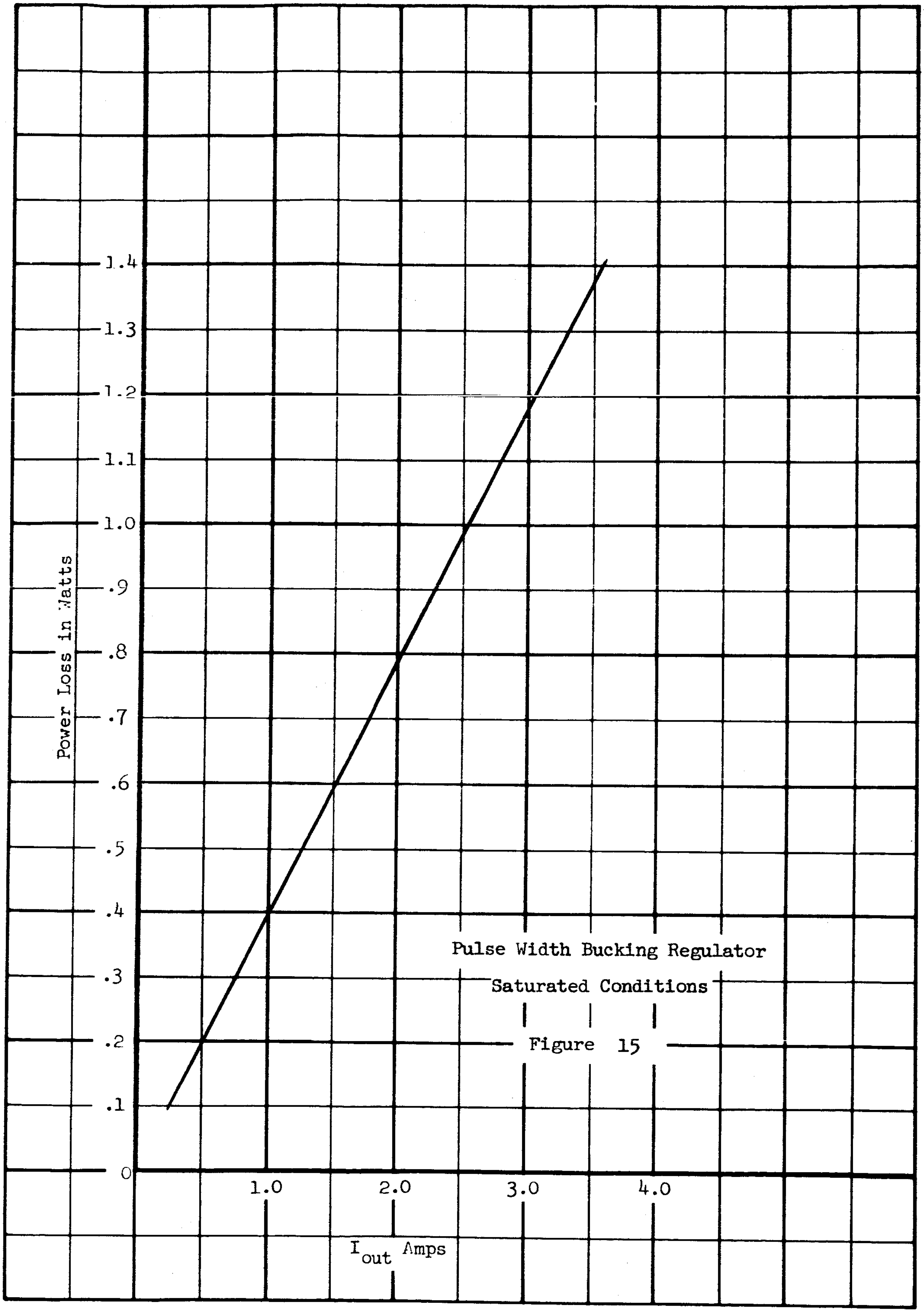

Pulse Width Bucking Regulator
Saturated Conditions

Figure 15

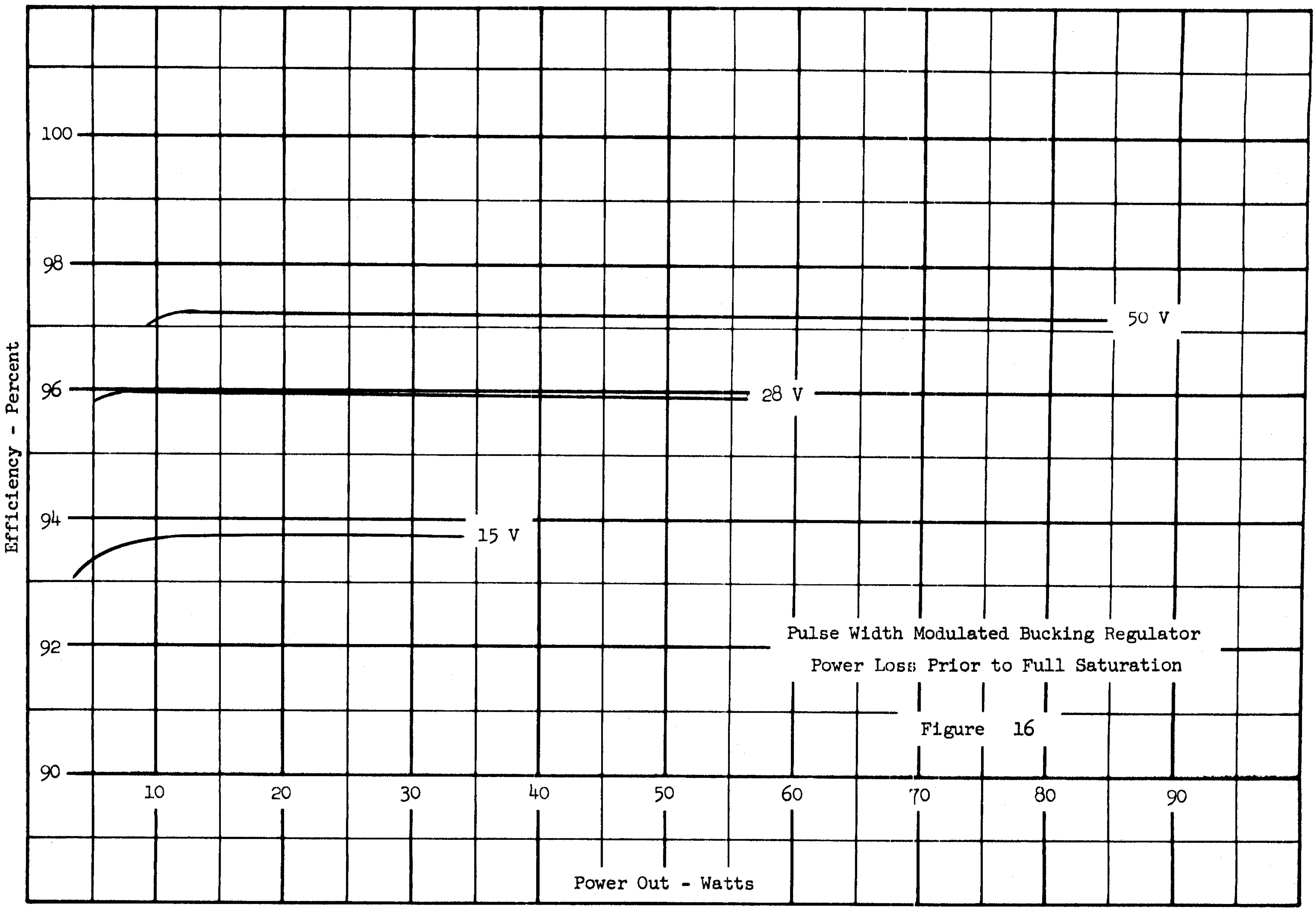

Pulse Width Modulated Bucking Regulator
Power Loss Prior to Full Saturation

Figure 16

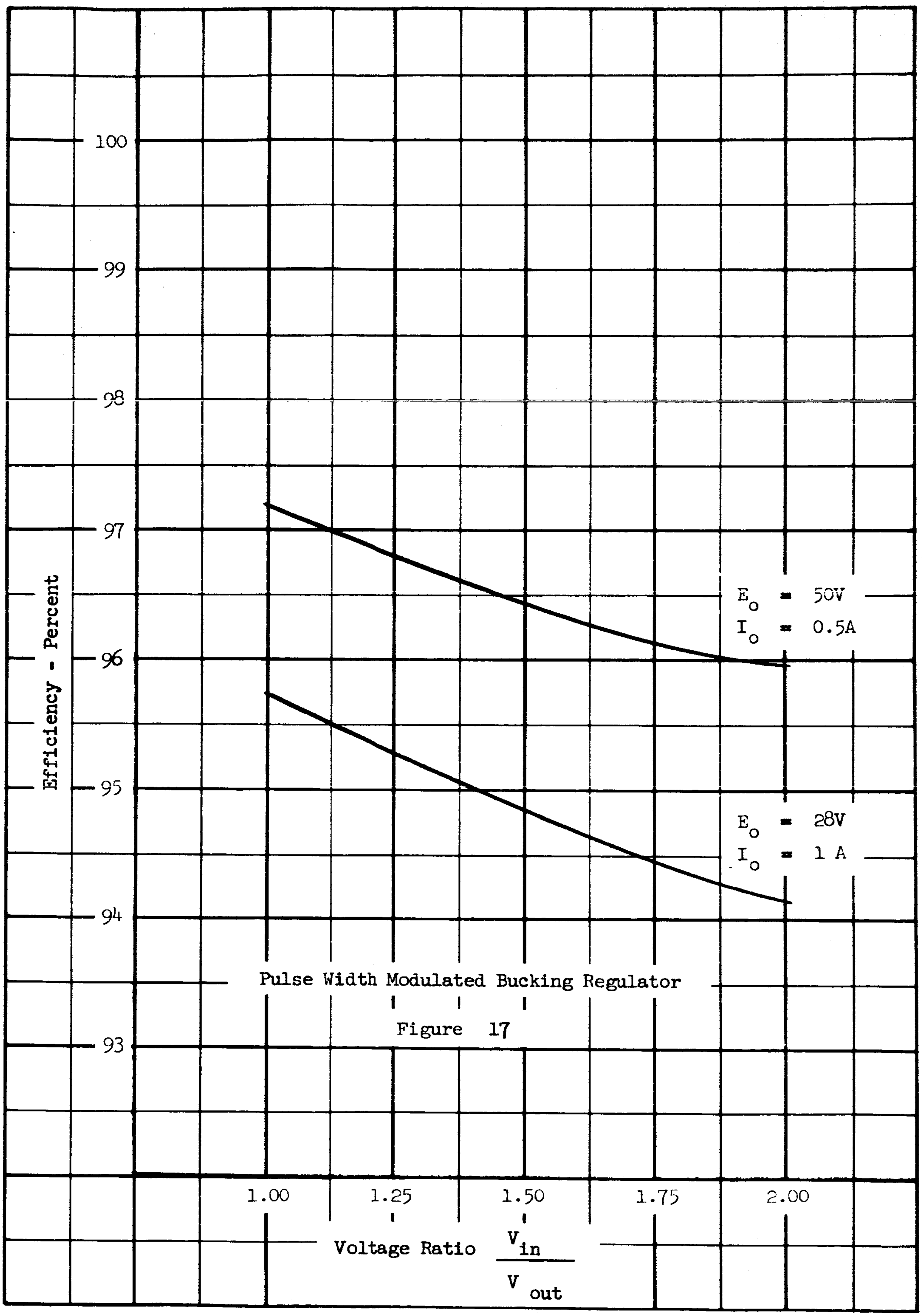

Pulse Width Modulated Bucking Regulator

Figure 17

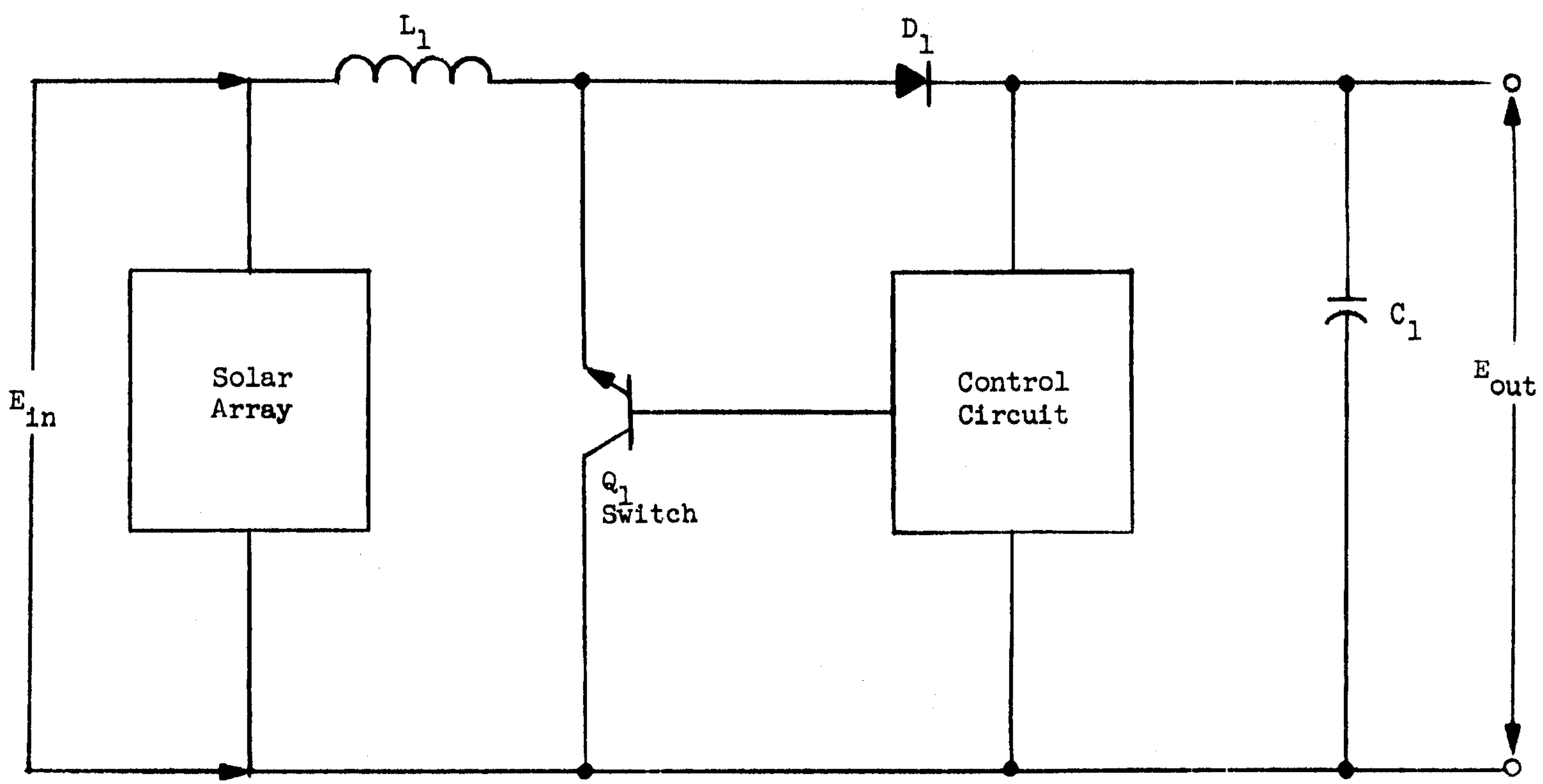

Pulse Width Modulated Boost Regulator Block Diagram

Figure 18

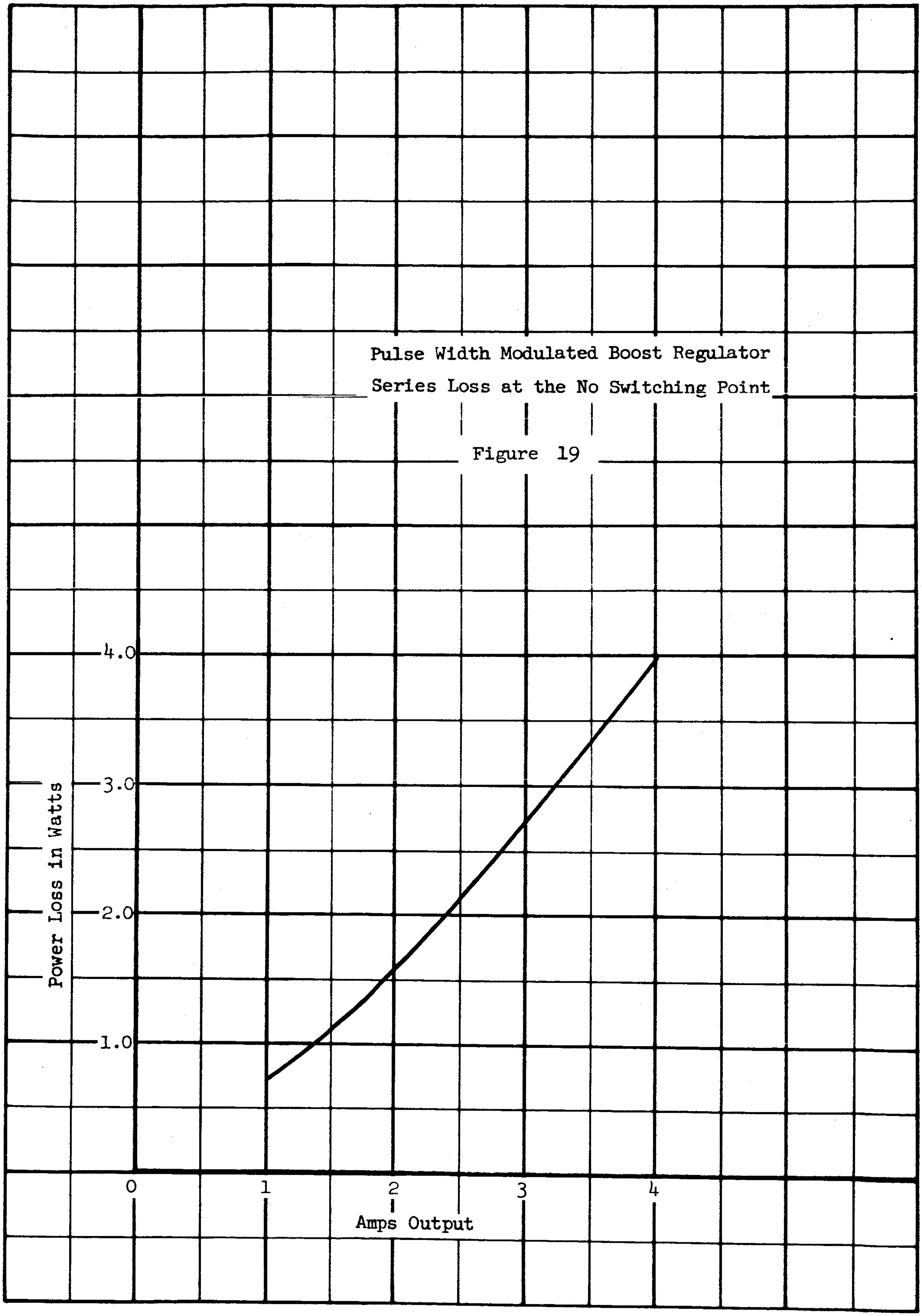

Pulse Width Modulated Boost Regulator
Series Loss at the No Switching Point
Figure 19
Power Loss in Watts
4.0
3.0
2.0
1.0
0
1
2
3
4
Amps Output

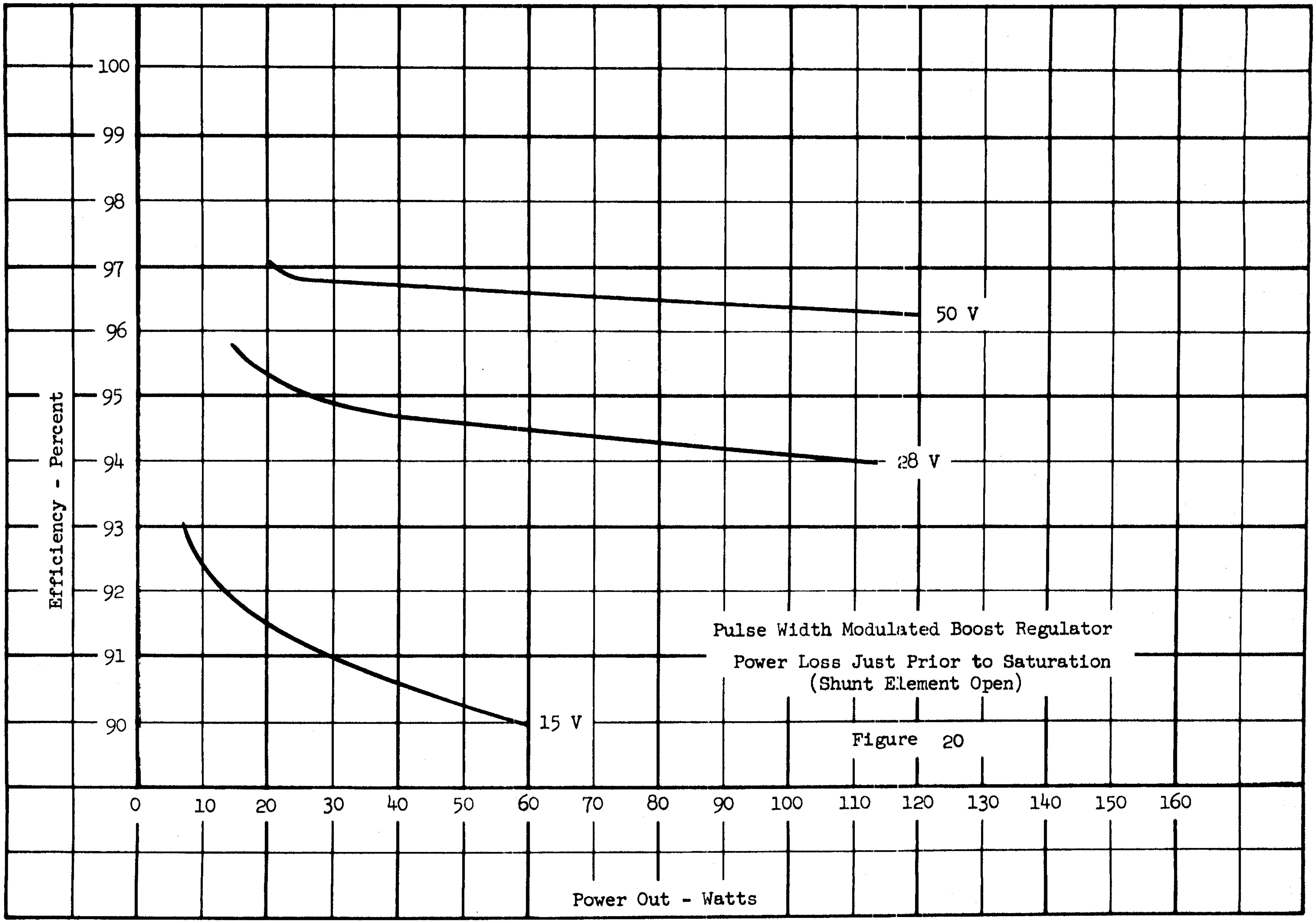

Pulse Width Modulated Boost Regulator
Power Loss Just Prior to Saturation
(Shunt Element Open)

Figure 20

for lower voltages. Figure 21 shows that for this type of regulation the efficiency is greater for high input/output voltage ratios.

In the third type of pulse width modulated regulator, the buck-boost type, output voltage is related to input voltage by the ratio t_{on}/t_{off}, which are respectively the On time and OFF time of the switch. At a 50 percent duty cycle for the switch these two values would be equal and the input and output voltages would also be equal. Where t_{on} is greater than t_{off} the circuit boosts the voltage, and the inverse case bucks (i.e., reduces) it. Figure 22 is a basic block diagram of this type of regulator. In this case also, efficiency is greatest when the voltage ratio is nearest unity, as shown in Figures 23 and 24, but varies with the output voltage chosen. As in the other cases, the higher output voltage shows the smallest losses. The major disadvantage to this type of regulator in comparison to the buck or boost types is its lower efficiency (note the lower absolute values of efficiencies shown in Figure 24 for a given voltage ratio as compared to Figures 17 and 21). When the regulator is in the boost mode the saturated switch and series choke losses are predominant, while in the buck mode the switch losses predominate.

3.3.2 Power Conditioning Equipment

Design. Power conditioning is the generic term used to describe the function of accepting electrical power of specified characteristics and altering it to meet the specific requirements of using equipment. The resulting power, sometimes called secondary power to distinguish it from the prime or unconditioned power, is supplied to the using equipment at the required voltages (and with any other required characteristics). The units used to perform this function are ordinarily classified as inverters, converters, and transformer-rectifiers. The three basic functions usually performed by power conditioning equipment are:

- o Regulation
- o Inversion (DC to AC)
- o Rectification (AC to DC)

In some cases it is possible to combine regulation and inversion in the same circuitry by modulating the drive to the inverter switching transistors so as to produce a constant volt-second integral to the inverter transformer. This

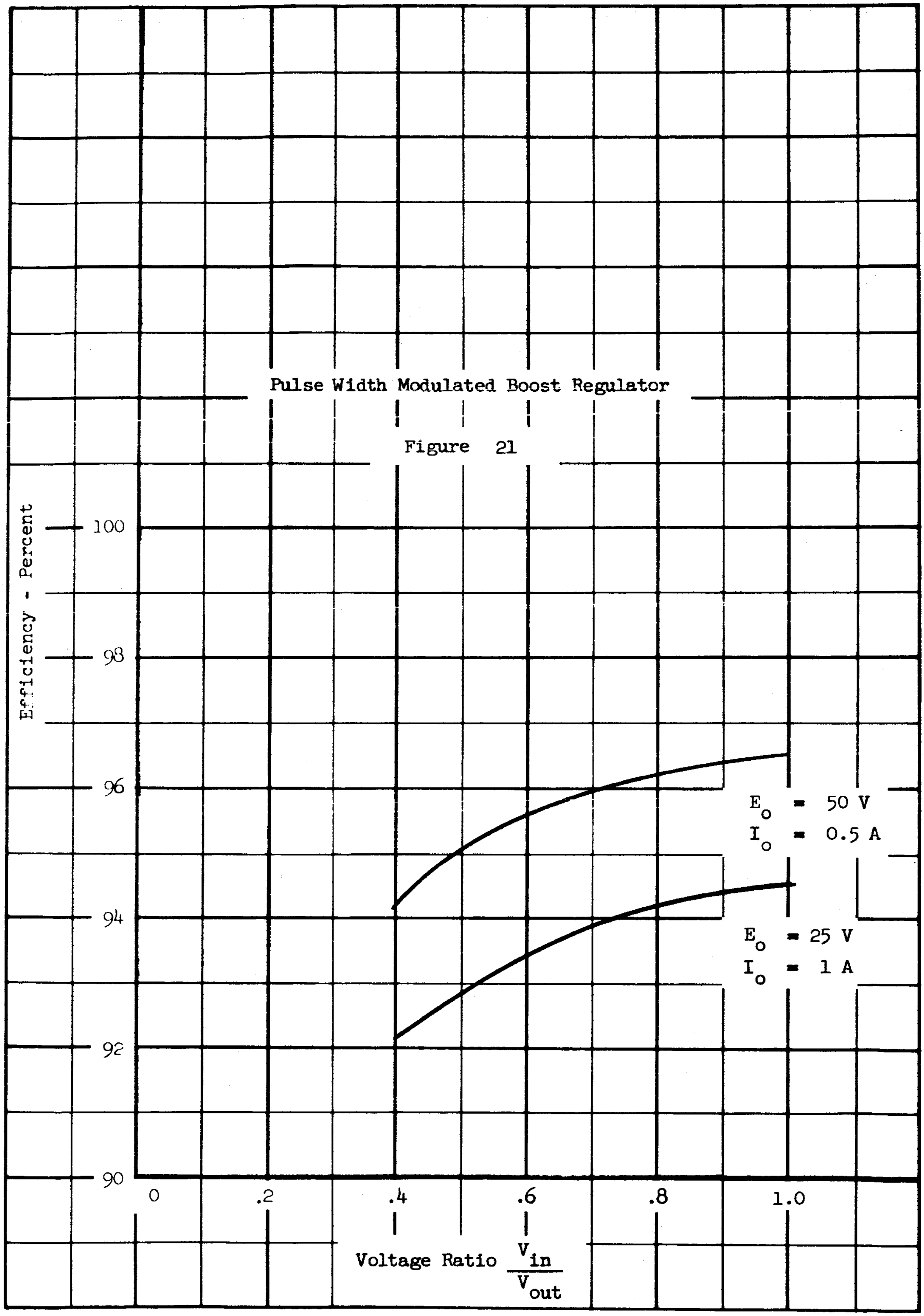

Pulse Width Modulated Boost Regulator
Figure 21
Efficiency - Percent
100
98
96
94
92
90
0
.2
.4
.6
.8
1.0
Voltage Ratio $\frac{V_{in}}{V_{out}}$
E_o = 50 V
I_o = 0.5 A
E_o = 25 V
I_o = 1 A

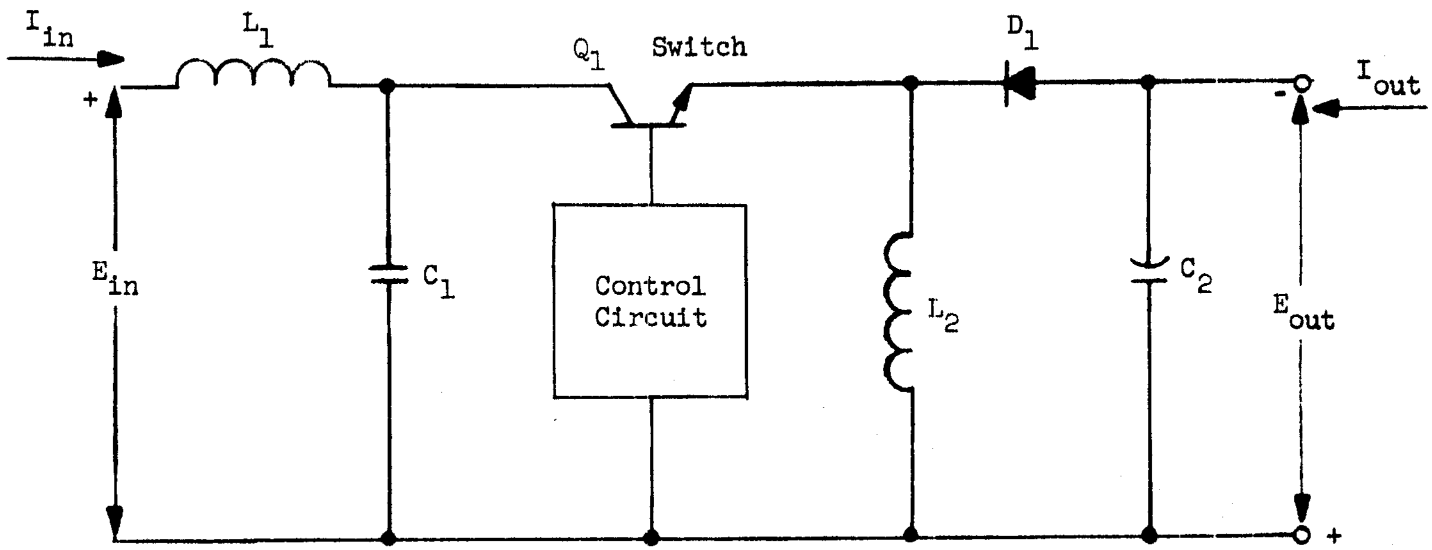

Pulse Width Modulated Buck-Boost Regulator Block Diagram

Figure 22

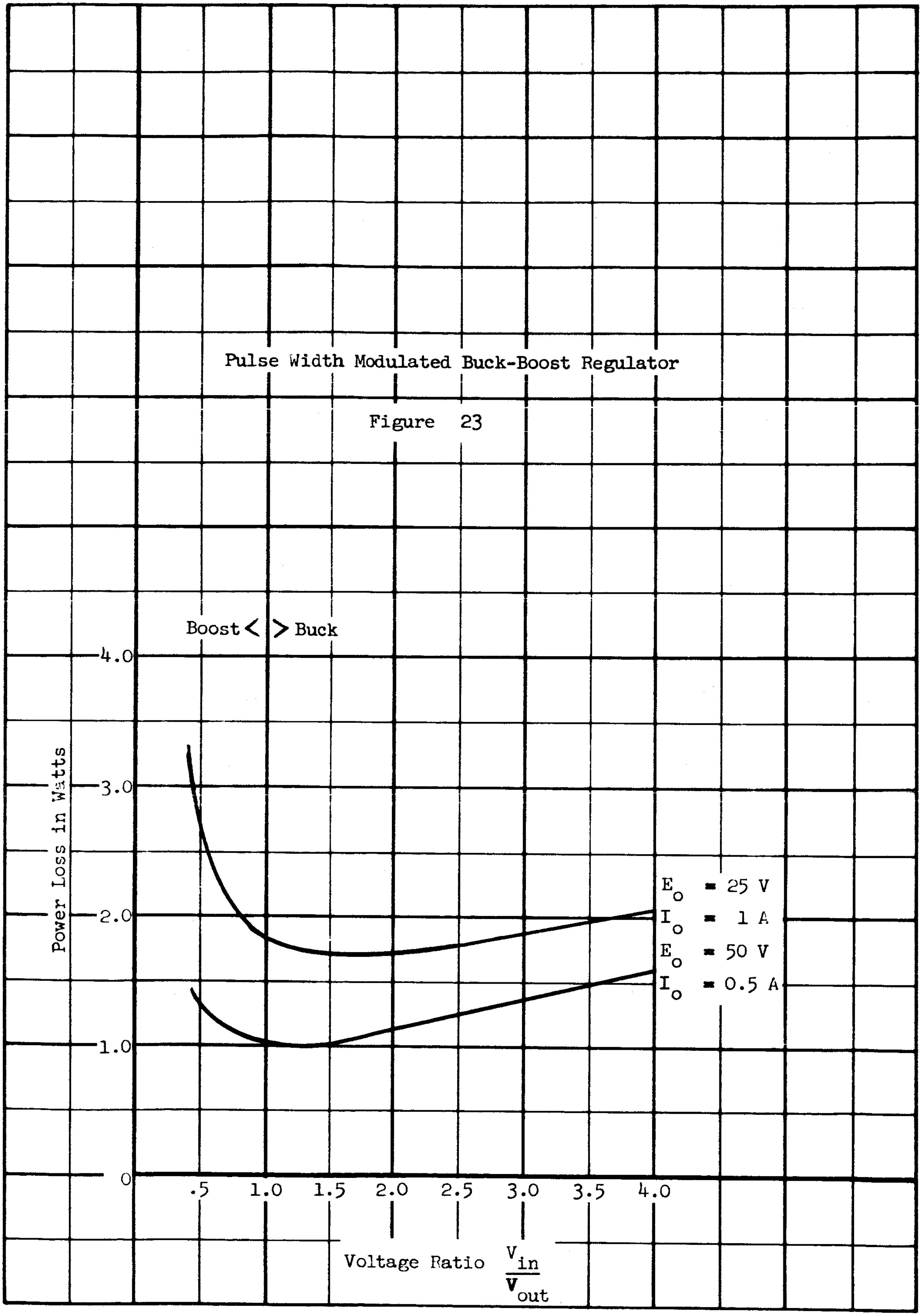
Pulse Width Modulated Buck-Boost Regulator
Figure 23
Boost < > Buck
Power Loss in Watts
4.0
3.0
2.0
1.0
0
.5
1.0
1.5
2.0
2.5
3.0
3.5
4.0
Voltage Ratio $\frac{V_{in}}{V_{out}}$
E_o = 25 V
I_o = 1 A
E_o = 50 V
I_o = 0.5 A

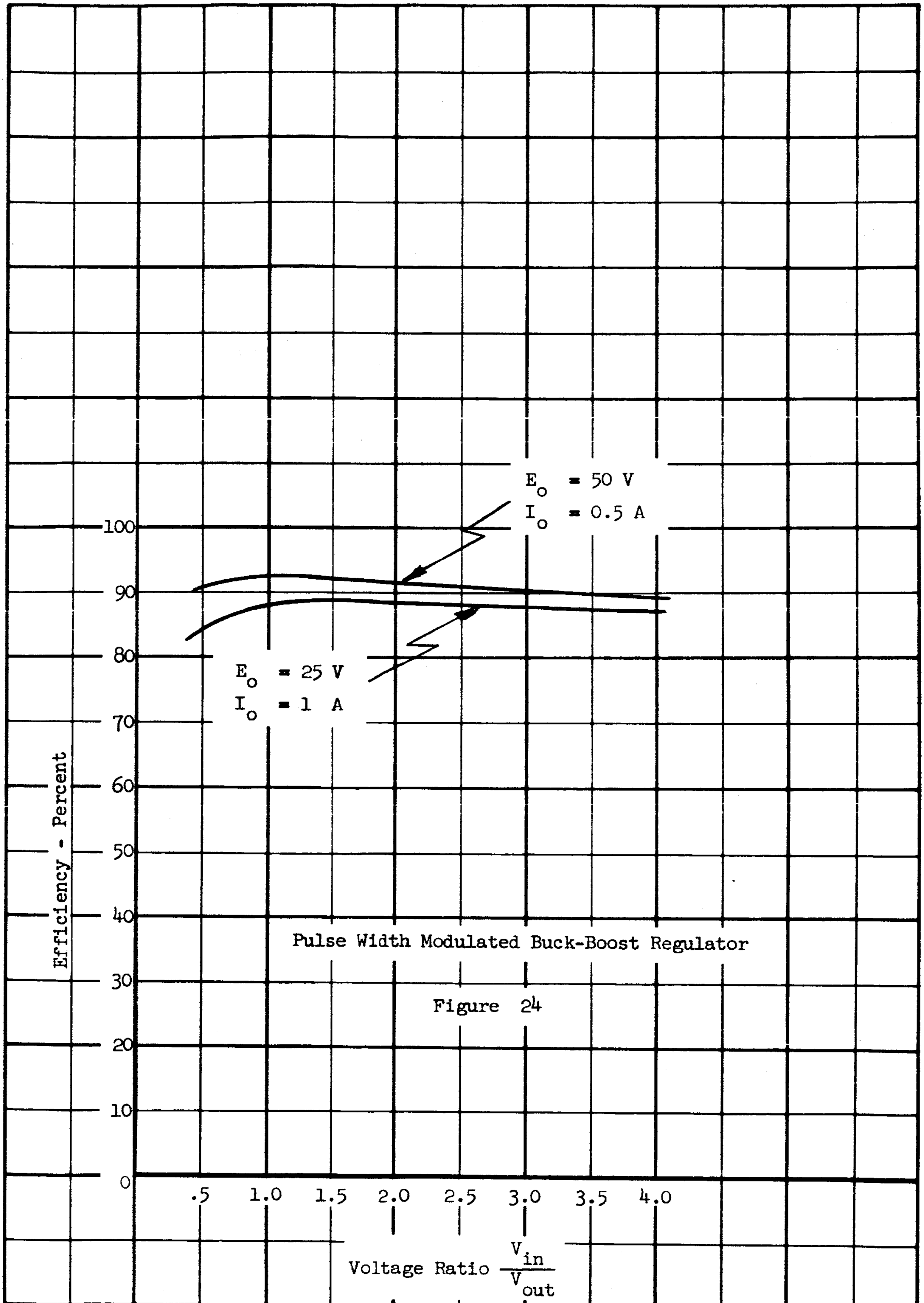
E_o = 50 V
I_o = 0.5 A
E_o = 25 V
I_o = 1 A
100
90
80
70
60
50
40
30
20
10
0
Efficiency - Percent
.5 1.0 1.5 2.0 2.5 3.0 3.5 4.0
Voltage Ratio $\frac{V_{in}}{V_{out}}$
Pulse Width Modulated Buck-Boost Regulator
Figure 24

approach can only be used, however, with low input voltages and relatively low power levels; the limiting factor is the peak collector voltage and current of the switching transistor.

Where separate pre-regulation is necessary, a circuit such as that shown in Figure 25 can be used. In this design, the input filter serves to smooth out spikes and high-frequency transients with large peak values but low volt-second intervals, to eliminate input ripple having frequency components at or near the modulating frequency of the switching transistor (which would produce low-frequency components by heterodyning; these would go through the integrator and back to the primary bus without attentuation), and to attenuate AC components produced by transistor switching. The integrator portion of the circuit serves to smooth the "chopped" DC, and the diode conducts when the transistor is off, permitting continuous current flow through the integrator inductor. The inductor then becomes, along with its capacitor, a means of storing electrical energy. The switching transistor "chops" the DC at the output of the input filter in such a way as to produce a constant volt-second integral into the integrator.

Implementation of the inversion function is relatively simple. Figure 26 illustrates three versions of inverters, two with transformers and one without. The inverter can obtain its drive from the same source that produces the unmodulated drive for the pre-regulator. Some current feedback from collector to base of the inverter transistor will reduce drive source power and improve efficiency.

Conversion can take various forms, as shown in Figure 27. When the secondary power is DC, the inverter output must be rectified and filtered. The designs of Figure 27 show isolation transformers such as would be needed with those source options shown as (a) and (c) of Figure 26, but the secondary for each converter in Figure 27 can be the secondary of (b) in Figure 26.

<u>Details of Implementation</u>. Probably the heaviest single part in the power conditioning equipment is the inverter transformer or the converter transformer (Figure 26 (a) and (b) or Figure 27). However, not all of the windings are used for the full switching cycle; for center-tapped windings, half

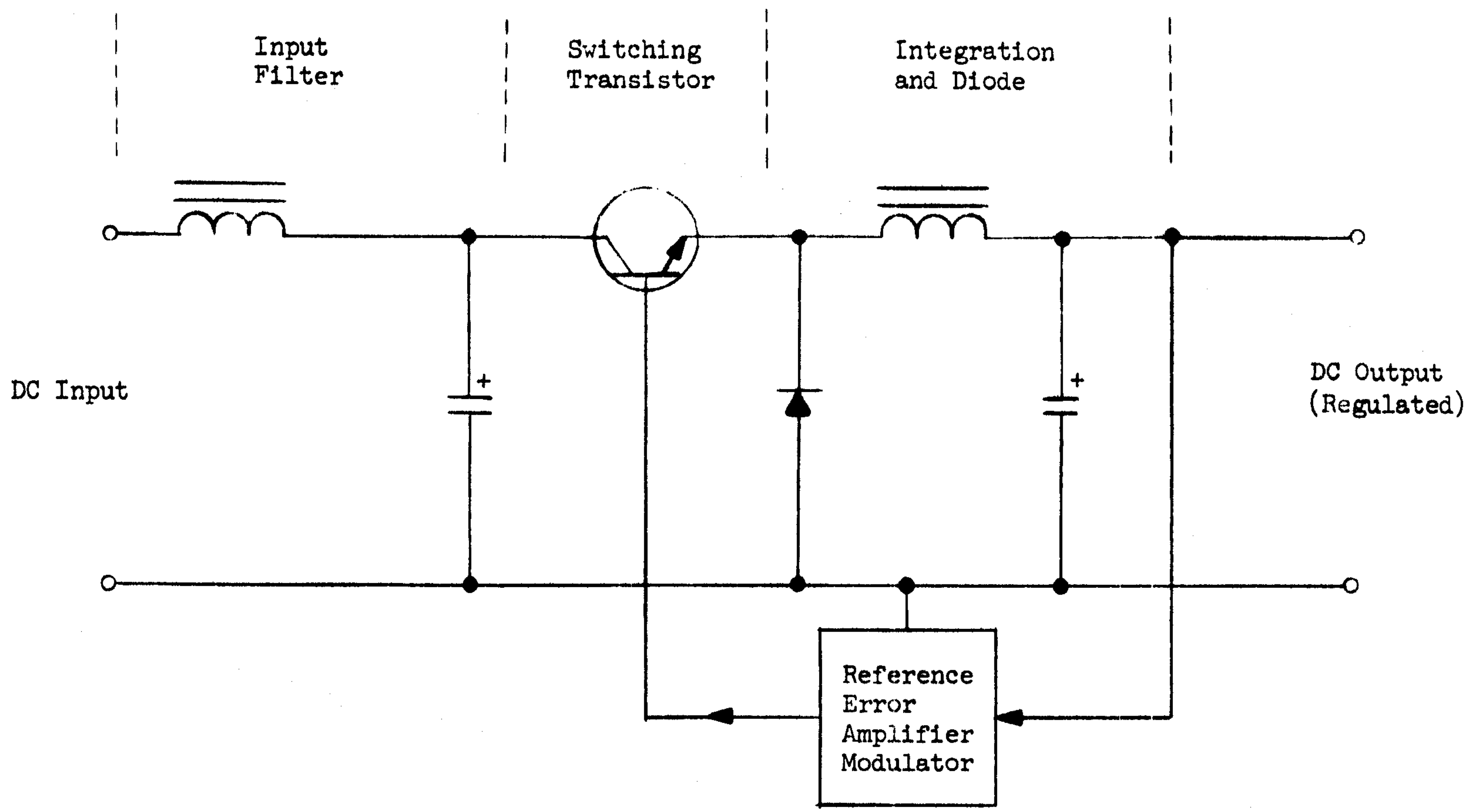

Typical Pre-regulator (Series)
Figure 25

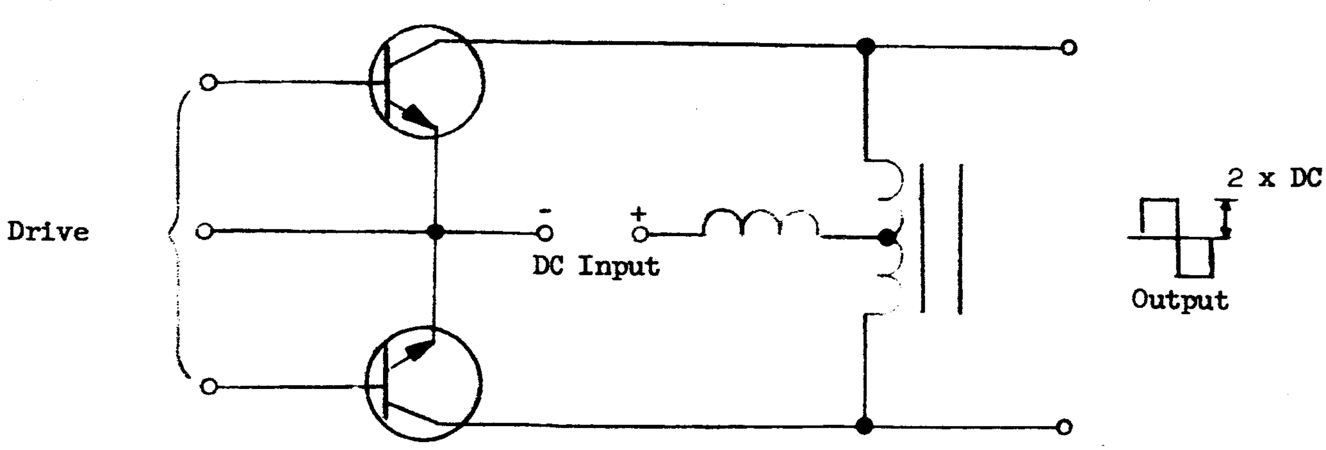

a) "Choppers" with Auto-Transformer

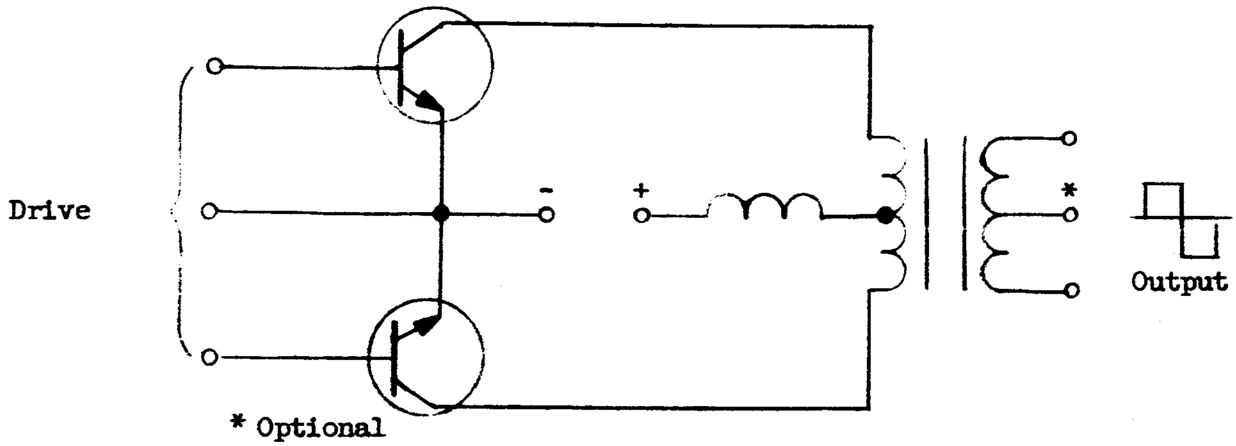

b) "Choppers" with Isolation Transformer

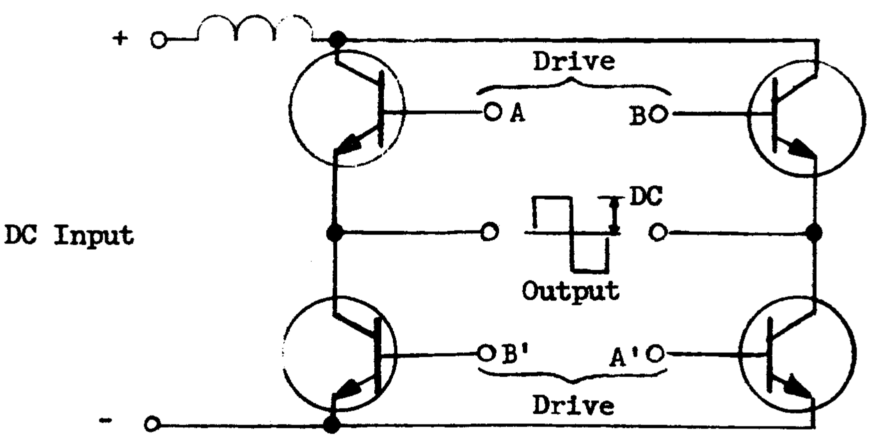

c) Bridge "Choppers" without Transformer

Types of Inverters
Figure 26

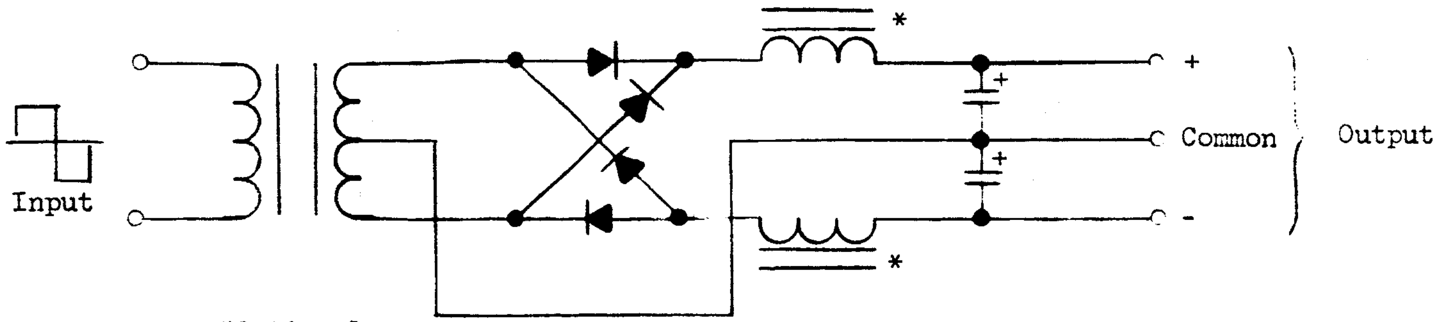

*Optional

a) Equi-voltage, Duo-polarity Converter

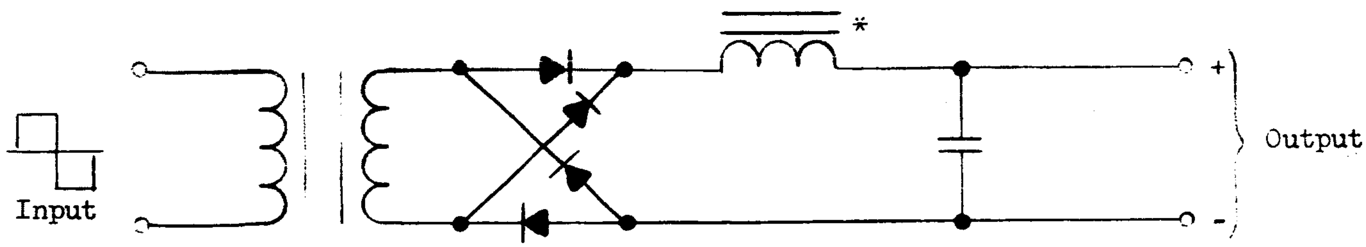

*Optional

b) Bridge Circuit for High Voltage or Improved Transformer Utilization

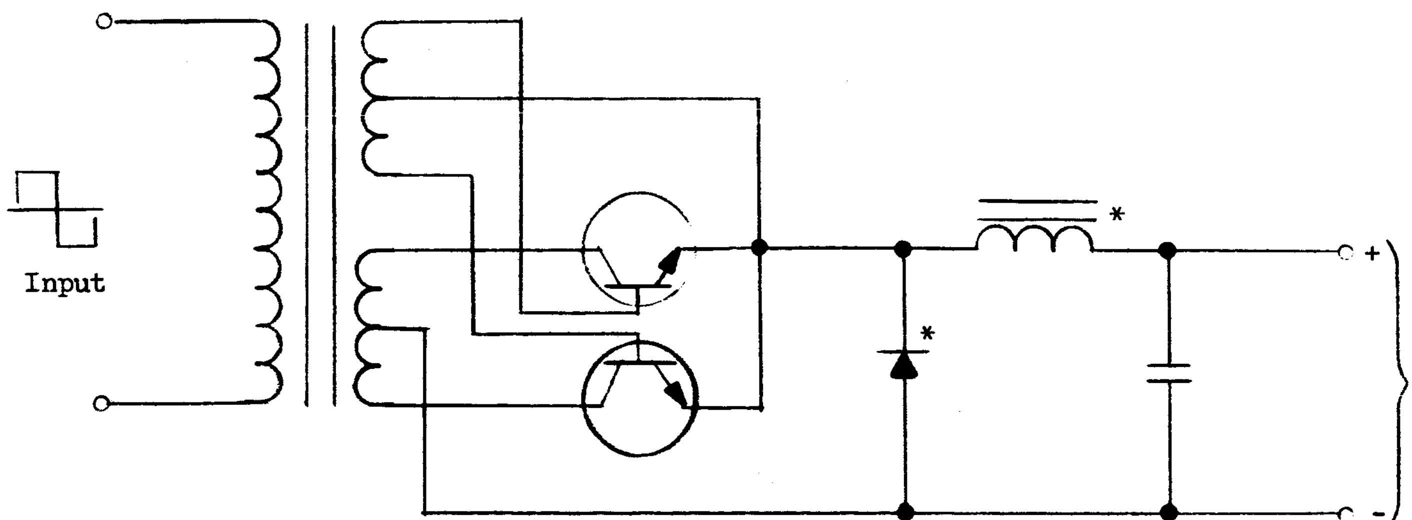

*Optional

c) Synchronous Converter (Very Low Voltage Only)

Typical Converters
Figure 27

are dormant for each half cycle. Figure 27 (a) shows a shared secondary winding that would be completely utilized if both output currents were equal, and is utilized to the extent that this is the case. In Figure 26 (a) the inverter transformer has a 100 percent utilization factor.

The filter capacitors shown in Figures 25 and 27 are usually ceramic or tantalum types, with the tantalum type available in foil, solid, or wet versions. Selection of capacitors has a significant effect on weight, since they are in the same weight range as transformers. Consideration must also be given to system frequencies, since these capacitors tend to become inductive at frequencies in the megacycle range. This makes it difficult to achieve low output impedance at high frequency, compensate a high-gain amplifier, or suppress high-frequency components for EMC (electromagnetic compatibility) reasons.

The inductors shown in Figures 25 and 27 are the DC carrying types which make use of the air gap to store most of the energy while leaving the core with sufficient permeability to act as an inductor toward AC components of energy. In those cases where the inductors are shown as optional they can be eliminated if the AC waveform is square or nearly square. They are needed in applications with severe noise (EMC) or ripple requirements. Care must be taken with inductors at high frequencies, since they tend to become capacitive above one megacycle. Weight is also an important consideration in their use, since they weigh more than resistors, low-value capacitors, transistors, or diodes.

With regard to semiconductors, most high-reliability or high-temperature applications call for silicon rather than germanium types, even though silicon has a larger saturation voltage drop than does germanium. When semiconductors are used in switching modes, there is the usual I-V loss for forward conduction and in addition a storage carrier effect, which causes the device to remain conducting into the next half cycle, after the complementary diode or transistor has turned on. This results in a short circuit for a brief period. These losses can be significant and may be within an order of magnitude of the other losses.

There are times when the secondary power circuits must perform with better than normal ripple or regulation, or lower than average output impedance due to dynamic loading (pulsed loads). When this is ncessary, active filtering must be used in the outputs following those converter circuits shown in Figure 27. Series regulators, Figure 28 (a), may be used where the dynamic range of regulation is not too great. Normally the pre-regulator function produces about one percent regulation to the inverter transformer secondaries for line, DC load, and temperature variations combined. The dynamic loads are usually pulsed demands for current which otherwise would produce significant voltage transients. The shunt regulator, Figure 28 (b), may be used for wide range dynamic loads.

Parametric Data. The parametric data accumulated to date on power conditioning equipment relates almost entirely to DC-DC converters. The following discussion will therefore cover power converters only, with discussion of inverters and transformer-rectifiers left to a subsequent report. Since DC-DC converters include an inversion function and a transformer-rectifier function, much of the technology is applicable to units performing those functions alone.

Table IX summarizes the pertinent electrical data on the converters included in the eight power systems under consideration. It can be seen that there is a wide range of characteristics, corresponding to the wide range of using equipment requirements previously noted.

With regard to converter weight, packaging densities for electronic components of 0.030 to 0.045 pounds/ cu. in. are being achieved; the total weight of mechanical hardware ranges from 33 to 100 percent of the weight of the electronic parts used in the unit, with the average about 50 percent. Operating temperature affects weight, since high temperature require more structural mass to remove heat.

The parameter of most interest for this study is converter efficiency. Weight in turn is affected by efficiency and switching frequency. Figure 29 shows the relationship of all these parameters. It can be seen that:

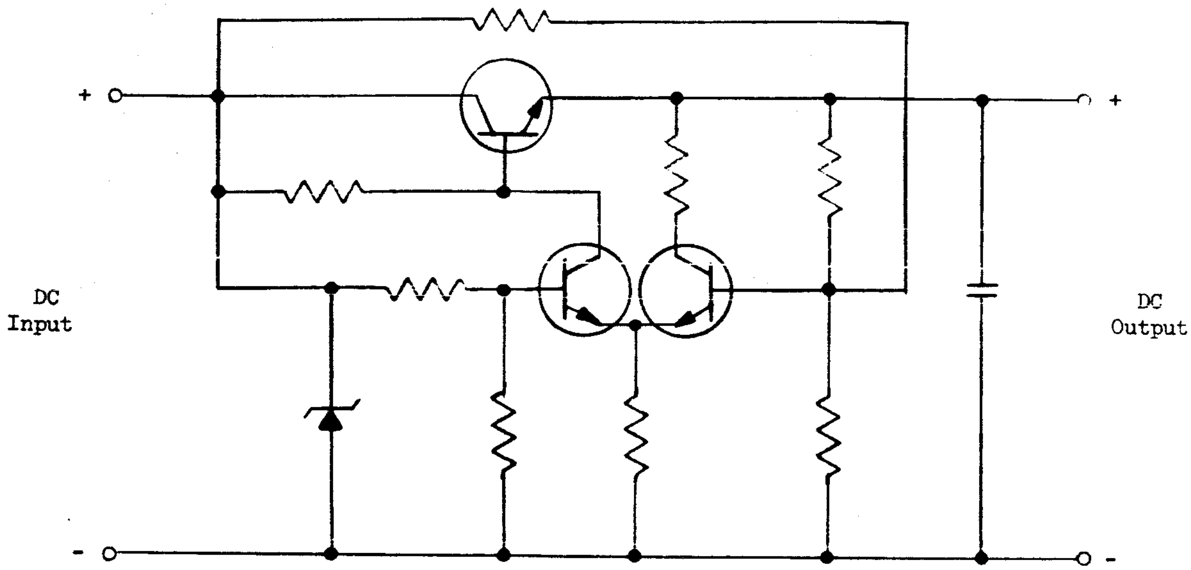

a) Typical Series Regulator

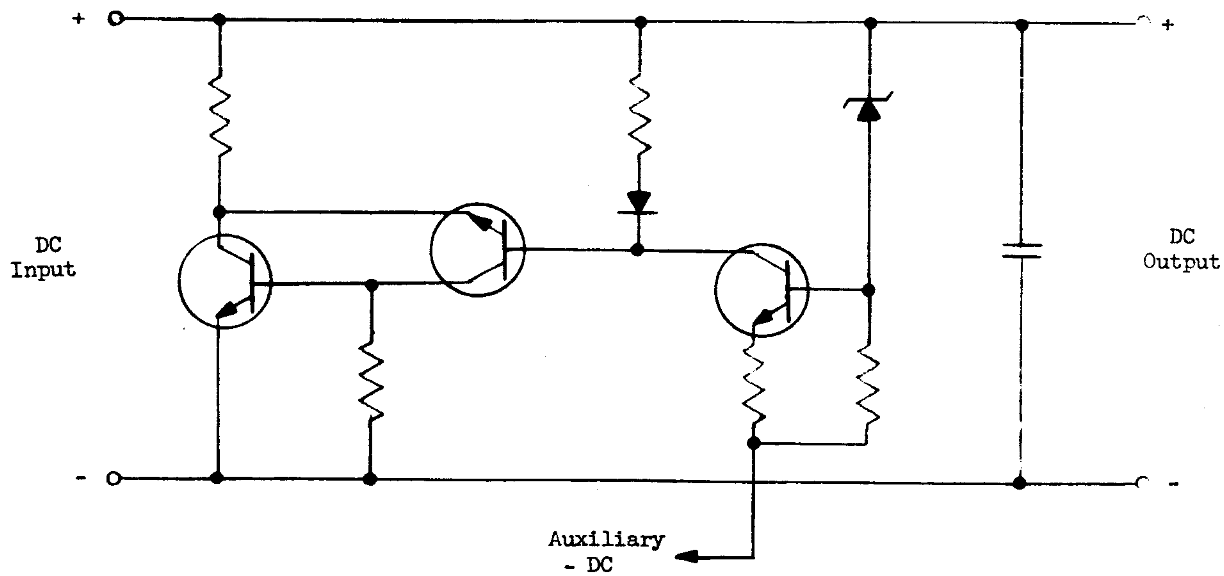

b) Typical Shunt Regulator

Active Filters
Figure 28

TABLE IX

CONVERTERS

Usage	Input Voltage	Input Regulation %	Output Voltage	Output Current ma	Output Regulation %	Output Ripple (p-p)	Overload Protection	Switching Frequency	Transients	Output Power (watts)	Efficiency %
Able V No. 2 Transmitter	18	+28 -22	+210 V	30	±5	1%	Yes	1.6 to 2.2KC	< 10 millisecond	6.3	73
			-20 V	3	±5	1%	Yes	1.6 to 2.2KC		0.6	
			-12 V	130	±5	1%	Yes	1.6 to 2.2KC		1.56	
			6.3 VAC	750	±5			1.6 to 2.2KC		4.7	
			+6.0 V	10	±5	1%	Yes	1.6 to 2.2KC		0.6	
										12.66	
Able V No. 1 Payload	18	+28 -22	+6.0 V	150	±0.3	1%	Yes	1.6 to 2.2KC	< 10 millisecond	.9	67
			-6.0 V	28	±0.3	1%	Yes	1.6 to 2.2KC		.2	
			+10 V	280	±0.3	1%	Yes	1.6 to 2.2KC		2.8	
			+16 V	51	±0.3	1%	Yes	1.6 to 2.2KC		.8	
			-16 V	18	±0.3	1%	Yes	1.6 to 2.2KC		.3	
			6.0 VAC	125						5.0	
Vela Payload	22.5	+10 -15	+6.5 V	275	±3.0	10 MV	Yes	3.0 to 3.5KC	< 13%	.138	64
			-6.5 V	1840	±3.0	10 MV	Yes	3.0 to 3.5KC	< 13%		
Vela Transmitter	22.5	-20 +10	+70 V	270	±2.0	350 MV	Yes	3.0 to 3.5KC	< 13%	21.8	70
			+23 V	130	±2.0	160 MV	Yes	3.0 to 3.5KC	< 13%		
Vela Communications	22.5	-13 +10	+16.2 V	20	±2.0	160 MV	Yes	3.0 to 3.5KC	< 13%		29
			+10.0 V	140	±2.0	100 MV	Yes	3.0 to 3.5KC	< 13%	1.91	
			-6.2 V	15	±2.0	60 MV	Yes	3.0 to 3.5KC	< 13%		
			-16.2 V	6	±2.0	160 MV	Yes	3.0 to 3.5KC	< 13%		
			+28.0 V	15	±5.0	560 MV	Yes	3.0 to 3.5KC	< 13%		39
			+12.2 V	250	±3.0	130 MV	Yes	3.0 to 3.5KC	< 13%	3.67	
			+10.0	10	N.A.	100 MV	Yes	3.0 to 3.5KC	< 13%		
			-6.2 V	20	± 5.0	120 MV	Yes	3.0 to 3.5KC	< 13%		

TABLE IX

CONVERTERS (CONTINUED)

Usage	Input Voltage	Input Regulation %	Output Voltage	Output Current ma	Output Regulation %	Output Ripple (p-p)	Overland Protection	Switching Frequency	Transients	Output Power (watts)	Efficiency %
Pioneer Transmitter	28	+18	-940 V	2-10	±0.5	± 0.1%	Yes	5.6 KC	± 0.2	5.64	80
		-16	-545 V	32-40	±1.0	± 1.0%	Yes		± 0.2	19.62	
			+80 V	.02-.2	±1.0	± 1.0%	Yes		± 0.2	.16	
			+4.875 VAC	300-400	±2.5		Yes		± 0.2	1.68	
										26	
Pioneer Equipment	28	+18	+12.8 V	10	±2%	±2.0%	Yes	5.6KC	± 5.0	.128	60
		-16	-12.4 V	76	±2%	±2.0%	Yes	5.6KC	± 5.0	.942	
			+16.7 V	22.2	±2%	±2.0%	Yes	5.6KC	± 5.0	.376	
			+16.0 V	54	±2%	±2.0%	Yes	5.6KC	± 5.0	.864	
			+10.0 V	246	±2%	±2.0%	Yes	5.6KC	± 5.0	2.46	
			-16.0 V	134	±2%	±2.0%	Yes	5.6KC	± 5.0	2.14	
			+16.7 V	22.2	±2%	±2.0%	Yes	5.6KC	± 5.0	.367	
			+12.8 V	10.0	±2%	±2.0%	Yes	5.6KC	± 5.0	.128	
			-12.4 V	76	±2%	±2.0%	Yes	5.6KC	±5.0	.942	
			+15.0	No Load		±2.0%	Yes	5.6KC	±5.0		
			+15 VAC	1.66		±2.0%	Yes	5.6KC	±5.0	.024	
			+15 VAC	1.66		±2.0%	Yes	5.6KC	±5.0	.024	
			+10 V	60	±3%	±2.0%	Yes	5.6KC	±5.0	.6	
										9.0	
OGO No. 1 and 10	28	+20	+70 V	330	±2.0	±2.0%	Yes	2461 CPS	±5%	23.1	70
		-16	+23 V	125	±2.0	±2.0%	Yes	2461 CPS	±5%	2.9	
										26.0	
No. 2	28	+20	+16 V	60	±1.0	±1.0%	Yes	2461 CPS	± 5%	1.0	44
		-16	+9 V	560	±1.0	±1.0%	Yes	2461 CPS	± 5%	5.0	
			+5 V	100	±1.0	±1.0%	Yes	2461 CPS	± 5%	0.5	
			-6 V	60	±1.0	±1.0%	Yes	2461 CPS	± 5%	0.36	
			-6 V	20	±1.0	±1.0%	Yes	2461 CPS	± 5%	0.12	
										6.98	
No. 3 and 4	28	+20	+70 V	275	±2.0	±2.0%	Yes	2461 CPS	±5%	19.2	69
		-16	+23 V	125	±2.0	±2.0%	Yes	2461 CPS	±5%	2.9	
										22.1	

TABLE IX

CONVERTERS (CONTINUED)

Usage	Input Voltage	Input Regulation %	Output Voltage	Output Current ma	Output Regulation %	Output Ripple (p-p)	Overload Protection	Switching Frequency	Transients	Output Power (watts)	Efficiency %
No. 5 and 6	28	+20	+16 V	300	1.0	1.0%	Yes	2461 CPS	± 5%	4.8	60
		-16	+9 V	789	1.0	1.0%	Yes	2461 CPS	± 5%	7.1	
			-6 V	280	1.0	1.0%	Yes	2461 CPS	± 5%	1.7	
			-16 V	10	1.0	1.0%	Yes	2461 CPS	± 5%	0.2	
										13.8	
No. 7 and 8	28	+20	+16 V	20	2.0	2.0%	Yes	2461 CPS	± 5%	0.32	28
		-16	+ 9 V	107	2.0	2.0%	Yes	2461 CPS	± 5%	0.97	
			+-6 V	20	2.0	2.0%	Yes	2461 CPS	± 5%	0.12	
										1.41	
No. 9	28	+20	+20 V	350	1.5	1.5%	Yes	2461 CPS	± 5%	7.0	75
		-16	+10 V	50	3.0	3.0%	Yes	2461 CPS	± 5%	0.5	
			-20 V	350	1.5	1.5%	Yes	2461 CPS	± 5%	7.0	
			+28 VAC,CT	385	3.0	3.0%	Yes	2461 CPS	± 5%	10.8	
										25.3	
ACS Inverter 350 V A 2 ϕ 400 cps	28	+20	+115 V	130	2.0	**		400	± 5%	15 max	75
		-16	+ 18 V	166	2.0				± 5%	3	
			+ 26 V	115	*				± 5%	3	
			+125 V	120					± 5%	15	
			+ 26 V	115						3	
			+135 V	110						15	
			+135 V	110						15	
			+125 V	1240						124	
			+135 V	1360						136	
			+135 V	1360						136	
										350	

*Varies proportionally with input

**No voltage spikes greater than 15% at the output

TABLE IX

CONVERTERS (CONTINUED)

Usage	Input Voltage	Input Regulation %	Output Voltage	Output Current ma	Output Regulation	Output Ripple (p-p)	Overload Protection	Switching Frequency	Transients	Output Power (watts)	Efficiency %
OGO NON-Gated Inverter	28	+20 -16	+ 115 V	130	± 2%	**		400 CPS	± 5%	15	80
			+ 18 V	167	± 2%					139	
			+ 26 V	115	Varies proportionally with input						
			+ 125 V	1110						139	
			+ 26 V	115						3	
			+ 135 V	1110						151	
			+ 135 V	1110						151	
										350	
Comsat Equipment Converters	28	± 15	+ 28 V	77	± 3%		Yes	12 KC		2.5	73
			+ 15 V	165	± 3%					2.47	
			+ 10 V	208	± 3%					2.08	
			+ 6 V	411	± 3%					2.46	
			-6 V	218	± 3%					1.3	
			-15 V	165	± 3%					2.47	
										12.99	

** No voltage spikes greater than 15% of the output

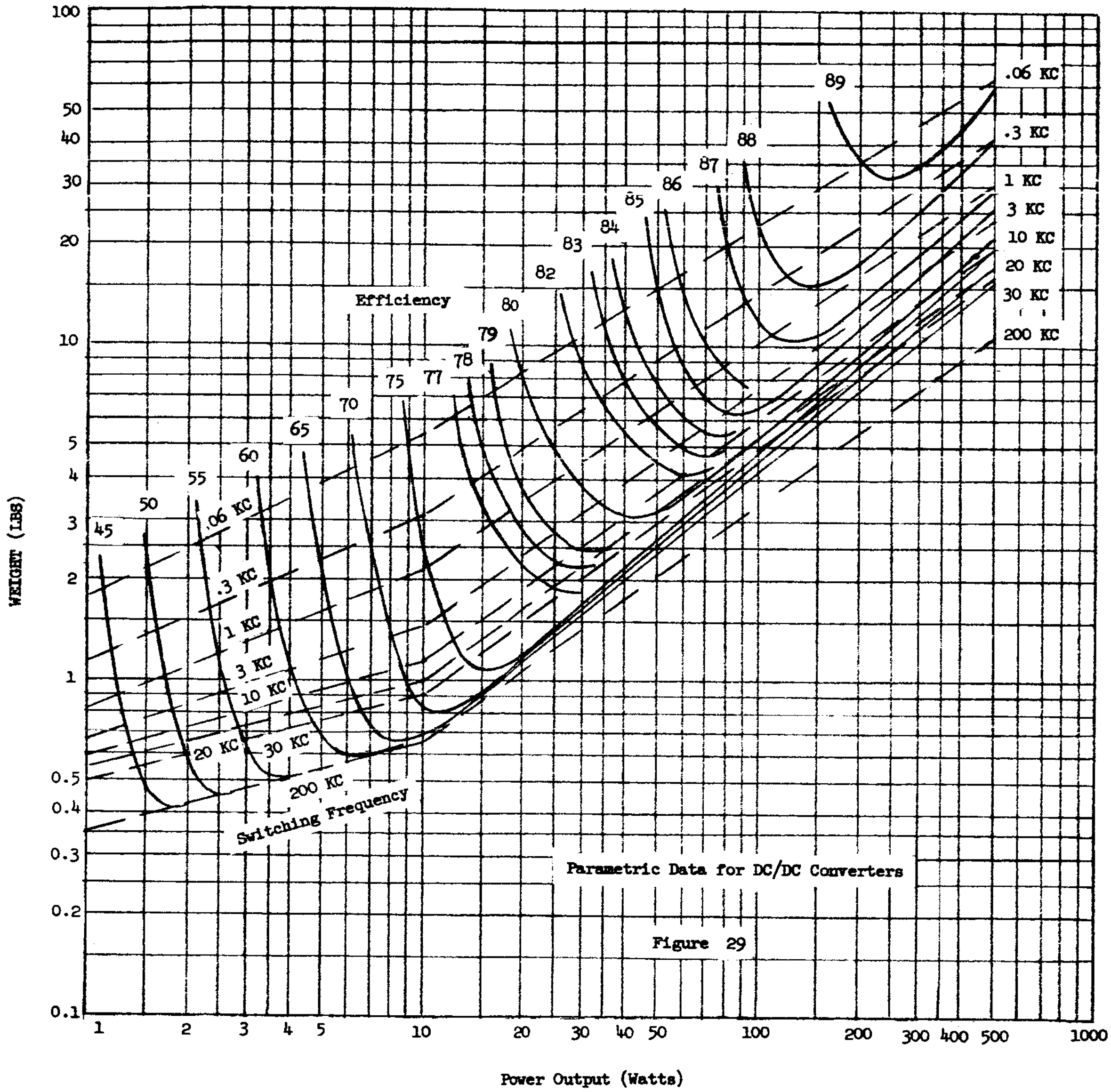

Parametric Data for DC/DC Converters

Figure 29

- Efficiency increases with power level. This results from the fact that there are certain fixed losses in a converter, and these naturally become a smaller percentage of the total as power is increased. In addition, the variable losses increase at a slower rate than the power level and thus also become smaller in proportion.
- Higher switching frequencies result in considerable reduction of weight, but at the same time in lower efficiency.
- High switching frequencies (100-200 KC) can be used at low power levels (up to 10 watts), but should not be used at higher power levels because of the loss in efficiency associated with long switching time characteristics of presently available power, switching transistors. The upper practical limit for a 500 watt power level, for example, is seen to be a switching frequency of 20-30 KC.

As the figure shows, there is a maximum efficiency attainable for any given power level. This is shown more simply in Figure 30, a curve of maximum efficiency versus power level for a typical 28 V DC-DC converter. As would be expected the efficiency increases with power level, but reaches a maximum at about 89 percent. This reflects the minimum attainable losses, which are attributable to I-V losses in the power switches, rectifiers, and magnetic components as well as to the fixed losses. Some increase in maximum efficiency may be attainable for low-power units by design innovations, and in high-power units by incorporating regulation in the inversion state.

Efficiency is affected, in part, by the magnitude and number of outputs. For single outputs other than 28 VDC, an efficiency correction factor, Figure 31, must be applied to compensate for rectification losses. At high voltage output, the efficiency correction factor (ECF) is greater than unity while at low voltages the correction factor is substantially less than unity due to the high rectification losses. For multiple outputs, the correction factor will also be utilized. An example calculation will be instructive. The problem is to determine the efficiency

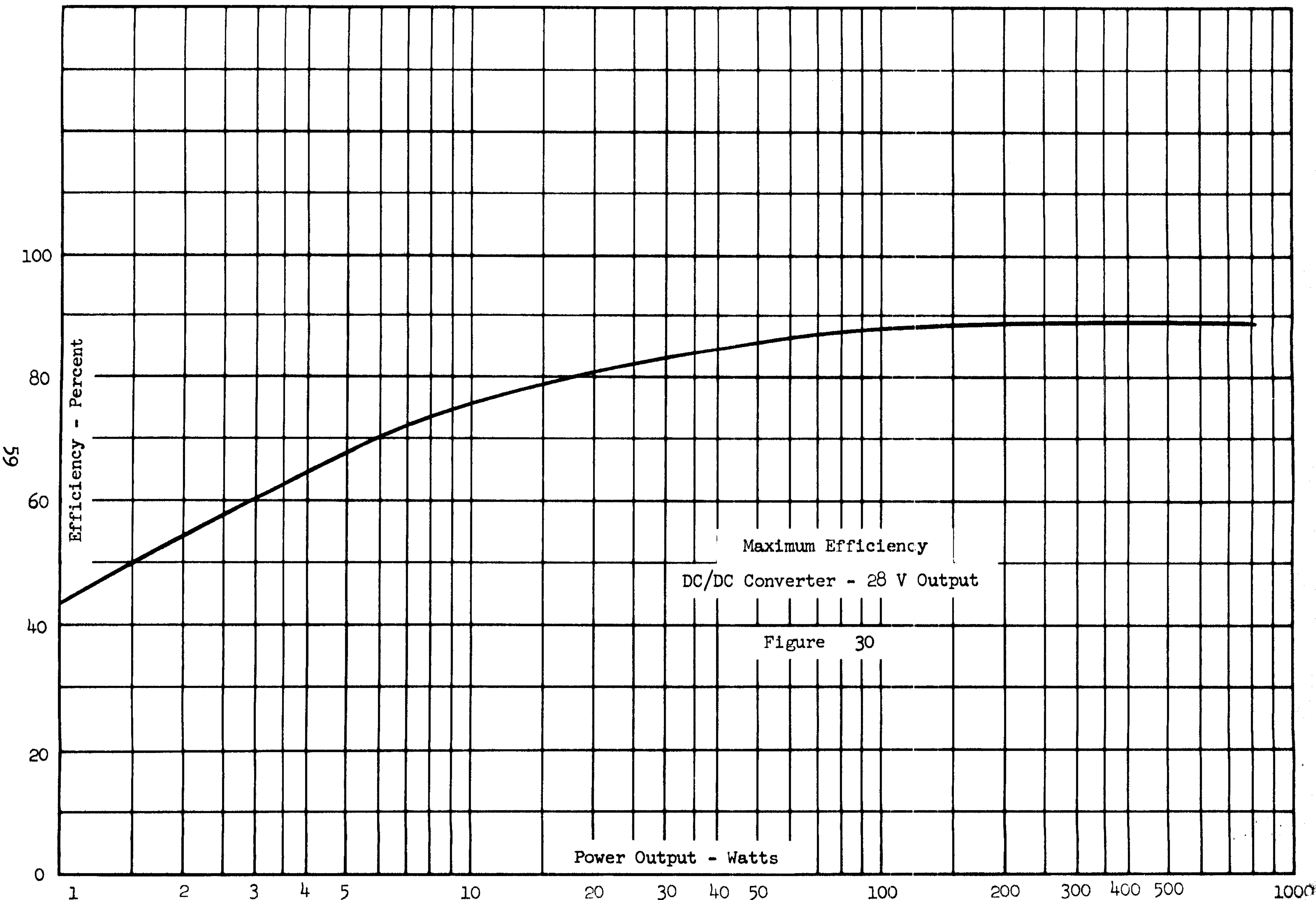
Maximum Efficiency
DC/DC Converter - 28 V Output
Efficiency - Percent
Power Output - Watts
0
20
40
60
80
100
1
2
3
4
5
10
20
30
40
50
100
200
300
400
500
1000

Figure 30

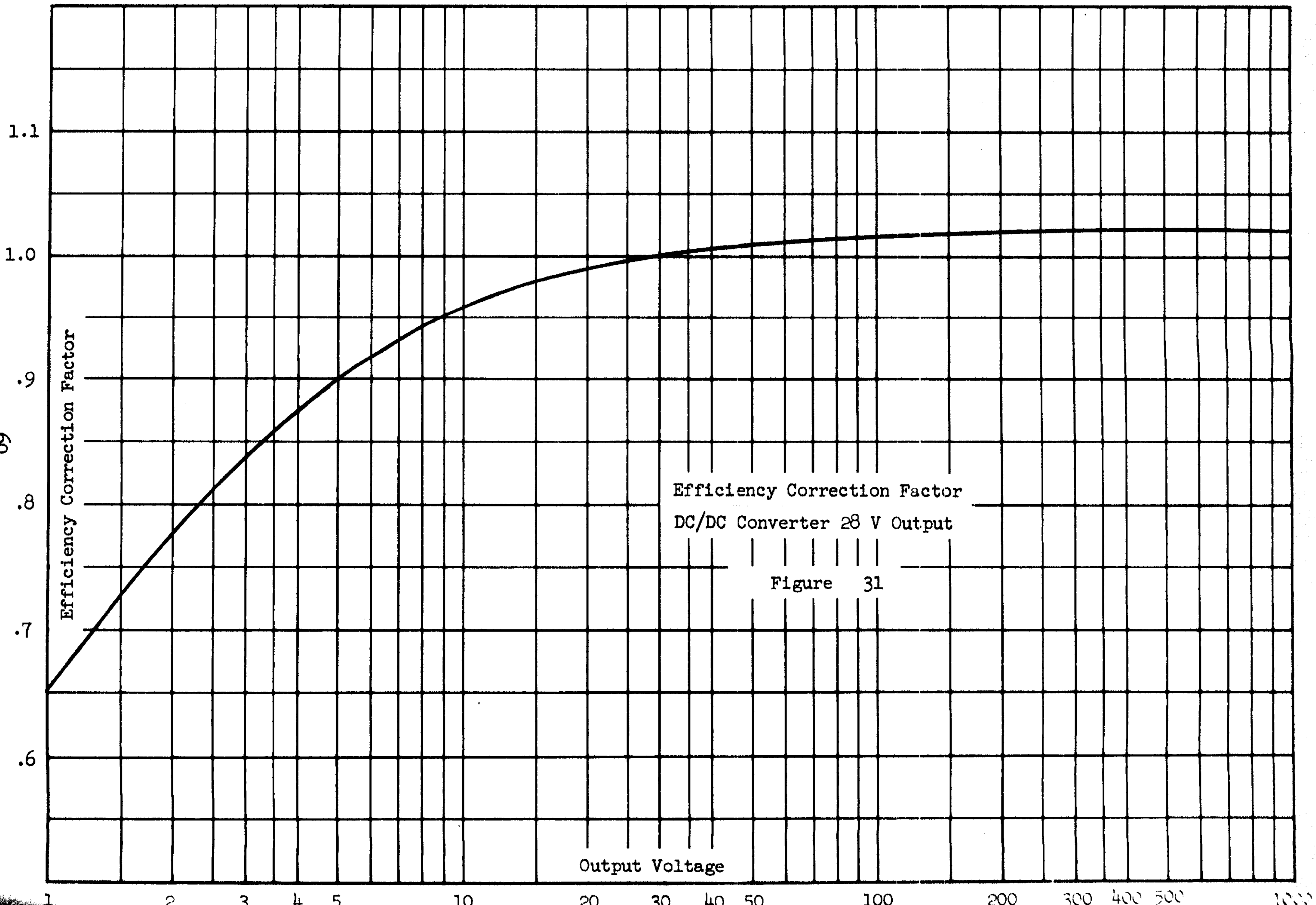

Efficiency Correction Factor
DC/DC Converter 28 V Output

Figure 31

of a 30 watt converter with five outputs as follows:

1. +15 at 5 W
2. -15 at 5 W
3. +28 at 10 W
4. +50 at 8 W
5. +3 at 2 W

The efficiency of a 30 watt converter at 10 KC switching rate from Figure 29, is 79%. The corrected efficiency is obtained by determining an overall efficiency correction factor (OECF) taking into account the respective power outputs and the ECF's.

Output	Efficiency Correction Factor (ECF)
+15	.98
-15	.98
+28	1.0
+50	1.01
+3	.835

$$OECF = \frac{.98(5) + .98\,(5) + 1.0\,(10) + 1.01\,(8) + .835\,(2)}{30}$$

OECF = .985

Corrected Efficiency = 79% (.985) = 77.7%

For DC/DC converters designed to operate at a particular input voltage when connected to a variable bus, efficiency decreases with higher input voltages. For a nominal 50 VDC input, converter efficiencies may increase approximately 2% reflecting the lower losses due to lower input current as compared to 28 VDC design. Voltages significantly greater than 50-60 volts will compromise the collector voltage breakdown ratings for available power transistors.

Standardization. Spacecraft requirements sometimes place undesirable physical and electrical performance constraints on the power conditioning equipment. Such factors as multiple output voltages, power proportioned for each output, tight regulation, low ripple, current limiting, and large input voltage range, cause the power conditioning equipment design to be less than optimum. All of these constraints limit serious design attempts toward standardization. However, despite this situation, attempts toward standardization are being made within TRW and presumably other companies. Discrete components such as resistors, capacitors, transistors, diodes, transformers, and inductors are assembled into packages called modules, which are named according to function and sub-function. These modules of cordwood and welded wire construction contained in a protective plastic housing reduce the number of visible nodes (terminals) and allow standardization. The finished "standard" module then becomes an entity which can be combined with four or more other modules to make a converter or inverter. These modules may be used unchanged in other applications, or with slight modification such as a change in resistor value.

The use of standard modules of this type helps to reduce costs, improve schedules, improve reliability and minimize electro-magnetic interference. The module approach yields an orderly arrangement of parts more readily producible with good packaging densities (.035 to .05 lbs/cu. in.).

3.3.3 Batteries

Electrical power systems for satellites or spacecraft basically have three choices of battery types - silver zinc, silver cadmium, and nickel cadmium. Because the state-of-the-art of sealed secondary (rechargeable) silver zinc batteries is not as advanced as the other two types, silver zinc batteries are not used for long life cycle operation. The primary (one shot) silver zinc is predominately used for short missions not requiring charge and discharge, and for peak power or emergency requirements on those vehicles having another source of continuous electrical power. The nickel cadmium battery has been in use the longest. However, the silver cadmium battery is being used more and more for two reasons: (1) it has a higher energy per unit weight, and (2) it is not magnetic in nature like the nickel cadmium. The nickel cadmium battery has a residual magnetic field, even when not in use. The magnitude and direction of this field varies as a function of its previous history of charge and discharge conditions.

To date, the nickel cadmium battery has demonstrated a better cycle life, but a steady improvement of silver cadmium performance is being realized.

Design data for the silver cadmium batteries is presented in Figures 32 through 41. Most of these data have been reduced to parametric form such that reasonable comparison can be made with other battery types. Figure 32 presents data on cycle life as accumulated from various test programs, under varying conditions. Sufficient tests have not been completed and documented to provide the most reliable design data. Most of the data points were derived from available information on Yardney cells. The cell capacity ratings as defined by Yardney are based on a C/15 charge rate and C/10 discharge rate at room temperature. In the following discussion of silver cadmium batteries, the cell capacity ratings have been re-defined to C/12 and C/4 charge and discharge rates, respectively. This re-definition of rates de-rated the battery capacities to more realisticly agree with satellite applications which use only the higher rates. The criteria for "failure" is defined as an occurrence of a catastrophic failure such as a cell open or short condition - or the inability of the battery (not cell) to supply the required (DOD) depth-of-discharge in a given cycle.

Figure 33 provides packaged battery weight per cell as a function of rated capacity. A packaging factor of 30% was used since the few existing designs fall in this area. However, as larger batteries are manufactured and used, a factor as low as 20% appears reasonable. The plot of temperature vs. ampere-hour efficiency in Figure 34, applies to any state of charge within the operating life of the battery. The maximum achievable input capacity is a function of the charge rate and temperature as shown in Figure 35, in terms of the end of life capacity.

Output capacity varies with temperature, charge rate, and discharge rate. Figures 36 and 37 present the family of these curves in terms of (Ce) end of life capacity. The charge and discharge voltage curves as a function of capacity and at several temperatures appear on Figures 38 and 39. The relationships of discharge rate and temperature on energy efficiency and weight are shown in Figures 40 and 41.

A similar set of parametric design data are presented in Figures 42 through 54, for the nickel cadmium batteries. Because this type of battery has a longer history, the data is more refined and lends itself to a systematic design approach. An example of a battery design will be used to demonstrate the use of these curves.

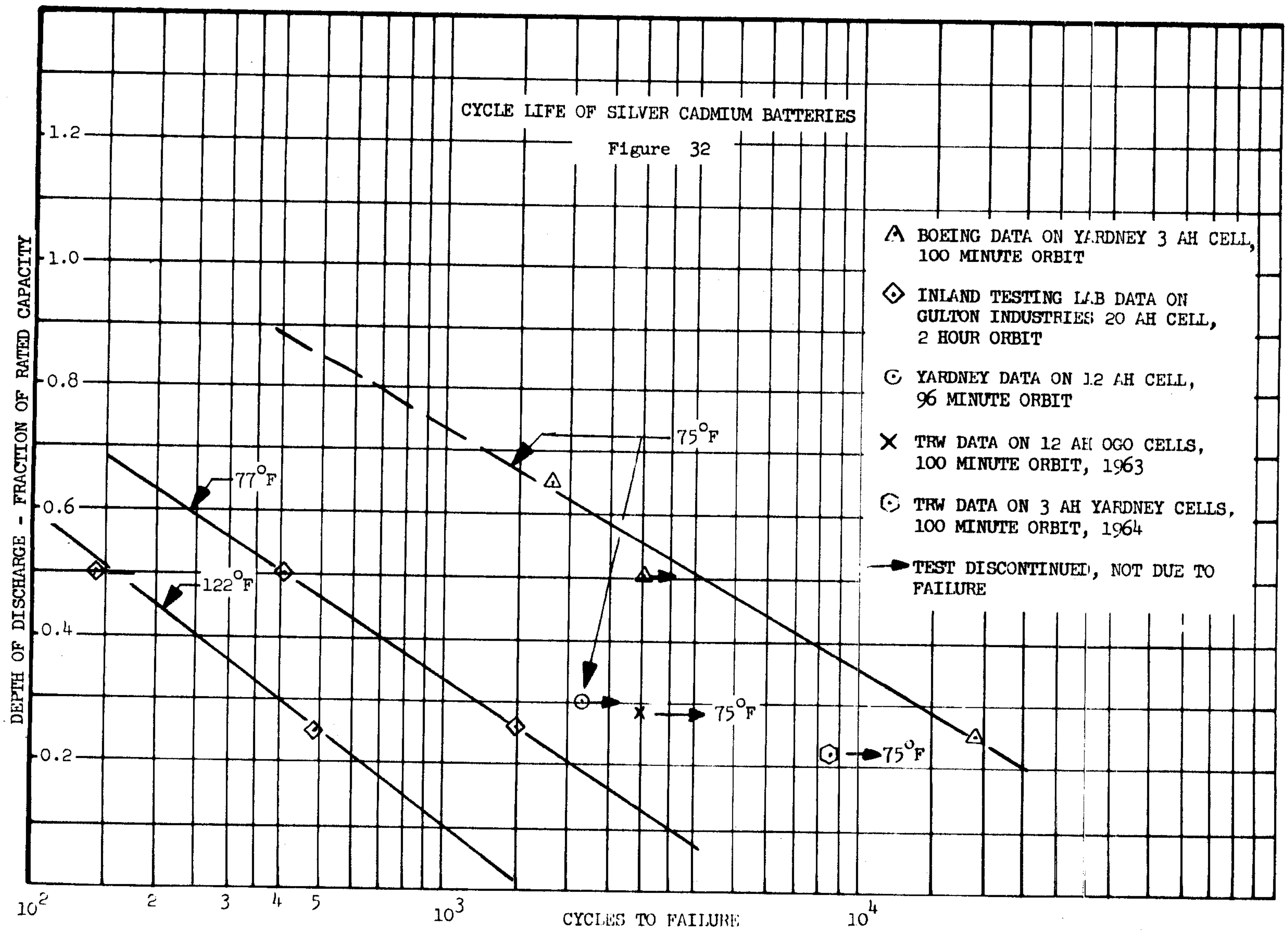
CYCLE LIFE OF SILVER CADMIUM BATTERIES
Figure 32
BOEING DATA ON YARDNEY 3 AH CELL, 100 MINUTE ORBIT
INLAND TESTING LAB DATA ON GULTON INDUSTRIES 20 AH CELL, 2 HOUR ORBIT
YARDNEY DATA ON 12 AH CELL, 96 MINUTE ORBIT
TRW DATA ON 12 AH OGO CELLS, 100 MINUTE ORBIT, 1963
TRW DATA ON 3 AH YARDNEY CELLS, 100 MINUTE ORBIT, 1964
TEST DISCONTINUED, NOT DUE TO FAILURE
75°F
77°F
122°F
75°F
75°F
1.2
1.0
0.8
0.6
0.4
0.2
DEPTH OF DISCHARGE - FRACTION OF RATED CAPACITY
10^2
2
3
4
5
10^3
10^4
CYCLES TO FAILURE

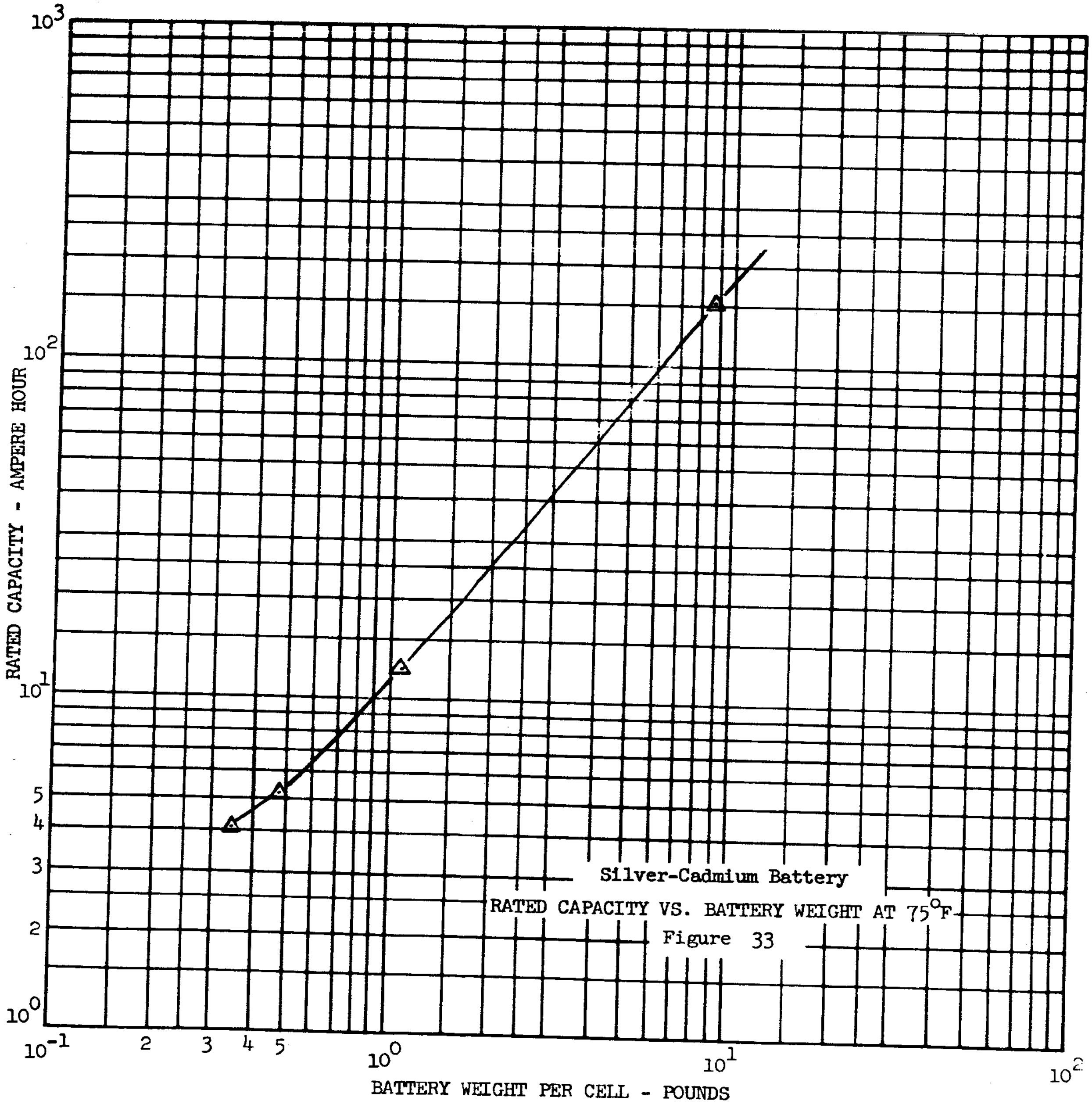

Silver-Cadmium Battery

RATED CAPACITY VS. BATTERY WEIGHT AT 75°F

Figure 33

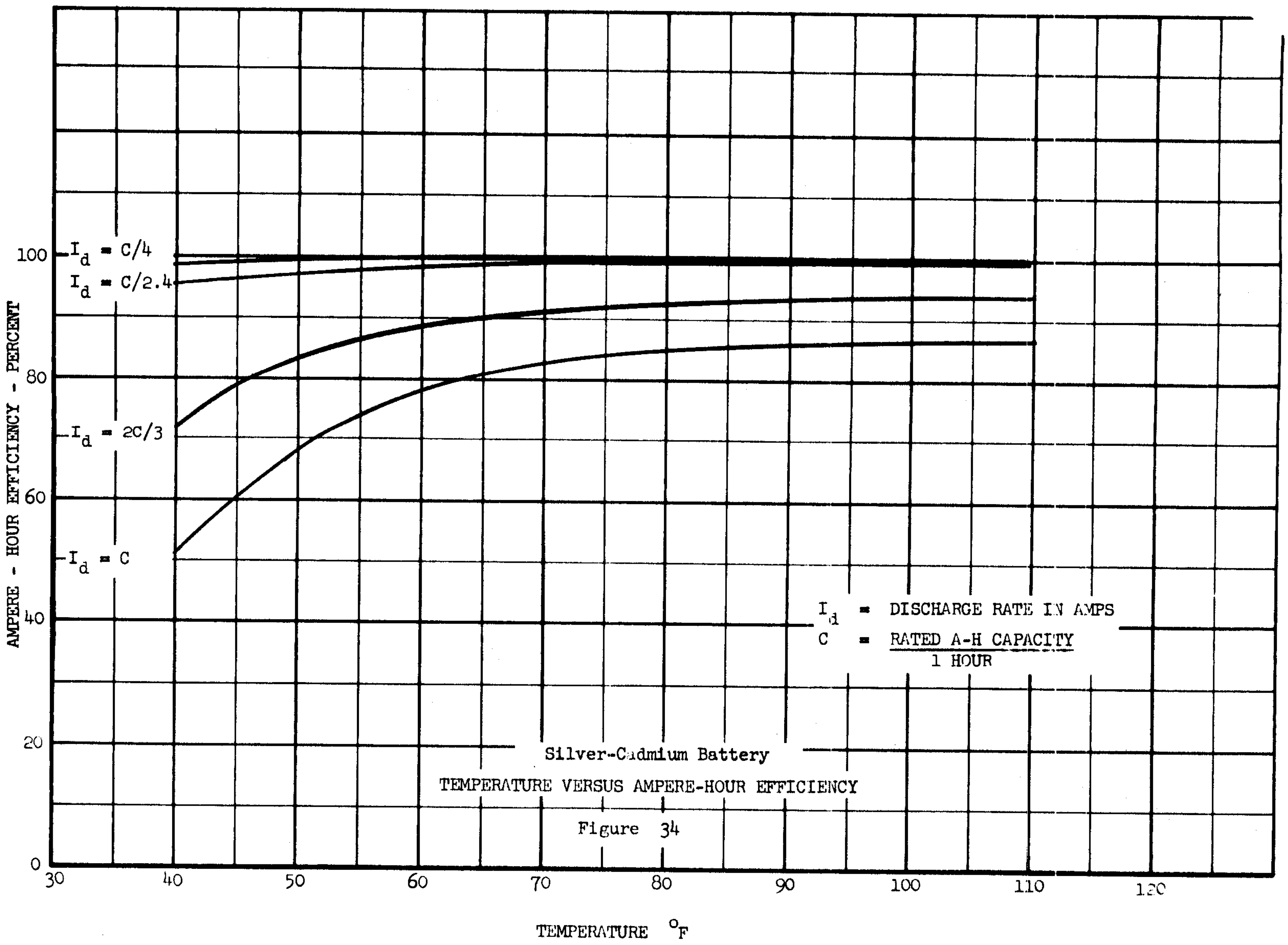

Silver-Cadmium Battery

TEMPERATURE VERSUS AMPERE-HOUR EFFICIENCY

Figure 34

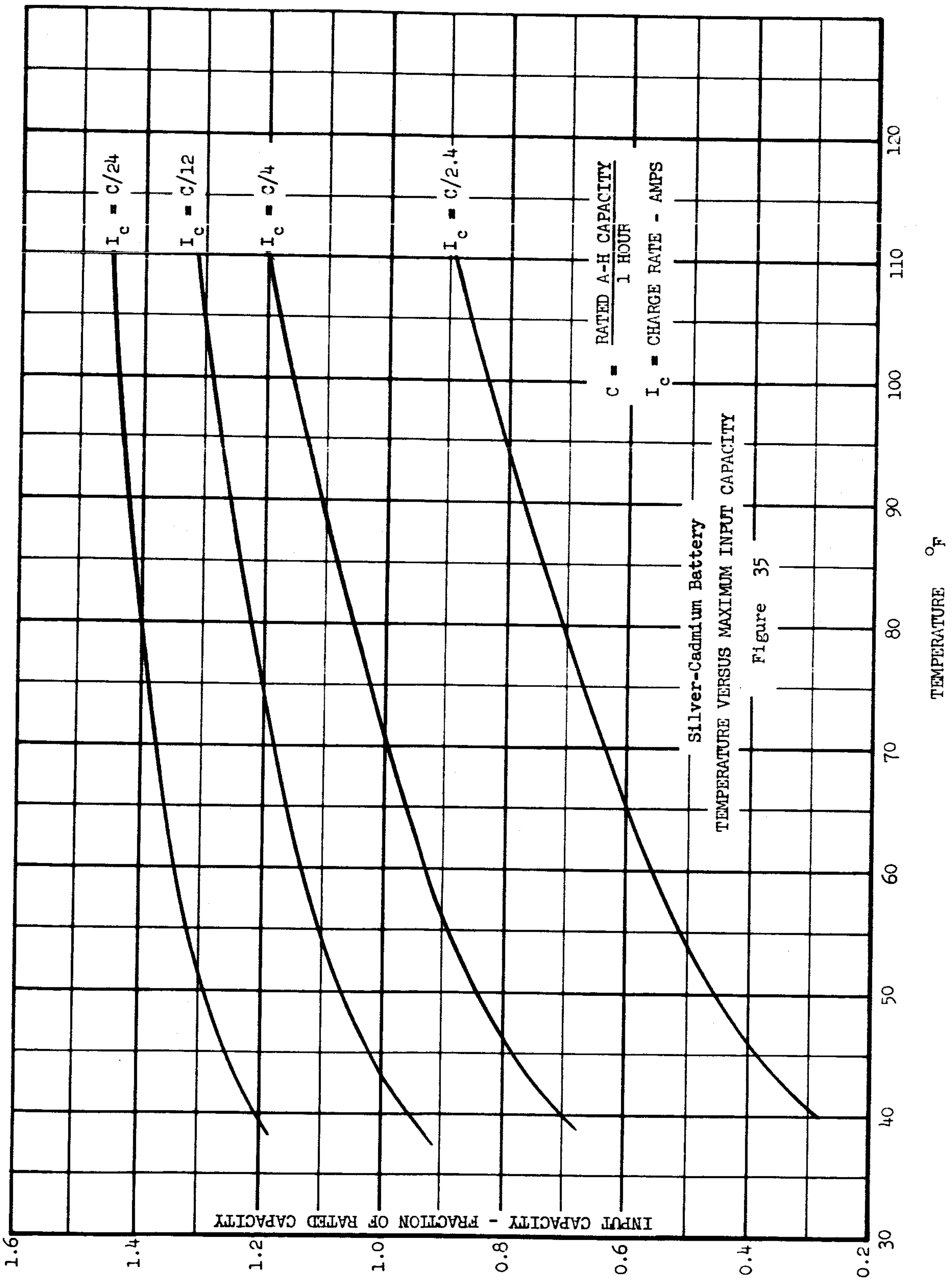

Silver-Cadmium Battery
TEMPERATURE VERSUS MAXIMUM INPUT CAPACITY
Figure 35

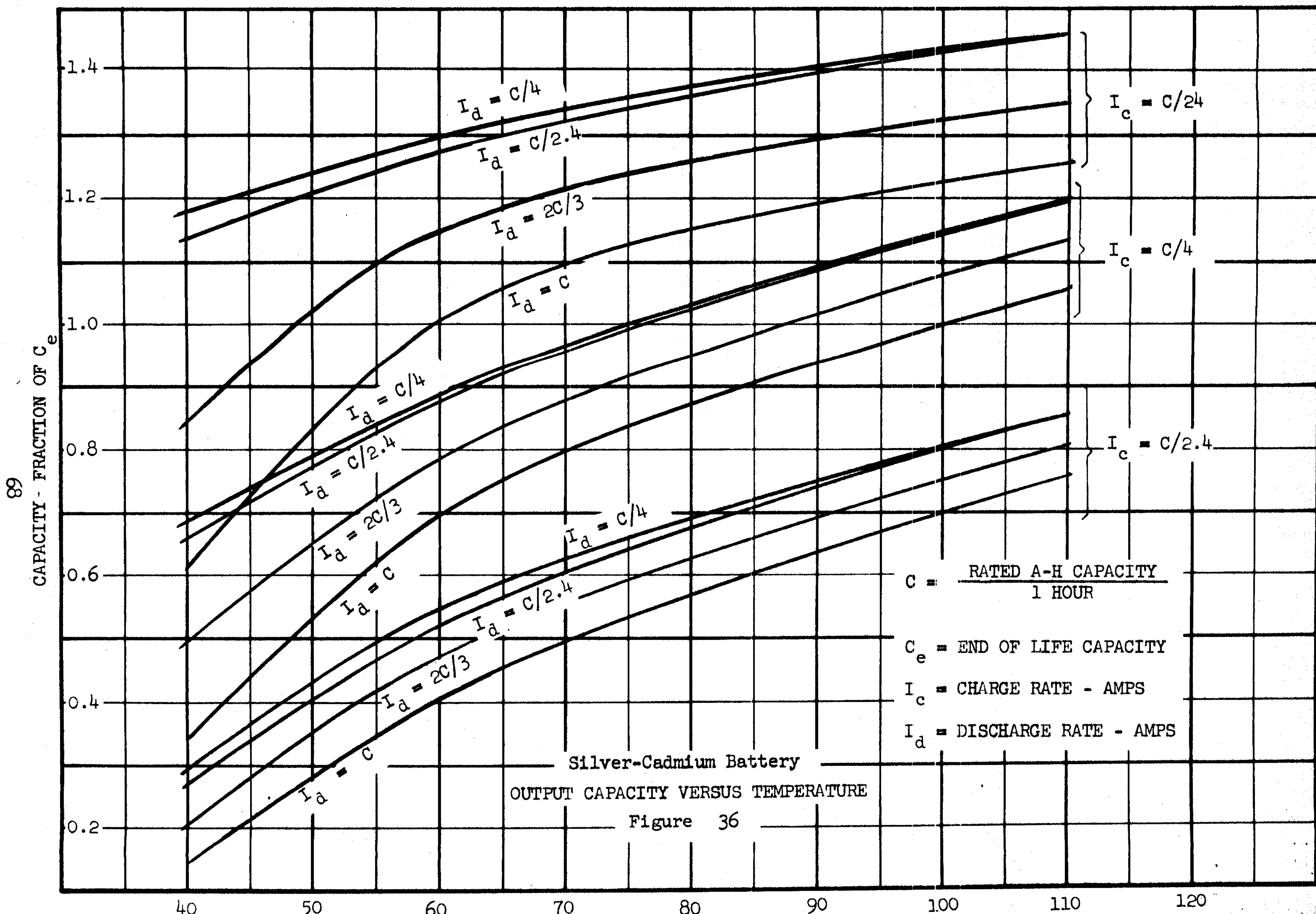

Silver-Cadmium Battery
OUTPUT CAPACITY VERSUS TEMPERATURE
Figure 36

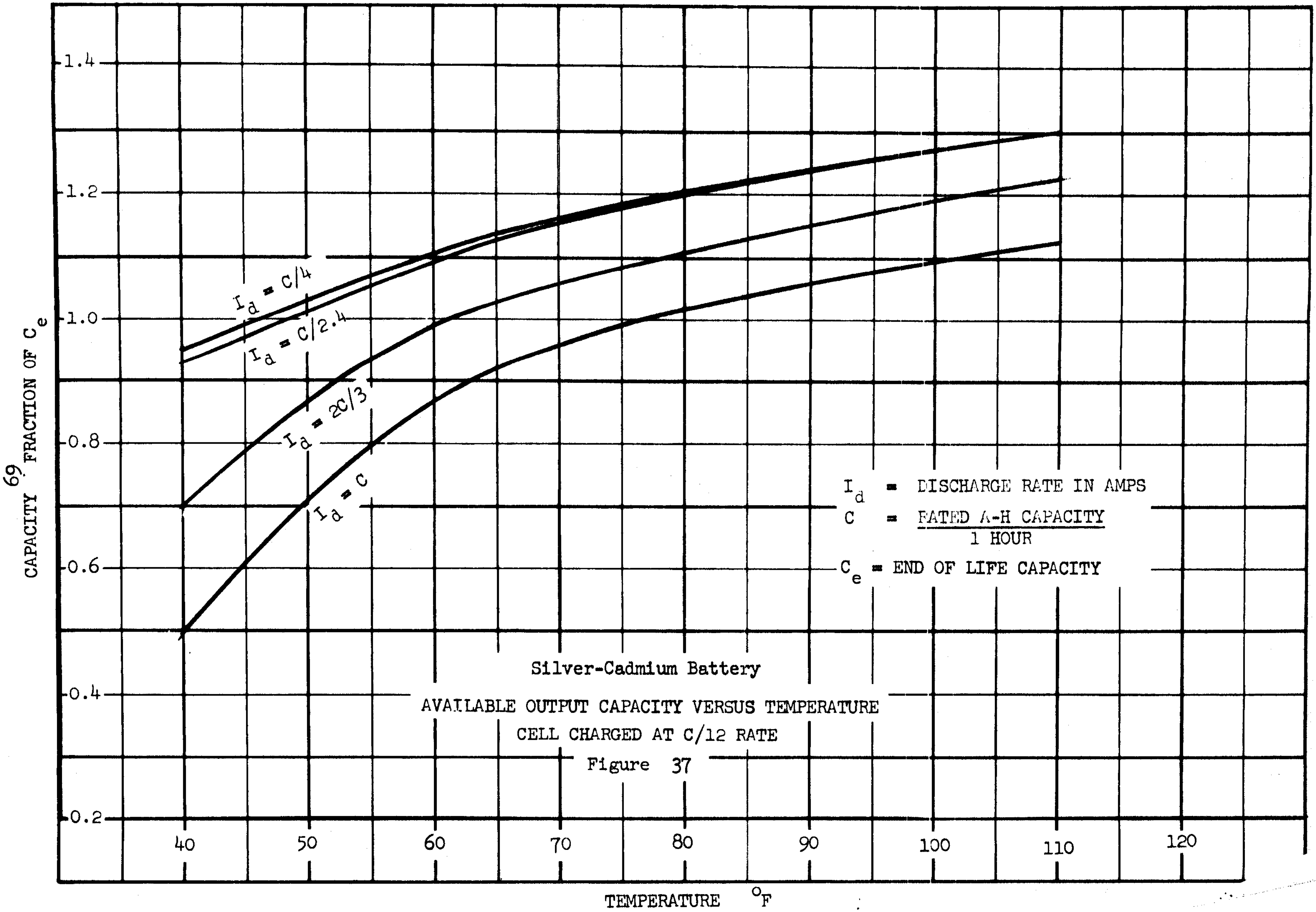

Silver-Cadmium Battery

AVAILABLE OUTPUT CAPACITY VERSUS TEMPERATURE

CELL CHARGED AT C/12 RATE

Figure 37

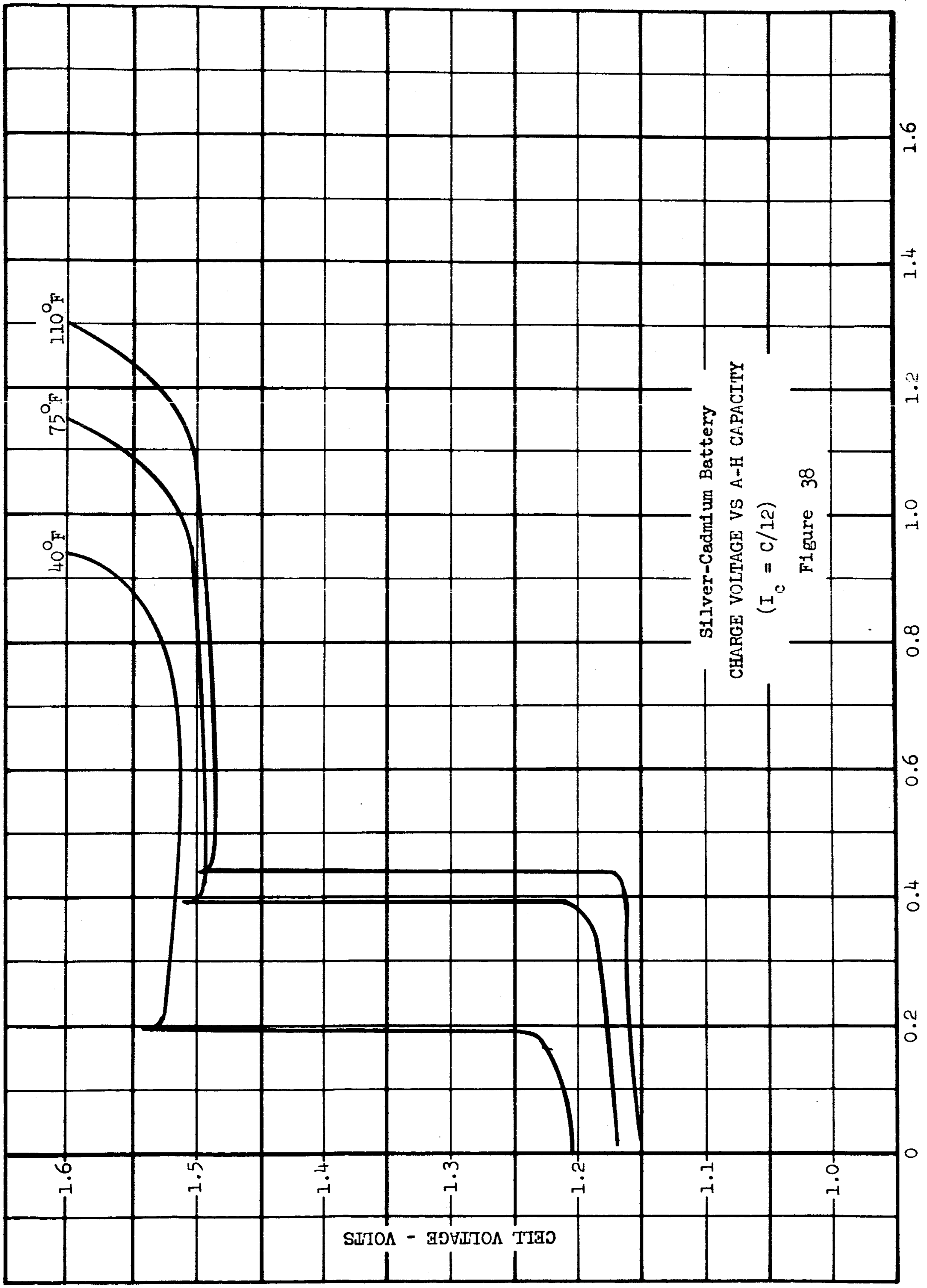

Silver-Cadmium Battery
CHARGE VOLTAGE VS A-H CAPACITY
(I_c = C/12)
Figure 38

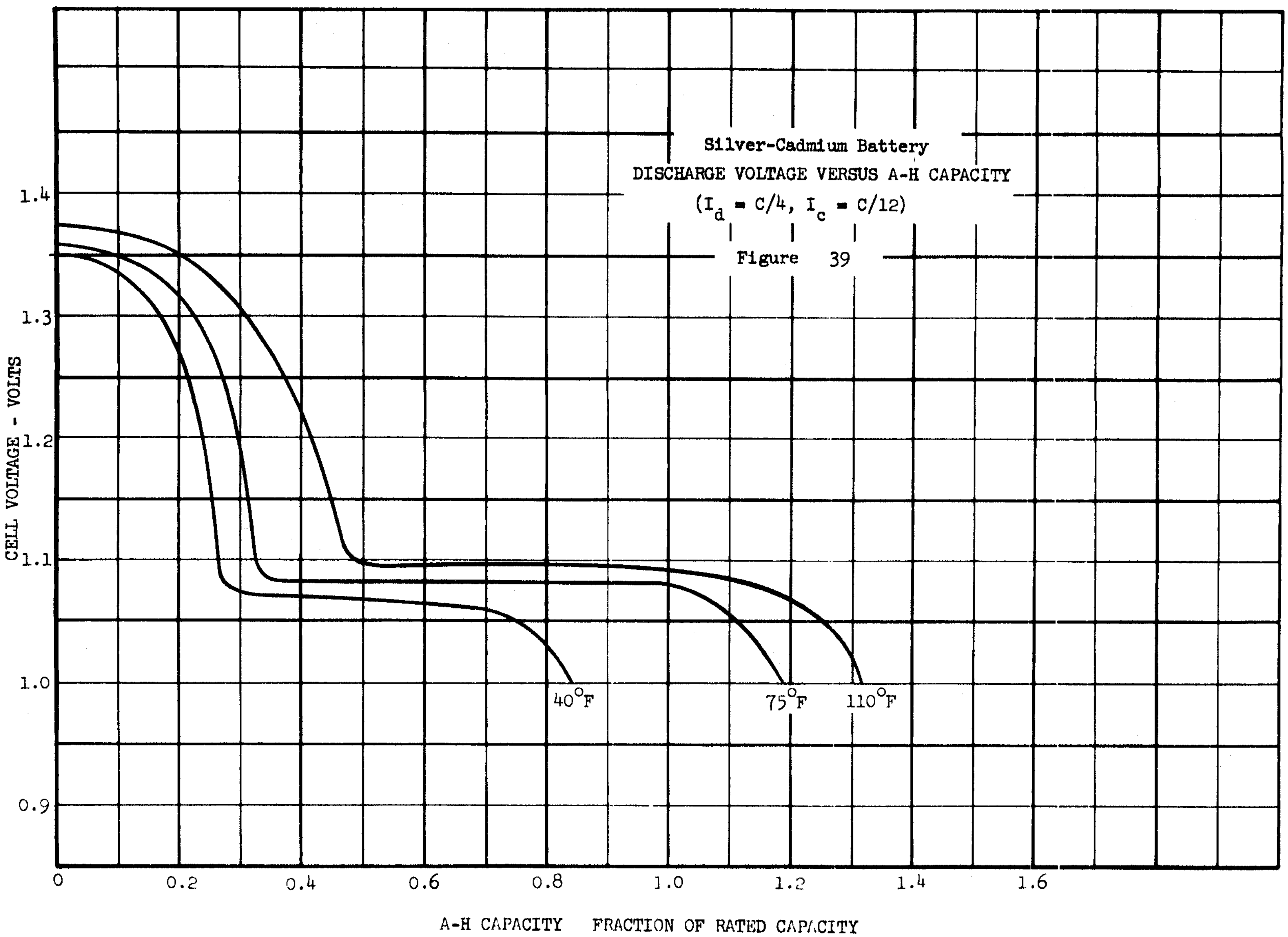
Silver-Cadmium Battery
DISCHARGE VOLTAGE VERSUS A-H CAPACITY
(I_d = C/4, I_c = C/12)
Figure 39
40°F
75°F
110°F
1.4
1.3
1.2
1.1
1.0
0.9
CELL VOLTAGE - VOLTS
0
0.2
0.4
0.6
0.8
1.0
1.2
1.4
1.6
A-H CAPACITY FRACTION OF RATED CAPACITY

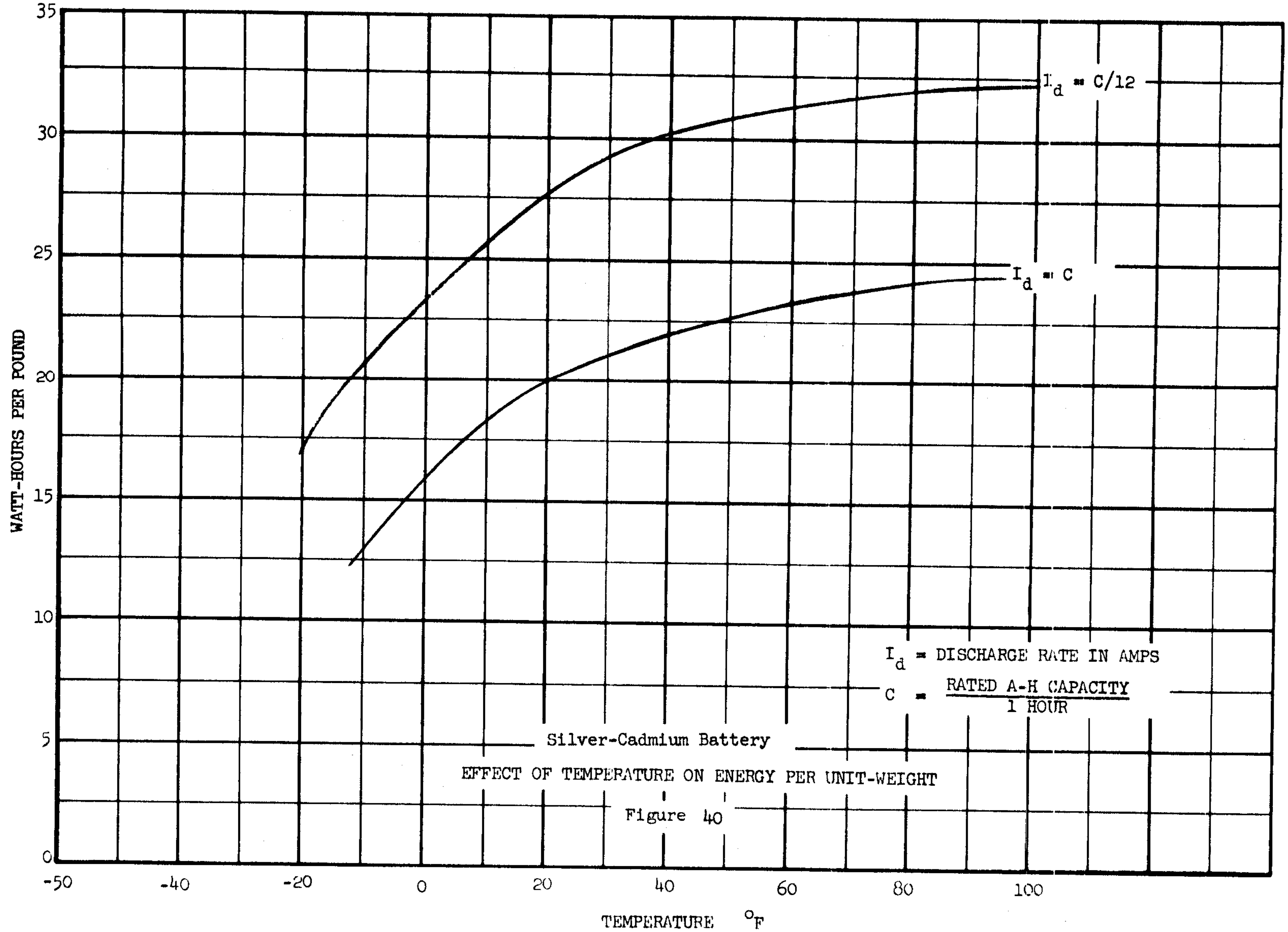

Silver-Cadmium Battery

EFFECT OF TEMPERATURE ON ENERGY PER UNIT-WEIGHT

Figure 40

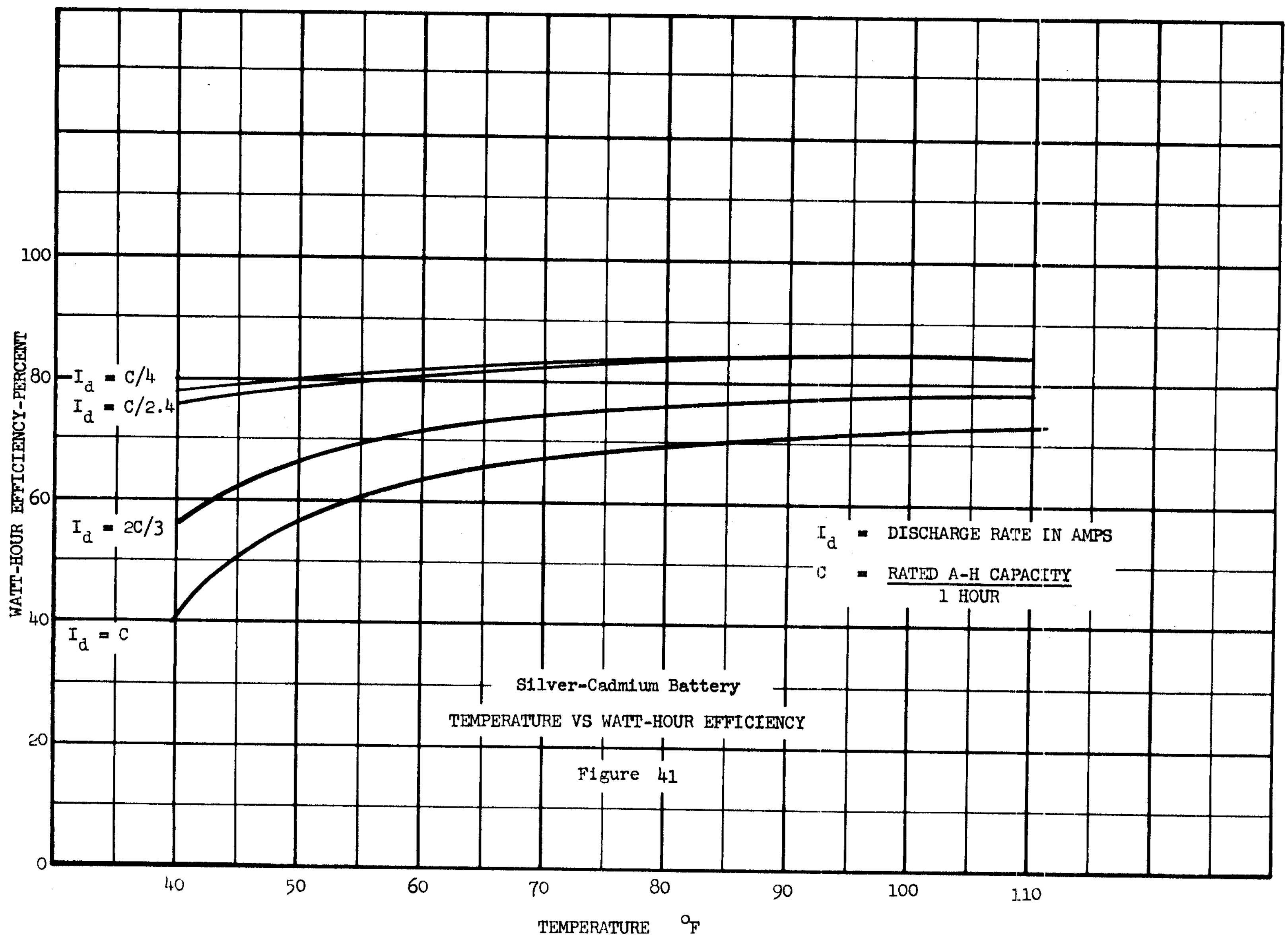

Silver-Cadmium Battery

TEMPERATURE VS WATT-HOUR EFFICIENCY

Figure 41

Example:

From the spacecraft mission and orbital considerations the following requirements are given:

Life	1000 cycles
Load Capacity (C_d) at end of life	3 AH
Discharge current (I_d)	3.0 Amps
Discharge Temperature (T_d)	50° F
Charge current (I_c)	1.5 Amps
Charge temperature (T_c)	96° F

Step (a): Assume $i_d = 0.5 \frac{\text{Amps}}{\text{AH}} = 0.5$ 1/hr

Define: $i_d = \frac{I_d}{C_e}$ $\qquad i_c = \frac{I_c}{C_e}$

C_d = Discharge capacity at end of life for a given charge current density (i_c) and ampere-hour efficiency (η).

C_e = Maximum available capacity at end of life for a given charge current density (i_c) and discharge current density (i_d).

C_e' = Maximum available capacity at end of life for a given optimum charge and discharge current.

C_r = Manufacturers ampere-hour rated capacity.

Step (b): From Figure 42, at $i_d = 0.5$ and $T_d = 50^{\circ}$F.

$C_e/C_e' = 0.825$

(Before any derating occurs, $C_e = C_d = 3$ AH.)

$$C_e' = \frac{C_d}{0.825} = 3.636 \text{ AH}$$

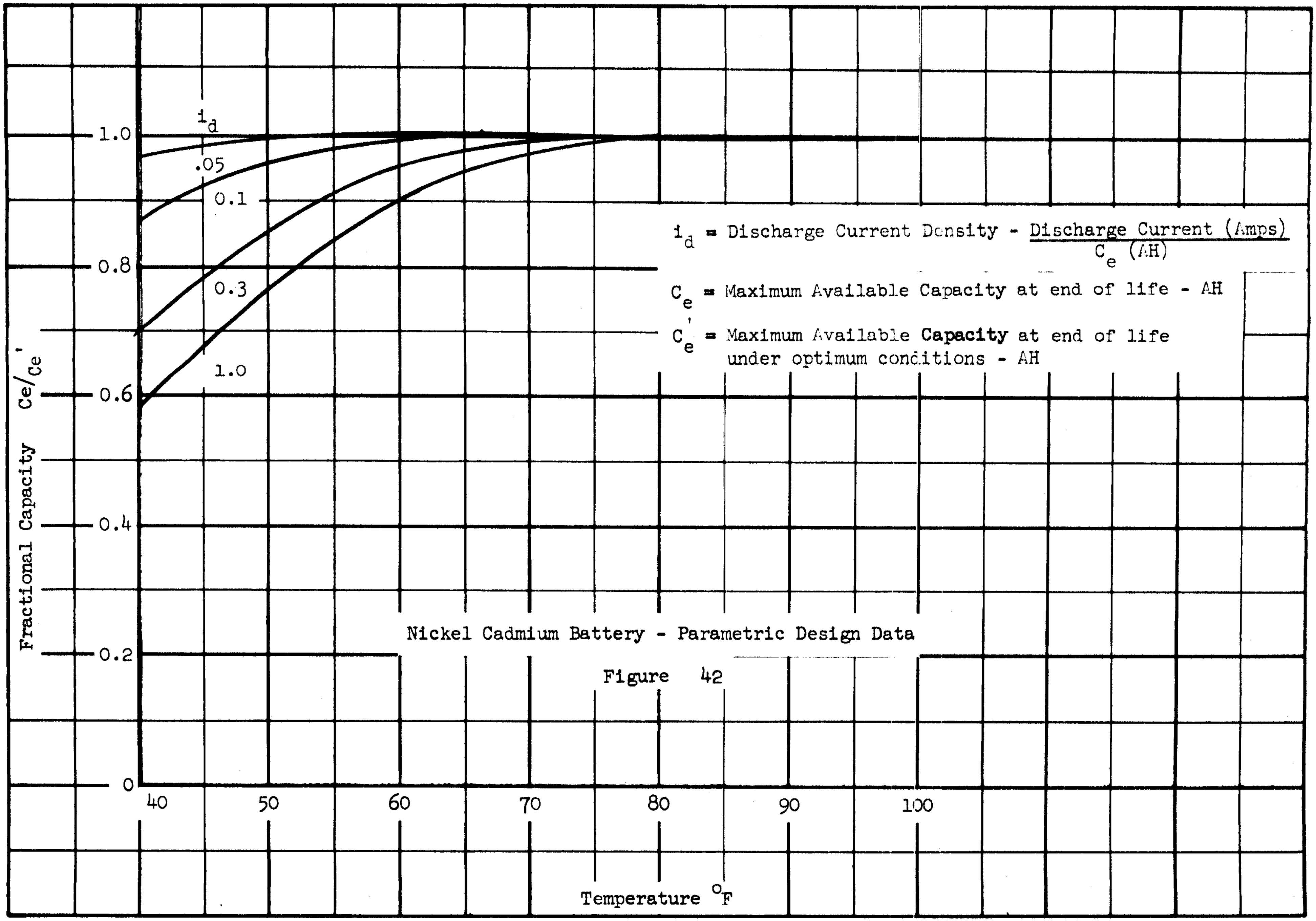

Nickel Cadmium Battery - Parametric Design Data

Figure 42

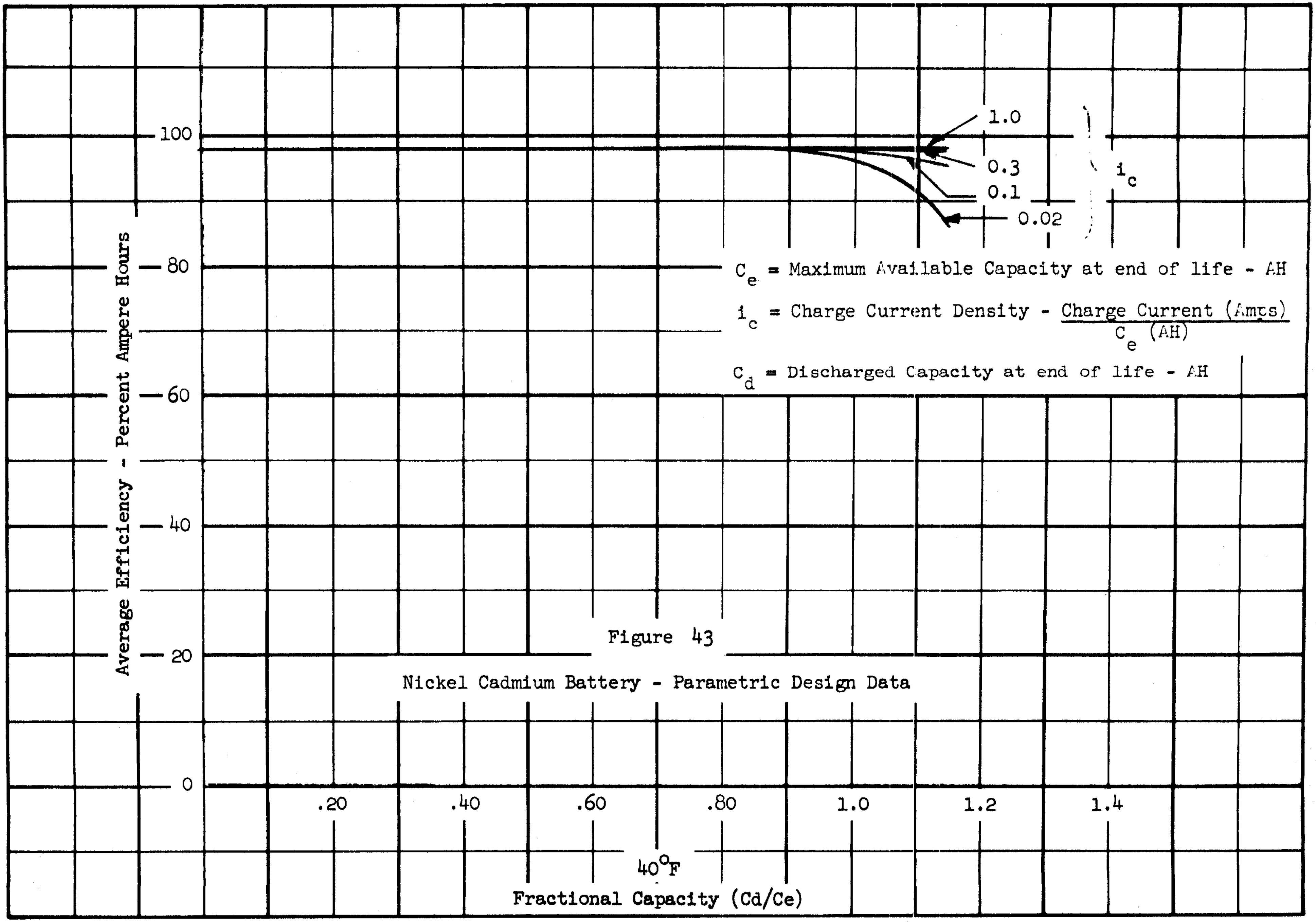

Figure 43

Nickel Cadmium Battery - Parametric Design Data

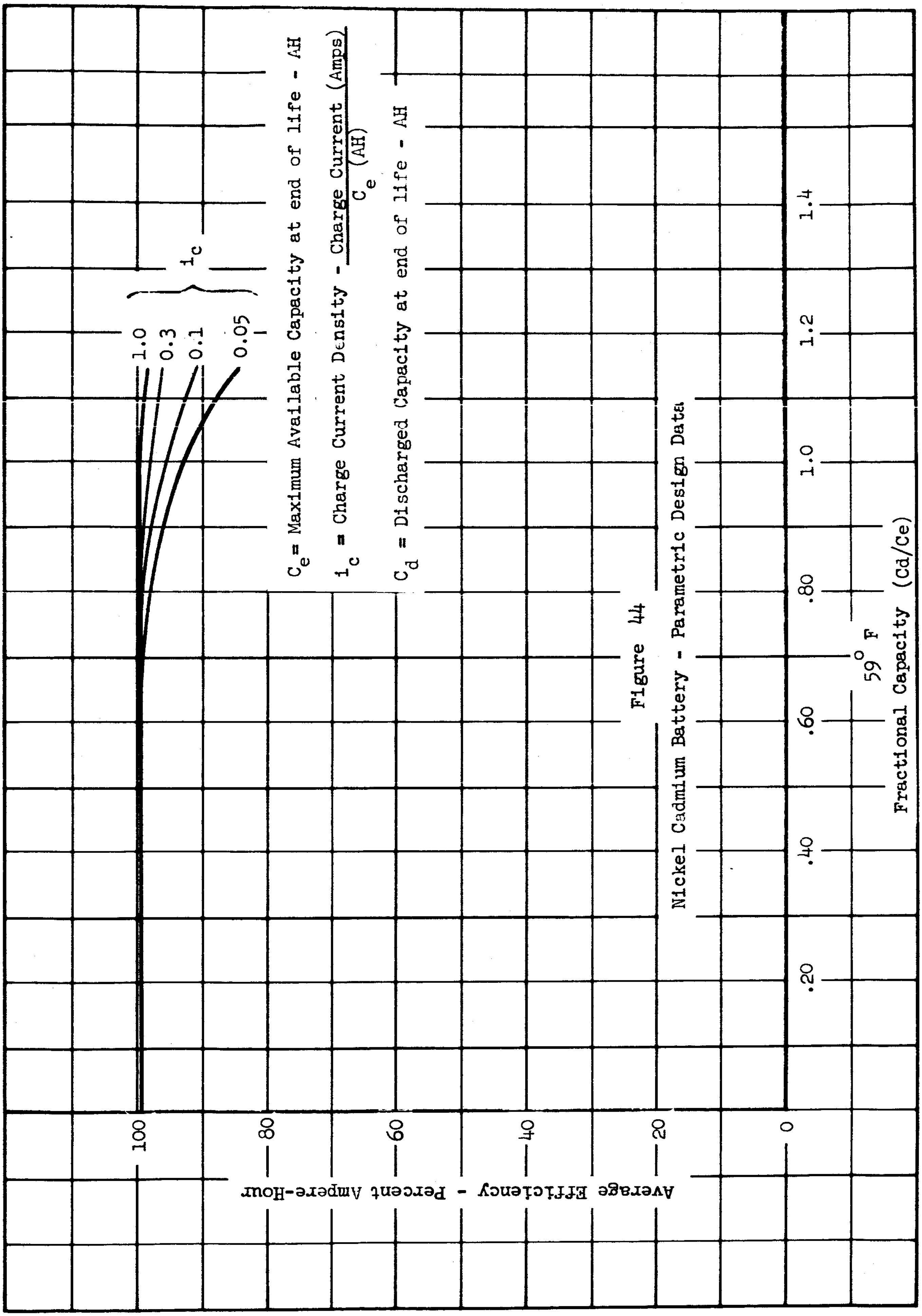

Figure 44
Nickel Cadmium Battery - Parametric Design Data

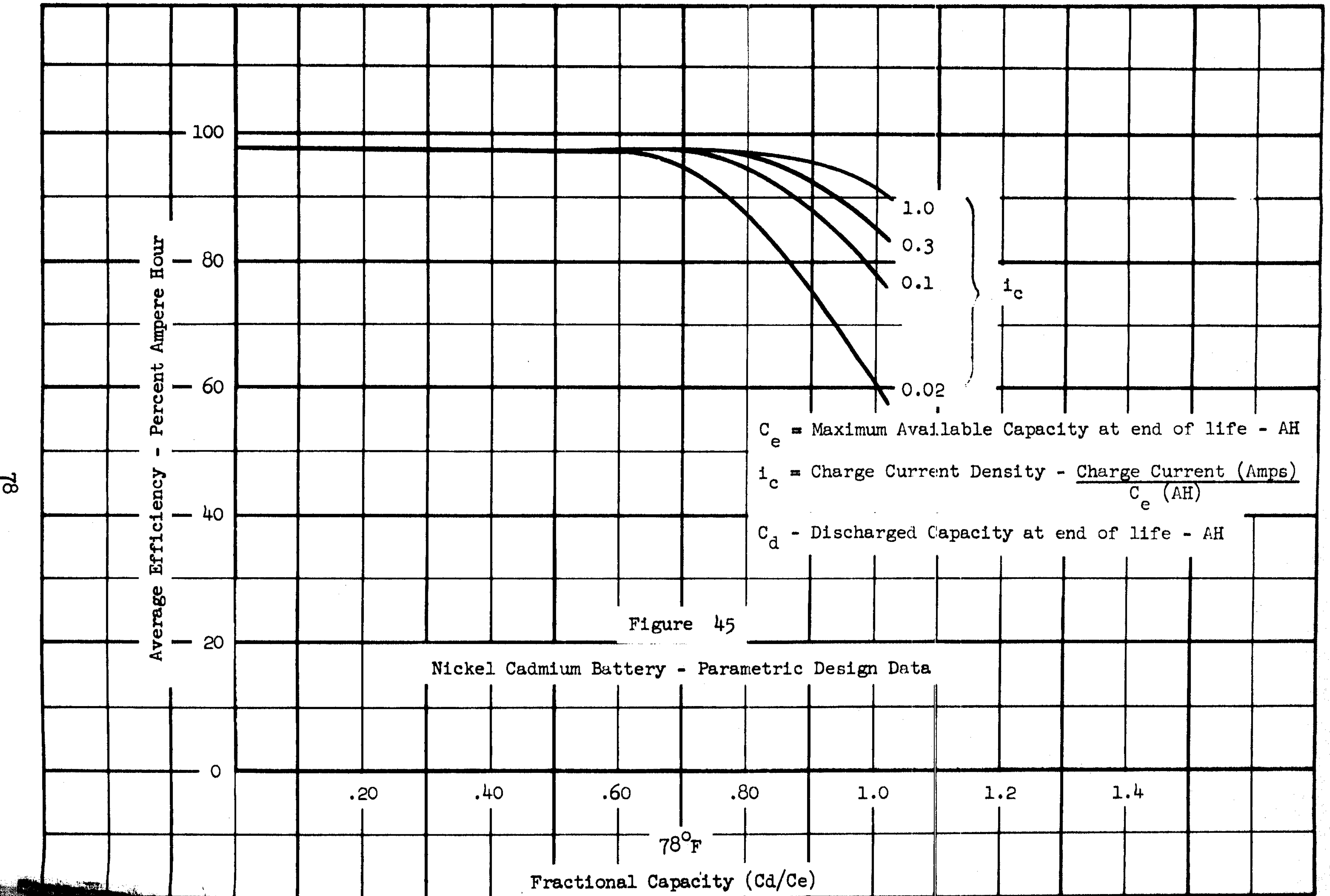

Figure 45

Nickel Cadmium Battery - Parametric Design Data

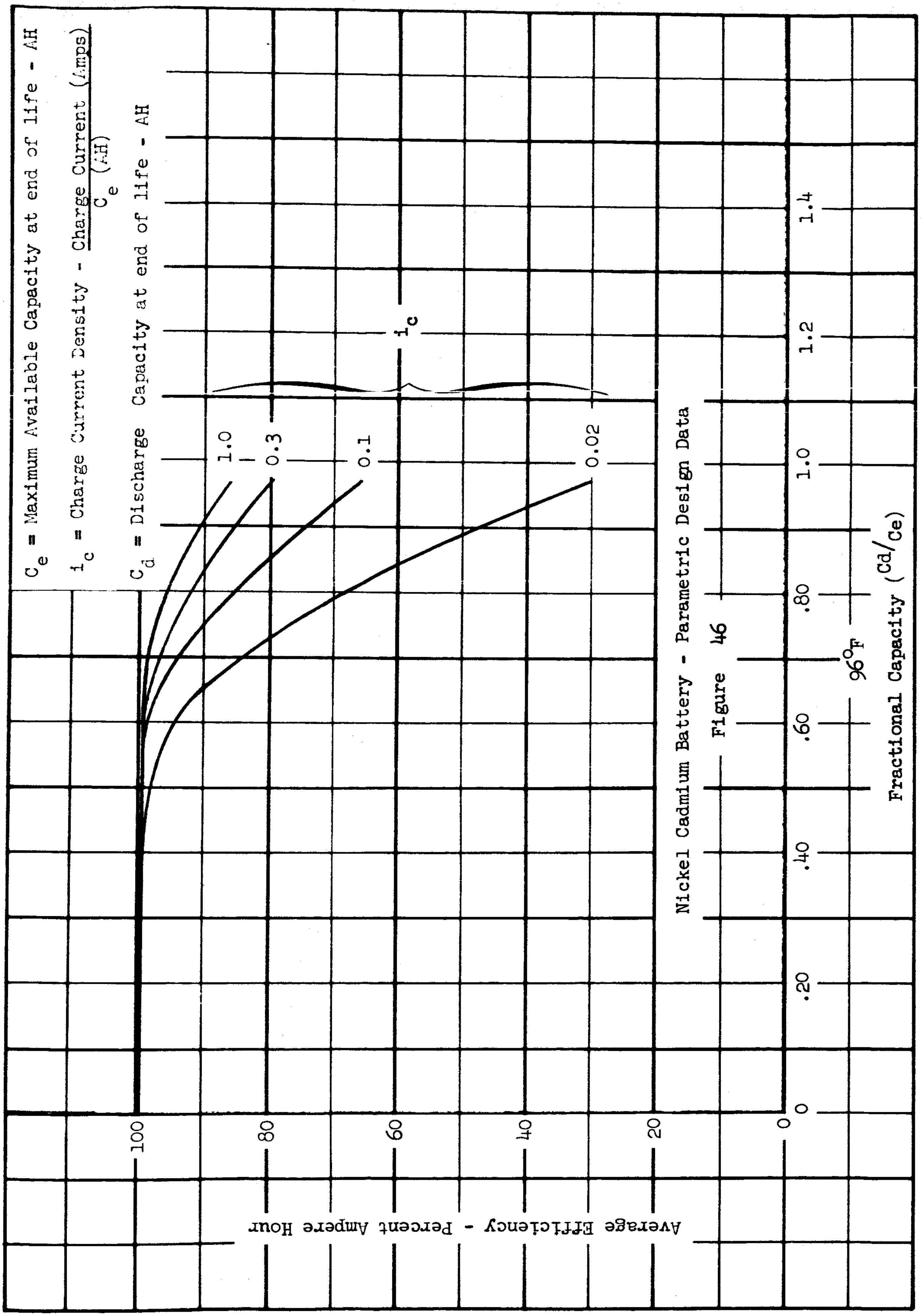

Nickel Cadmium Battery - Parametric Design Data

Figure 46

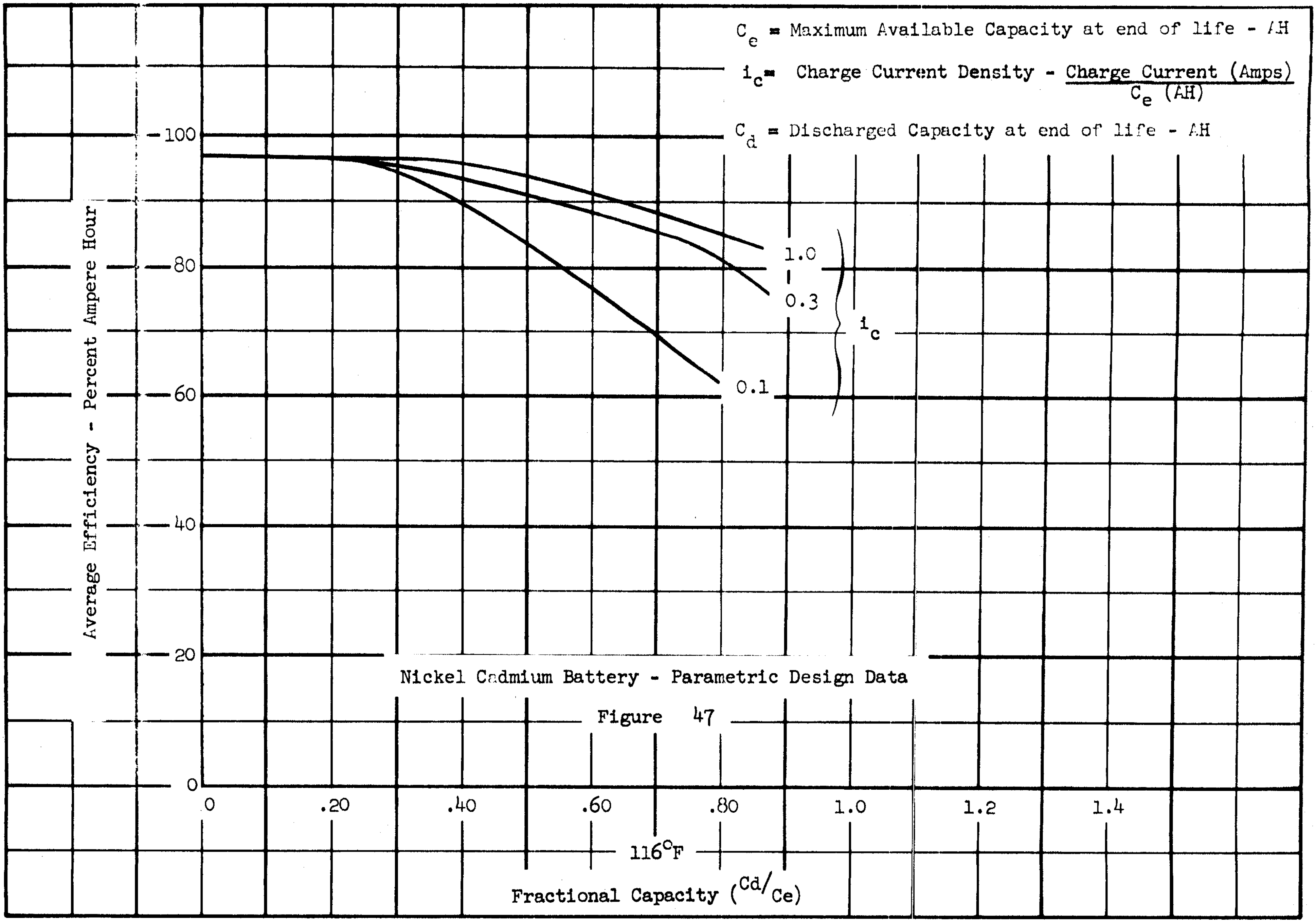

Nickel Cadmium Battery - Parametric Design Data

Figure 47

$$i_c = \frac{I_c}{C_e'} = \frac{1.5 \text{ Amps}}{3.636 \text{ AH}} = 0.4125$$

Figures 43 through 47 are a set of efficiency curves for various charge temperatures.

Step (c): Assume a charge efficiency of 90%.

Step (d): From Figure 46 having a charge temperature of $96^{\circ}F$ - read $C_d/C_e = 0.835$ for $\eta = 90\%$, $i_c = 0.4125$

Step (e): Let a new $C_d = 3.636$ AH from the previous C_e' calculation.

The new $C_e = \frac{C_d}{0.835} = \frac{3.636}{0.855} = 4.354$ AH

This should be the de-rated AH capacity required for these specific charge and discharge conditions. However $i_d = 0.5$ was assumed.

Step (f): Examine $i_d = 0.5$ assumption.

$$i_d = \frac{I_d}{C_e} = \frac{3 \text{ Amps}}{4.354 \text{ AH}} = 0.689$$

Thus, $i_d \neq 0.5$ as assumed and a further iteration is required.

Step (g): Return to Figure 42 for $i_d = 0.689$ and $T_d = 50^{\circ}F$.

New $C_e/C_e' = 0.800$

$$C_e' = \frac{Ce}{0.8} = \frac{3 \text{ AH}}{0.80} = 3.750 \text{ AH}$$

Step (h): Calculate new i_c

$$i_c = \frac{I_c}{C_e'} = \frac{1.5 \text{ Amps}}{3.750 \text{ AH}} = 0.400$$

Step (i): From Figure 46 again obtain a new C_d/C_e where

$i_c = 0.400$, $\eta = 90\%$

$C_d/C_e = 0.830$

$$C_e = \frac{3.750}{0.830} = 4.518 \text{ AH}$$

Step (j): Re-examine last value of i_d used

$$i_d = \frac{I_d}{C_e} = \frac{3 \text{ Amps}}{4.518 \text{ AH}} = 0.664$$

This $i_d \neq 0.689$ last assumed. A further iteration is required.

Step (k): Return to Figure 42 for $i_d = 0.664$, $T_d = 50^\circ F$

New $C_e/C_e' = 0.805$

$$C_e' = \frac{3 \text{ AH}}{0.805} = 3.726$$

Step (l): Calculated new i_c

$$i_c = \frac{1.5 \text{ Amps}}{3.726 \text{ AH}} = 0.4025$$

Step (m): From Figure 46,

new $C_d/C_e = 0.832$

$$C_e = \frac{3.726}{0.832} = 4.478 \text{ AH}$$

Step (n): Re-examining i_d assumption

$$i_d = \frac{3 \text{ Amps}}{4.478 \text{ AH}} = 0.6699$$

This is close enough to assumed

$i_d = 0.664$

Therefore:

$C_e = 4.478$ AH

$I_d = 3$ Amps, $i_d = 0.67$

$I_c = 1.5$ Amps, $i_c = 0.335$

Step (o): From Figure 48,

The depth of discharge C_e/C_r for 1000 cycles is 55%.

Therefore the rated capacity required to be installed for minimum weight and maximum reliability is

$$C_r = \frac{4.478 \text{ AH}}{.55} = 8.4 \text{ AH or } 8 \text{ AH}$$

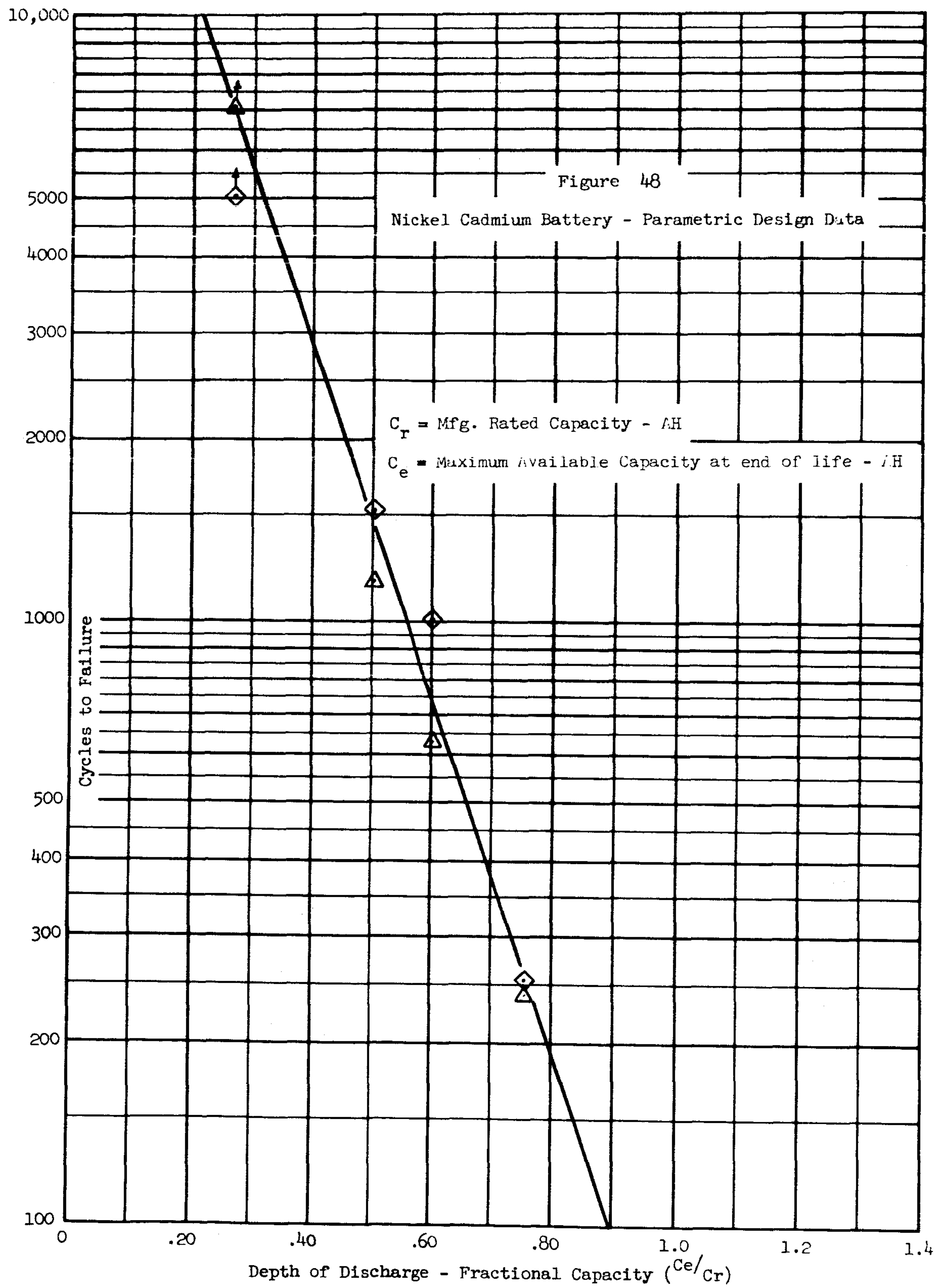
Figure 48
Nickel Cadmium Battery - Parametric Design Data
C_r = Mfg. Rated Capacity - AH
C_e = Maximum Available Capacity at end of life - AH
Cycles to Failure
10,000
5000
4000
3000
2000
1000
500
400
300
200
100
0
.20
.40
.60
.80
1.0
1.2
1.4
Depth of Discharge - Fractional Capacity ($^{Ce}/_{Cr}$)

Step (p): From Figure 49, the weight of packaged battery is 0.95 lbs per cell. The battery total weight is determined by multiplying this number by the number of cells required to meet the system bus voltage.

Efficiency data as a function of temperature, current and state of charge are extrapolations of experimental data obtained at a single current over a range of temperature. Experimental data at C/3 may be relied upon. Data at all other currents should be expected to show increasing error as the deviation from C/3 increases in either direction. No weighting, either for conversatism or optimism has been applied.

Cycling life versus depth of discharge data are those extracted from NASA - SP 5004, "Space Batteries", after eliminating the effects of discharge at low temperatures. Since these data already are statistically confounded with, and are inseparable from, the effects of current (which varies with depths of discharge in a 90 minute orbit cycle), when combined with earlier steps in the analysis, the result is a conservative approach.

Figures 51 through 54 show the effect that can be accomplished with a nickel cadmium battery by revitalization treatments. In effect, this restores the battery to near its original capacity after an extended period of cycling. By setting the period between revitalization treatments equal to or less than the original cycle life of the battery, mission life of the battery can be extended significantly. The limited data now available has not established any limit to the number of times a nickel cadmium battery can be revitalized and thereby multiply its original cycle life by the number of revitalization periods. This treatment has been used on some of the later TRW spacecraft power system designs.

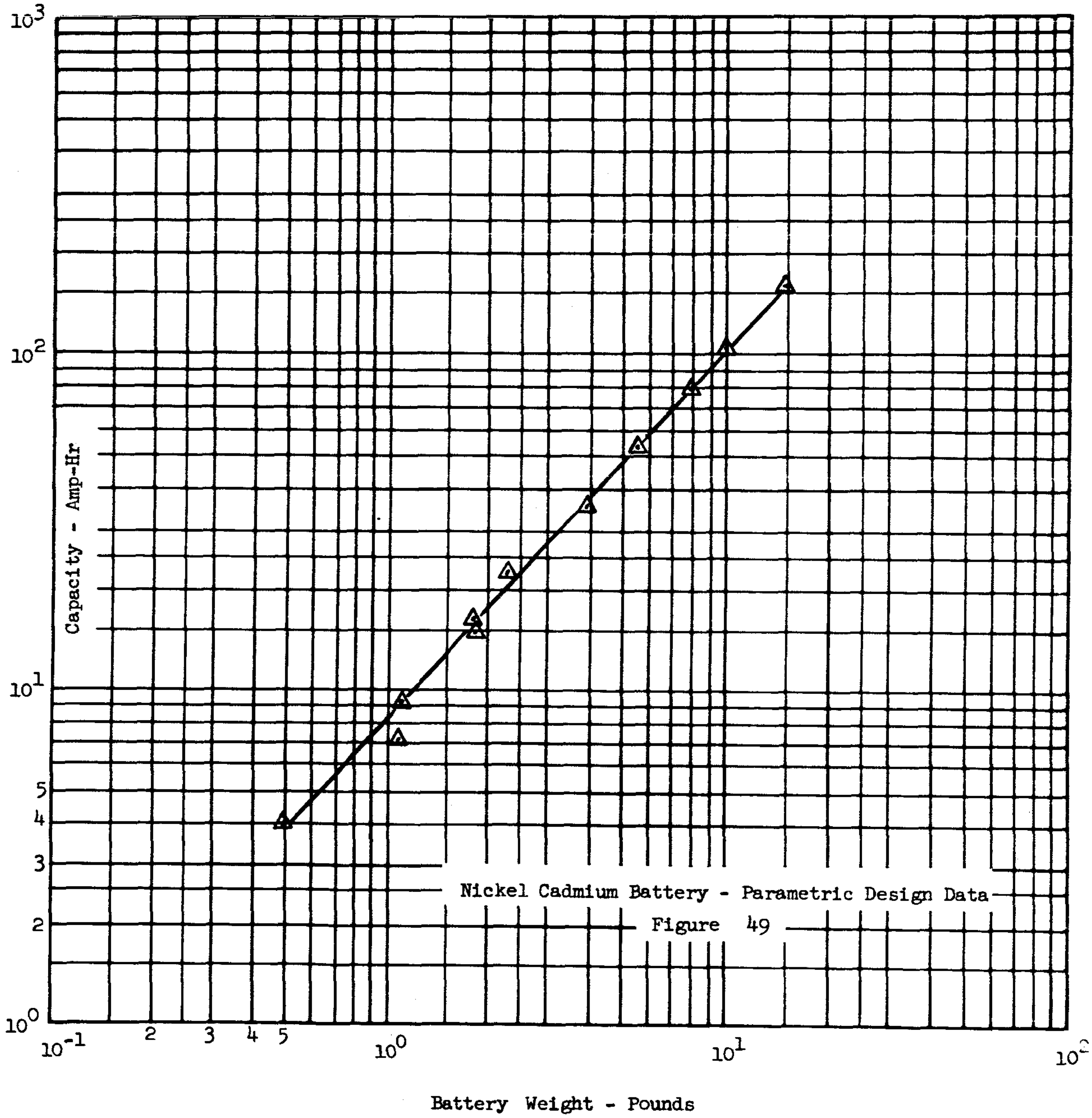

Nickel Cadmium Battery - Parametric Design Data

Figure 49

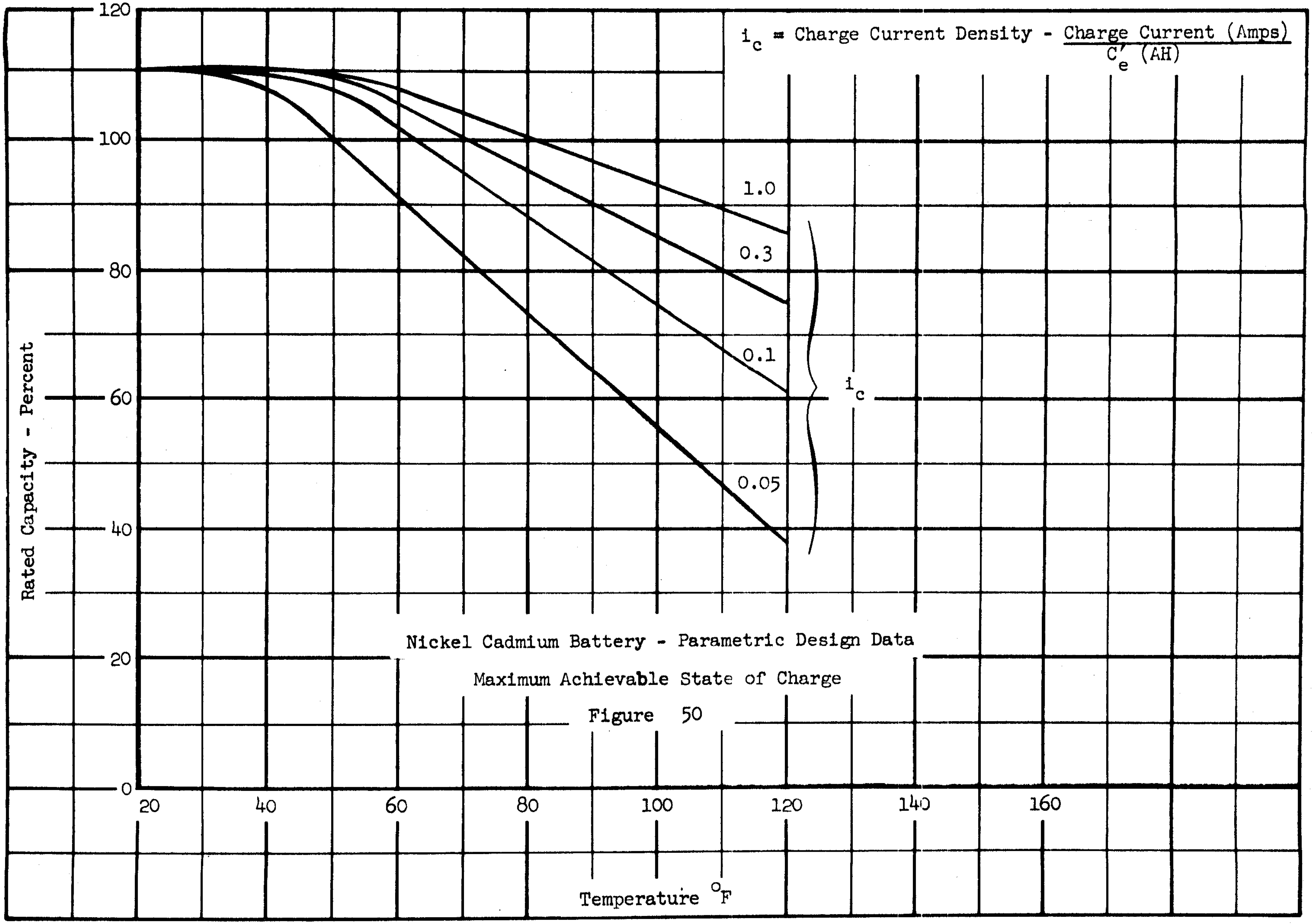

Nickel Cadmium Battery - Parametric Design Data

Maximum Achievable State of Charge

Figure 50

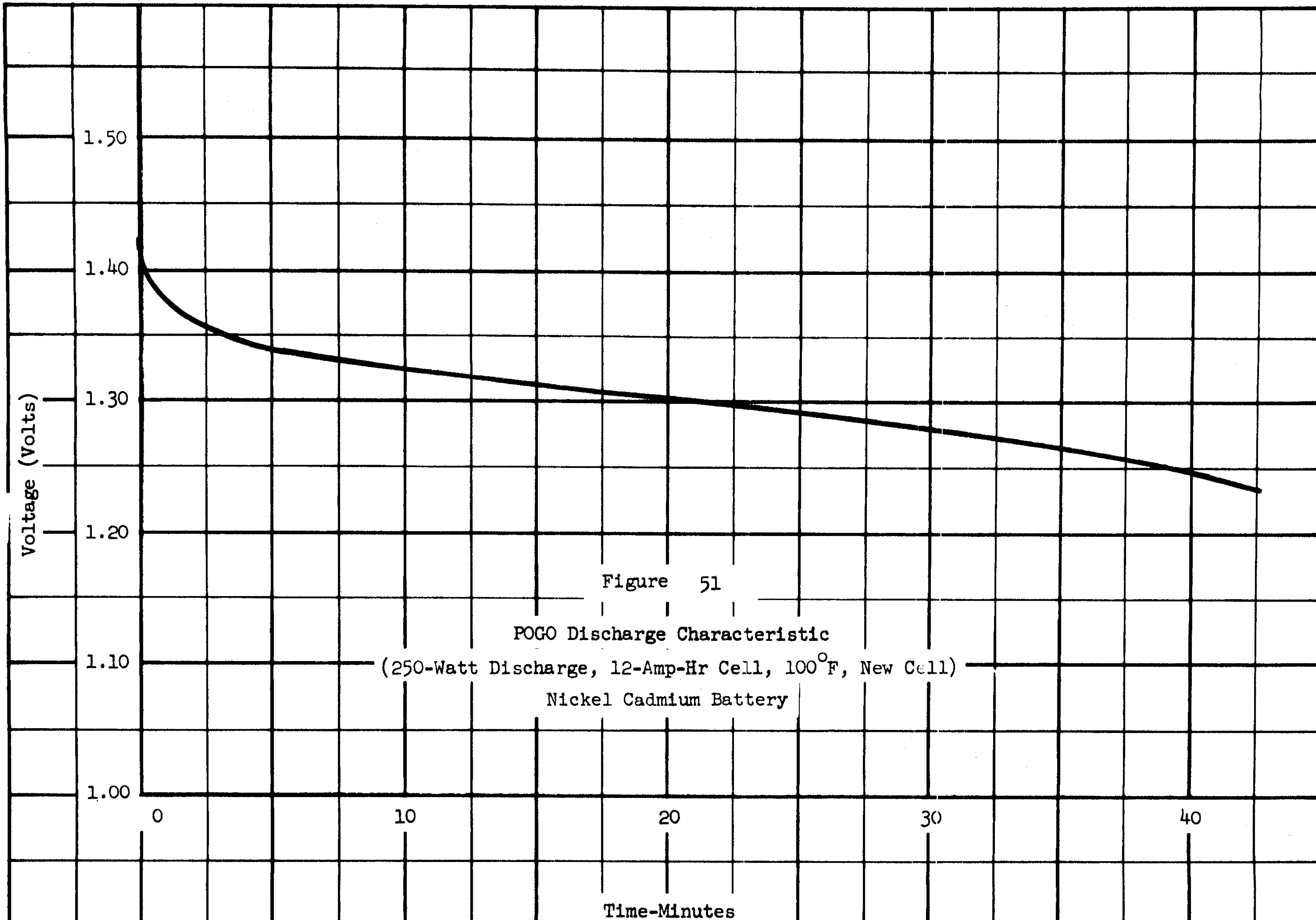

Figure 51

POGO Discharge Characteristic

(250-Watt Discharge, 12-Amp-Hr Cell, 100°F, New Cell)

Nickel Cadmium Battery

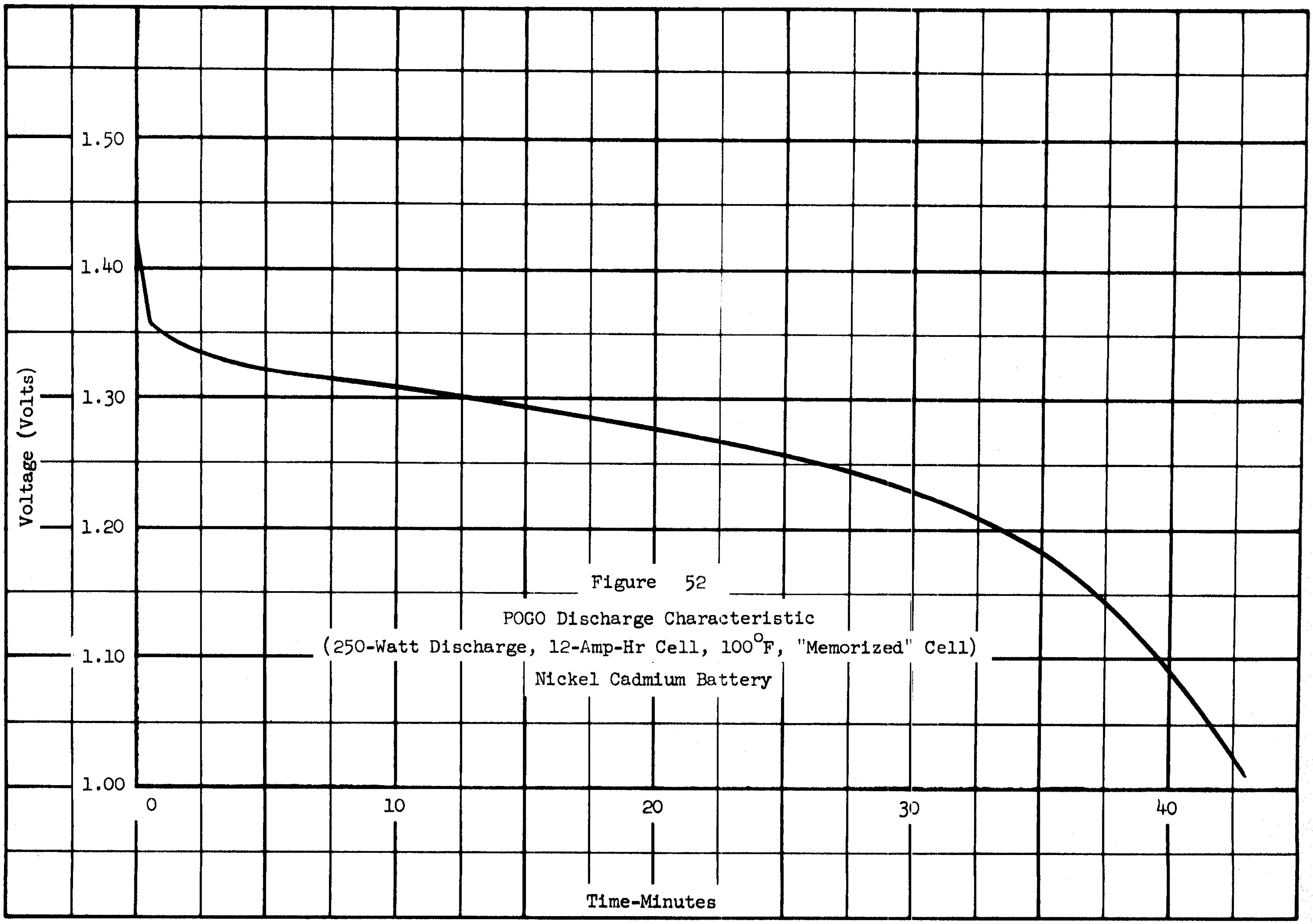

Figure 52

POGO Discharge Characteristic

(250-Watt Discharge, 12-Amp-Hr Cell, 100°F, "Memorized" Cell)

Nickel Cadmium Battery

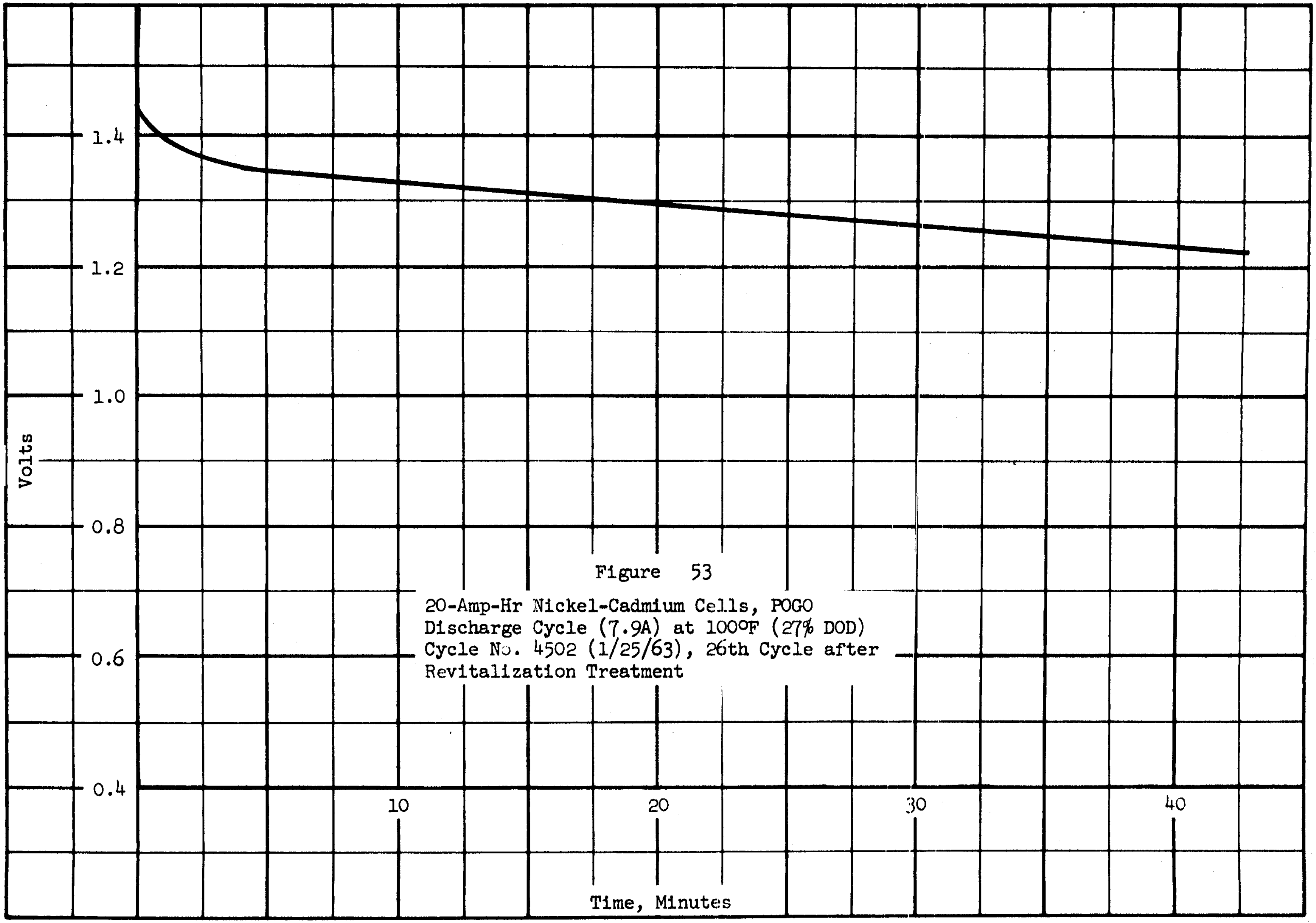

Figure 53

20-Amp-Hr Nickel-Cadmium Cells, POGO
Discharge Cycle (7.9A) at 100°F (27% DOD)
Cycle No. 4502 (1/25/63), 26th Cycle after
Revitalization Treatment

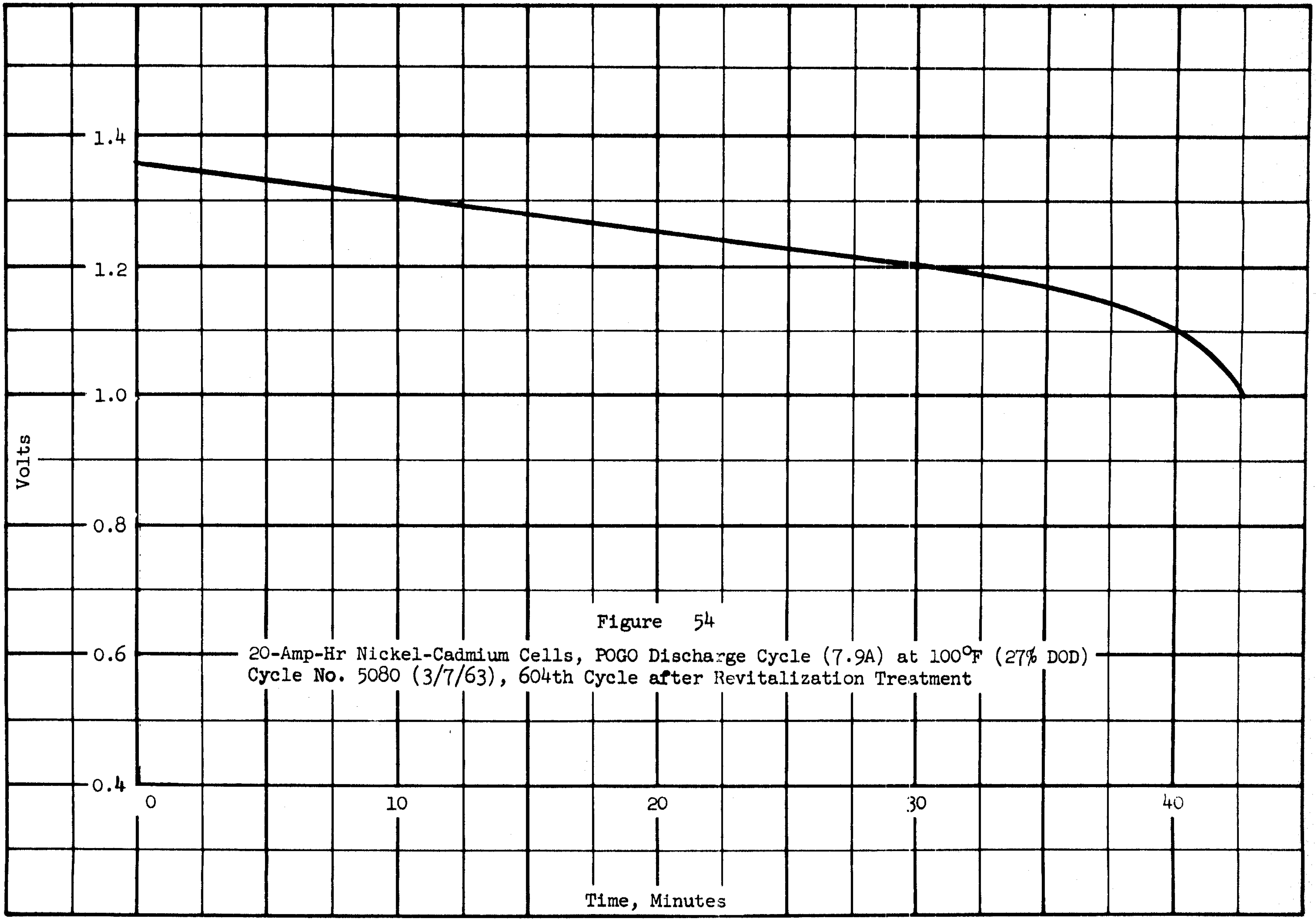

Figure 54

20-Amp-Hr Nickel-Cadmium Cells, POGO Discharge Cycle (7.9A) at 100°F (27% DOD)
Cycle No. 5080 (3/7/63), 604th Cycle after Revitalization Treatment

3.4.4 Power Distribution

Power distribution equipment is usually classified as harnesses, circuit protection or fuses, terminal blocks, power switching, and under or over voltage protection and isolation diodes.

Power loss, weight and wire gauge for the harnesses used on five of the considered programs is summarized in Table X. Considerable standardization of component parts for harnesses has already been accomplished. Except for changing of the wire sizes to reduce losses, very little contribution can be made by the harness area to the maximum utilization of power. At present, these power losses are very minimal.

Circuit protection has been accomplished by the use of fuses in all known vehicles to date. These devices operate in a linear mode as a function of I^2t. Other devices known as current limiters, which are non-linear with I^2t have been used in special cases requiring only current limiting.

The use of relays for switching power or transferring functions has been the established procedure so far. Solid state switches have been proposed and used on two programs - Pioneer and 2029. All other programs investigated have used relays. These devices each have advantages and disadvantages as summarized below.

Advantages

Relays: Low power consumption; not susceptable to radiation damage; essentially unlimited current carrying capacity; well advanced in the state-of-the-art; and reasonably high reliability.

TABLE X

Harness Characteristics

Program	Voltage Drop: Primary Power*	Voltage Drop: Secondary Power**	Weight lb.	Wire Gauge
OGO	<1.5%	<1.5%	110	20-28 AWG
ABLE	< 50 MV	—	~15	20-28 AWG
VASP	<1200 MV	< 80 MV	15	20-28 AWG
PIONEER	< 250 MV	< 50 MV	9.87	20-28 AWG
VELA	750 MV	60 MV	12	20-28 AWG

*Primary power losses are from primary sources to the users'equipment.

**Secondary power losses are from secondary sources to the users'equipment.

Solid State Switch:	Light weight; very compact; no magnetic properties; no moving parts; and predicted high reliability.

Disadvantages

Relays:	Poor magnetic field properties; high volume; high weight; and subject to contact chatter causing interruptions and/or noise.
Solid State Switches:	Subject to radiation damage; limited current carrying capacity; power consumption proportional to current carried; and relatively new in development.

For the purpose of this study, it would appear that characteristics other than power consumption may dictate the selection of switching device. All other things being equal, solid state switches would be used for low power circuits, and relays for high power circuits in order to obtain maximum power system efficiency.

Under and over voltage protection has been accomplished by two methods in the spacecrafts surveyed. The Able V, Vela and OGO vehicles have used unijunction transistors. The Pioneer, Comsat and 2029 program are using the differential amplifier method. The later method is superior to using a unijunction, but has only recently been fully developed. Its advantages are: lower power consumption, narrower hysteresis band width, matrix logic outputs, better temperature range stability, and low DC voltage signals which can drive the power switching devices.

From a power efficiency point of view, the state-of-the-art in over/under voltage control is moving in the correct direction. At this time, no better choice is available.